

A Compositionally Zoned Ash-Flow Sheet in Southern Nevada

GEOLOGICAL SURVEY PROFESSIONAL PAPER 524-F

*Prepared on behalf of the
U.S. Atomic Energy Commission*



A Compositionally Zoned Ash-Flow Sheet in Southern Nevada

By P. W. LIPMAN, ROBERT L. CHRISTIANSEN, and J. T. O'CONNOR

SHORTER CONTRIBUTIONS TO GENERAL GEOLOGY

GEOLOGICAL SURVEY PROFESSIONAL PAPER 524-F

*Prepared on behalf of the
U.S. Atomic Energy Commission*

*A widespread ash-flow sheet grades from
phenocryst-poor rhyolite upward into
phenocryst-rich quartz latite, recording
in inverted order the compositional
zonation of magma in the source chamber*



UNITED STATES GOVERNMENT PRINTING OFFICE, WASHINGTON : 1966

UNITED STATES DEPARTMENT OF THE INTERIOR

STEWART L. UDALL, *Secretary*

GEOLOGICAL SURVEY

William T. Pecora, *Director*

For sale by the Superintendent of Documents, U.S. Government Printing Office
Washington, D.C. 20402 - Price \$1 (paper cover)

CONTENTS

| | Page | | Page |
|--|------|--|------|
| Abstract..... | F1 | Petrology..... | F26 |
| Introduction..... | 1 | Groundmass mineralogy and texture..... | 27 |
| Acknowledgments..... | 2 | Phenocryst mineralogy..... | 28 |
| Nomenclature of ash-flow tuffs..... | 2 | Chemistry..... | 30 |
| Geologic setting..... | 2 | Major oxides..... | 30 |
| General features..... | 3 | Minor elements..... | 34 |
| Welding and crystallization zones..... | 3 | Relations between bulk-rock and groundmass chemistry..... | 35 |
| Vertical compositional variations..... | 7 | Relations between chemical and mineralogical com- positions..... | 38 |
| Busted Butte section..... | 7 | Compositional zonations in other ash-flow sheets..... | 39 |
| 311 Wash section..... | 11 | Interpretation of magmatic differentiation..... | 41 |
| Black Glass Canyon section..... | 11 | Correlation of normative compositions with ex- perimental data..... | 41 |
| Pah Canyon section..... | 13 | Hypothesis of crystal accumulation..... | 43 |
| Yucca Mountain section..... | 14 | Hypotheses of crystal-liquid fractionation at hid- den depth..... | 44 |
| Lathrop Wells section..... | 14 | References cited..... | 46 |
| Prospectors Pass section..... | 17 | | |
| Fluorspar Canyon section..... | 18 | | |
| Lateral compositional variations..... | 18 | | |

ILLUSTRATIONS

| | | Page |
|--------|---|-----------|
| PLATE | 1. Diagram showing correlation of measured sections from Lathrop Wells to Paintbrush Canyon..... | In pocket |
| FIGURE | 1. Index map showing the distribution and thickness of the Topopah Spring Member of the Paintbrush Tuff..... | F4 |
| | 2. Photograph of abundant lithophysal cavities in densely welded crystallized tuff..... | 5 |
| | 3. Photograph of thick stratigraphic section of the Topopah Spring Member..... | 6 |
| | 4. Measured section of the Topopah Spring Member at Busted Butte..... | 8 |
| | 5. Photograph and photomicrograph of crystal-rich quartz latitic caprock of the Topopah Spring Member..... | 10 |
| | 6. Measured section of the Topopah Spring Member at 311 Wash..... | 12 |
| | 7. Measured section of the Topopah Spring Member in Black Glass Canyon..... | 13 |
| | 8. Photograph showing typical appearance of the xenolithic unit..... | 14 |
| | 9. Photograph of contact between xenolithic and caprock flow units..... | 14 |
| | 10. Measured section of the Topopah Spring Member in Pah Canyon..... | 15 |
| | 11. Measured section of the Topopah Spring Member at the north end of Yucca Mountain..... | 16 |
| | 12. Measured section of the Topopah Spring Member near Lathrop Wells..... | 17 |
| | 13. Photograph showing the base of the ash-flow sheet of the Topopah Spring Member..... | 18 |
| | 14. Photographs and photomicrograph showing the swarm of quartz latitic pumice..... | 19 |
| | 15. Measured section of the Topopah Spring Member at Prospectors Pass..... | 20 |
| | 16. Photographs and photomicrograph showing the bedded welded tuff in the upper part of the ash-flow sheet of the Topopah Spring Member..... | 21 |
| | 17. Measured section of the Topopah Spring Member in Fluorspar Canyon..... | 23 |
| | 18. Diagrams showing the distribution of depositional subunits..... | 25 |
| | 19. Photomicrographs of crystal-poor rhyolitic tuff..... | 27 |
| | 20. Photomicrograph showing phenocryst of plagioclase mantled by alkali feldspar..... | 28 |
| | 21. Graph showing variations in plagioclase compositions and in $2V_x$ of alkali feldspars..... | 29 |
| | 22. SiO_2 variation diagrams for weight percent of major oxides..... | 31 |
| | 23. SiO_2 variation diagrams of minor elements..... | 36 |

| | Page |
|---|------|
| FIGURE 24. Graph showing relation between SiO_2 and total phenocryst contents of 11 analyzed rocks of the Topopah Spring Member..... | F39 |
| 25. Graphs showing relations between phenocryst proportions and total phenocryst content of tuffs of the Topopah Spring Member..... | 40 |
| 26. Triangular diagrams showing normative compositions of tuffs of the Topopah Spring Member in the system Q-Or-Ab..... | 42 |

TABLES

| | Page |
|--|------|
| TABLE 1. Partial analysis of alkali feldspar from quartz latitic caprock of Topopah Spring Member..... | F28 |
| 2. Composition of tuffs of the Topopah Spring Member..... | 32 |
| 3. Calculated groundmass composition of tuffs of the Topopah Spring Member..... | 35 |
| 4. Analysis of glassy groundmass of quartz latitic tuff from the Busted Butte section..... | 38 |

SHORTER CONTRIBUTIONS TO GENERAL GEOLOGY

A COMPOSITIONALLY ZONED ASH-FLOW SHEET IN SOUTHERN NEVADA

By P. W. LIPMAN, ROBERT L. CHRISTIANSEN, and J. T. O'CONNOR

ABSTRACT

Several ash-flow sheets in the vicinity of the Atomic Energy Commission's Nevada Test Site in southern Nevada display systematic chemical and mineralogical zonations; in each of these zoned sheets, basal crystal-poor rhyolite grades upward into crystal-rich quartz latite. These compositional changes appear to reflect vertical variations in the magmas from which the ash-flow sheets were erupted. The Topopah Spring Member, a widespread ash-flow sheet of the Paintbrush Tuff of Miocene(?) and Pliocene age, is typical of such compositionally zoned units and is here discussed in detail.

The Topopah Spring Member is a multiple-flow compound cooling unit which originally covered about 700 square miles and had a volume of about 40 cubic miles. Because it was erupted over irregular terrain, thickness and other lithologic features of the sheet vary considerably within short distances. Zones of welding and crystallization are well developed; in general, a densely welded crystallized center is enveloped by nonwelded to densely welded glassy rocks. Thick stratigraphic sections contain a central lithophysal zone within the crystallized zone.

The principal compositional zonation of the tuffs is from basal crystal-poor rhyolite (77 percent SiO_2 ; 1 percent phenocrysts) to capping crystal-rich quartz latite (69 percent SiO_2 ; 21 percent phenocrysts). In addition, concentrations of pumice blocks and lithic inclusions vary systematically, permitting recognition of at least six flow units. Flow-unit contacts, which vary laterally in character, may be sharp in some places and gradational in others. Most individual flow units are present in only part of the area in which the ash-flow sheet occurs. Their thicknesses tend to be compensating; where the underlying flow unit is thick, the overlying one is thin. In three-dimensional form, the flow units have a shingled pattern rather like the divergent distribution of successive mudflows on an alluvial fan.

The main phenocrysts of the Topopah Spring Member are sanidine (about $\text{Or}_{50}\text{Ab}_{50}$), oligoclase (An_{20-30}), biotite, clinopyroxene, and magnetite. Although a few crystals may be xenocrysts, most are magmatic phenocrysts. The upward increase in phenocryst content is accompanied by systematic variations in phenocryst proportions. In crystal-poor rhyolite, plagioclase and alkali feldspar occur in subequal amounts and clinopyroxene is absent; in the crystal-rich quartz latite, alkali feldspar is more abundant than plagioclase, and clinopyroxene is conspicuous.

The systematic sequence of compositional variations in the Topopah Spring Member and nine other nearby ash-flow sheets suggests that each sheet formed by eruption of successively

lower parts of a zoned magma body in which relatively crystal-poor rhyolitic magma overlay crystal-rich quartz latitic magma.

The chemical variation trend of the Topopah Spring tuffs closely follows fractionation curves for the liquid line of descent in the experimentally determined system $\text{NaAlSi}_3\text{O}_8\text{-KAlSi}_3\text{O}_8\text{-SiO}_2\text{-H}_2\text{O}$ at about 600 bars water pressure. This suggests that the compositional variation resulted from fractional separation of crystals from liquid under conditions of near equilibrium. However, phenocryst proportions and groundmass compositions show that the variation did not result from simple accumulation, in the quartz latitic part of the erupted magma, of crystals settled from the rhyolitic part. Although phenocryst proportions are incompatible with such a mechanism, they can be interpreted as the result of progressive crystallization in a previously zoned magma body. According to this interpretation, crystallization had progressed further in the quartz latite than in the rhyolite at the time of eruption. Three-fourths of the chemical variation results from differences in groundmass composition rather than differences in phenocryst content. Two compatible hypotheses for differentiation of the Topopah Spring magma are (1) fractional crystallization and the settling of crystals into a larger continuous magma body underlying the erupted part, and (2) fractional anatexis melting of sialic crust.

INTRODUCTION

Most described ash-flow tuffs are poorly sorted and compositionally homogeneous, presumably because of turbulent emplacement. Many of these tuffs, especially the thicker ones, have striking zones of crystallization and welding, the understanding of which has been greatly advanced through the work of R. L. Smith (1960a, b). However, formation of such crystallization and welding zones does not appear to modify appreciably the primary chemical uniformity of the tuffs (Lipman and Christiansen, 1964). Although most described ash-flow sheets, therefore, show little vertical or lateral variation in chemical or phenocrystic composition, at least three ash-flow sheets that show compositional zonations have been reported in addition to the one described here: the Mammoth Mountain Rhyolite in the Creede district, southwestern Colorado (Ratté and Steven, 1964), the pumice-scoria flows of Crater Lake, Oreg. (Howell Williams, 1942), and the pumice

flow of Shikotsu Volcano, northern Japan (Katsui, 1963). The descriptions of these ash-flow sheets are brief, but apparently in each sheet silicic tuff relatively poor in phenocrysts grades upward to more mafic tuff richer in phenocrysts.

Recent investigations of upper Tertiary volcanic rocks in the vicinity of the U.S. Atomic Energy Commission's Nevada Test Site by the authors and other members of the U.S. Geological Survey have disclosed 10 additional examples of systematic compositional variations in ash-flow sheets. Within each sheet relatively low-phenocryst rhyolite grades upward into crystal-rich quartz latite. The ash-flow deposits of largest volume most commonly show such compositional zonations. A major conclusion of this paper is that these compositional zonations record in inverted order vertical compositional sequences that were established in the magmas prior to eruption. Some of our petrographic studies have already been briefly reported (O'Connor, 1963; Quinlivan and Lipman, 1965). In this paper a representative ash-flow sheet for which relatively abundant field and laboratory data are available, the Topopah Spring Member of the Paintbrush Tuff, is described in some detail in order to document the characteristic features of the compositional variations and to provide a basis for petrogenetic interpretations.

ACKNOWLEDGMENTS

The detailed descriptions of variations in the Topopah Spring Member are based mainly on our observations in the western half of the ash-flow sheet. Discussions and field excursions with our colleagues who have studied the remainder of the sheet indicate that our generalizations are valid for the entire unit; we are indebted particularly to F. M. Byers, Jr., E. N. Hinrichs, E. J. McKay, F. A. McKeown, and P. P. Orkild. Stimulating discussions with R. L. Smith have greatly benefited our concepts of zonal features in ash-flow tuffs. Previously unpublished analyses of the Topopah Spring Member were contributed by E. N. Hinrichs and F. A. McKeown. The work on which this report is based was done on behalf of the U.S. Atomic Energy Commission.

NOMENCLATURE OF ASH-FLOW TUFFS

The nomenclature used in this report to describe ash-flow tuffs is that of Smith (1960a, b) and Ross and Smith (1961). Smith described features of ash-flow deposits resulting from both depositional and cooling processes. The basic depositional unit of these deposits is considered to be "the **ash flow** that is analogous to, or perhaps the same as, the deposit resulting from the pas-

sage of one nuée ardente" (Smith, 1960a, p. 800). The smallest recognizable virtually nonsorted layers in an outcrop section must necessarily be regarded as the local flow units, although it is probable that other similar units in densely welded sections go unrecognized and that some of those recognized are only pulsations of single ash flows. The principal genetic concept relating to ash-flow tuffs is that of the **cooling unit**, an "ash-flow deposit that can be shown to have undergone continuous cooling * * *" (Smith, 1960a, p. 801). A cooling unit may contain only a single ash flow, or it may contain many. The flows within the unit may have been emplaced rapidly and completely cooled together to produce a **simple cooling unit**; or, there may have been interruptions between certain of the ash flows, resulting in partial cooling of the lower parts of the deposit and the formation of a **compound cooling unit**. An ash-flow sheet in which separate cooling units grade laterally into a single compound or simple cooling unit is a **composite sheet**.

GEOLOGIC SETTING

The Paintbrush Tuff is part of a large ash-flow field in southwestern Nevada that represents a late Miocene and Pliocene episode of voluminous rhyolitic volcanism. Little detailed work had been done in this ash-flow field before that of Cornwall (1962) in the Beatty area and before the current geologic study of the Nevada Test Site, of which this study is a part. Most of the volcanism in this field occurred later than that in eastern Nevada and southwestern Utah, which was studied mainly by Mackin (1960), P. L. Williams (1960), and Cook (1958). Partly as a result of extensive mantling by relatively young volcanic deposits, basin-range topography is less conspicuous in the southwestern Nevada ash-flow field than in most parts of the Great Basin. The structural style of the area is, nevertheless, the typical basin-range pattern of tilted blocks bounded by antithetic normal faults. Basin-range block faulting clearly occurred before, during, and after the main period of volcanism, but the ranges and valleys outlined by these blocks are small in comparison with other Great Basin features.

The area of the southwestern Nevada ash-flow field is most aptly described as a highly faulted and eroded volcanic plateau. Within this plateau are several calderas that resulted from subsidence of the source areas after episodes of intense pyroclastic activity (Cornwall, 1962; Christiansen and others, 1965; Christiansen and Noble, 1965). Additional volcanic centers within the field are represented by local accumulations of rhyolitic to mafic lavas which markedly influenced the extent and shape of the extensive ash-flow deposits of the region. Struc-

tural control for the locations of the volcanic centers is not well understood, but the group of centers is within the right-lateral structural zone of the Walker Lane (Locke and others, 1940; Gianella and Callaghan, 1934; Longwell, 1960).

GENERAL FEATURES

The Topopah Spring Member, one of the most widespread and voluminous ash-flow cooling units in the southwestern Nevada volcanic field, was named for Topopah Spring (Hinrichs and Orkild, 1961) on the south side of Shoshone Mountain (fig. 1). It is the lowest major unit in the Paintbrush Tuff (Orkild, 1965), a predominantly ash-flow sequence that includes three other major ash-flow units. The other three are, in ascending order, the Pah Canyon, Yucca Mountain, and Tiva Canyon Members. Similar areal distributions and petrologic features of these four ash-flow units suggest that they are genetically related. The Tiva Canyon and the Topopah Spring Members are very similar and can be mistaken for one another in the field.

The Topopah Spring Member is predominantly pale-grayish-red to pale-reddish-brown¹ densely welded ash-flow tuff, but it includes varicolored nonwelded to partly welded tuffs at its base and top. Minor thicknesses of genetically related ash-fall tuff widely underlie and overlie the ash flows and are also included in the member. The tuff is mainly rhyolite, but it generally grades into quartz latite at its top. The ash-flow tuff forms a compound cooling unit, although the deviations from simple cooling are slight in many places.

The inferred original distribution and thickness of the Topopah Spring Member are shown in figure 1. This reconstruction is based on detailed (1:24,000) mapping of the entire area east and northeast of Crater Flat, augmented by reconnaissance mapping of the western part of the area shown in figure 1. Additional reconnaissance west and northwest as far as California has thus far failed to disclose other occurrences of the Topopah Spring Member, but the absence of the unit in these directions is as yet unproven. The unit has been identified in cores from three drill holes on Pahute Mesa; therefore, it once extended across the area of Timber Mountain. However, no outcrops of the Topopah Spring occur in the area between Pahute Mesa and the continuous exposures south of Timber Mountain, because the intervening area is entirely blanketed by younger rocks.

Virtually continuous outcrops of the Topopah Spring Member extend along a generally arcuate east-west belt, irregularly concave to the north and about 50

miles long. As reconstructed, the area originally covered was about 700 square miles (1,800 sq. km.) and the volume was approximately 40 cubic miles (170 cu. km.). Its thickness and various lithologic features vary markedly within short distances; these variations reflect emplacement on irregular terrain having at least several hundred feet of local relief. For instance, the elongate bulge in the zero isopach southwest of Shoshone Mountain (fig. 1) delimits a thick but areally restricted pile of older rhyolitic laval flows that the Topopah Spring Member surrounded but did not cover. The closely spaced isopachs and lobate zero isopach northeast of Skull Mountain mark the lapping of the Topopah Spring tuffs upon an older andesite-rhyodacite volcano, composed of the Miocene and Pliocene Wahmonie and Miocene Salyer Formations (Poole and others, 1965). Only 5 miles north of this barrier, in the 311 Wash area, the Topopah Springs tuffs reach their maximum known thickness—890 feet. The tuffs also thin abruptly against older volcanic rocks along the south side of Pinnacles Ridge and against Paleozoic carbonate rocks at the north end of Bare Mountain. More than 700 feet of the tuff accumulated in the relatively restricted valley just east of Beatty, and the tuff appears to have been channeled southeastward through this valley from a source area farther northwest, possibly in the Oasis Valley area. Structural evidence suggests a caldera-subsidence source area near Oasis Valley for at least part of the Paintbrush Tuff.

The Tertiary volcanic section in southwestern Nevada is very sparsely fossiliferous, and the Topopah Spring Member has not been dated paleontologically. Biotite from the unit has yielded a potassium-argon age of 13.2 ± 0.3 million years (R. W. Kistler, written commun., 1964). This age, which approximately coincides with the Miocene-Pliocene boundary (Kulp, 1961), is compatible with potassium-argon ages of underlying and overlying units.

WELDING AND CRYSTALLIZATION ZONES

The most striking vertical and lateral variations in the Topopah Spring Member, as in most other ash-flow cooling units in southwestern Nevada, are due to zonal welding and crystallization features. These zonal features tend to overshadow the primary compositional variations and, accordingly, are described first.

The welding and crystallization zones of the Topopah Spring Member correspond closely to those described by Smith (1960b). In general, the Topopah Spring ash-flow sheet consists of a densely welded crystallized center enveloped by nonwelded to densely welded glassy top, bottom, and distal edges. The nonwelded to partly welded zones are seldom more than 50 feet thick at the

¹ Color terms in this paper follow those of the "Rock-Color Chart," prepared by the National Research Council (Goddard and others, 1948).

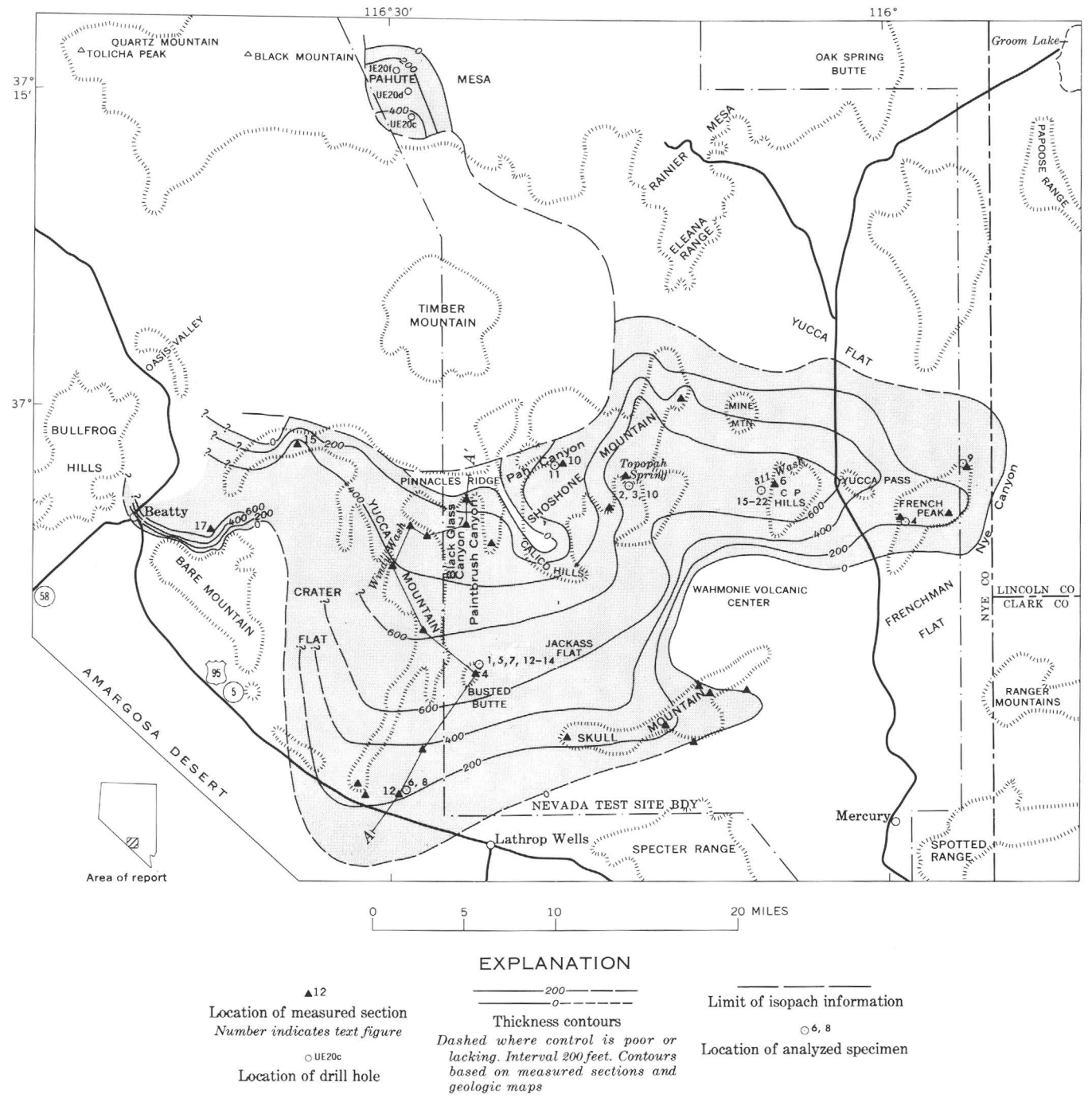


FIGURE 1.—Distribution and thickness of the Topopah Spring Member of the Paintbrush Tuff and location of measured sections and chemically analyzed samples. Section A-A' is shown on plate 1.

base of the cooling unit and are typically even thinner at the top; hence, the densely welded zone constitutes the bulk of most sections. The densely welded zone is crystallized in only its central part; commonly at its bottom there is a thick vitrophyre and at its top a thinner vitrophyre. The widespread presence of two vitrophyre horizons in the Topopah Spring Member tends to distinguish it from the other ash-flow members of the Paintbrush Tuff, in which the zone of crystallization typically extends into the zone of partial welding, and dense vitrophyres are accordingly absent. Sections of the Topopah Spring Member thicker than about 250 feet contain a central zone of lithophysae within the devitrified zone (fig. 2). Well-developed lithophysal zones are also typical of the other ash-flow members of



FIGURE 2.—Abundant lithophysae in densely welded crystallized tuff of the Topopah Spring Member. Small lithophysae, most clearly visible in the lower right corner, are spherical and are filled by products of vapor-phase crystallization. The larger lithophysae are incompletely filled and occur as lenticular cavities flattened parallel to the compaction foliation of the welded tuff. This configuration indicates that some compaction and welding of the ash-flow sheet occurred after formation of the lithophysae. Busted Butte measured section, 400-foot level.

the Paintbrush Tuff. A type of crystallization characterized by coarse intergrowths and mosaics of quartz and alkali feldspar, referred to as granophyric crystallization by Smith (1960b, p. 152), is striking in some specimens from the interiors of thick stratigraphic sections, especially in collapsed pumice lapilli.

Thicknesses of welding and crystallization zones in eight measured sections of the Topopah Spring Member are indicated diagrammatically in figures 4, 6, 7, 10, 11,

12, 15, and 17. The section at Busted Butte (figs. 3, 4) is described in detail in the following paragraphs to illustrate typical features of the zones. The Busted Butte section is representative of the Topopah Spring Member where it is thick and the margins are distant; in such places the welding and crystallization zones are most varied.

At the base of the Busted Butte section a thin (10 ft) nonwelded zone of moderate-orange-pink ash-flow tuffs sharply overlies bedded ash-fall tuff. The nonwelded zone grades upward into a zone of pale-yellowish-brown partly welded tuff about 20 feet thick. As the welding increases in this zone, the color of the shards grades upward to dark yellow brown; toward the top of the zone, collapsed pumice lapilli become black and are conspicuously darker than the shard matrix. With complete loss of porosity in the shard matrix, the rock grades upward into densely welded black vitrophyre. The transition from vitrophyre to overlying crystalline welded tuff is strikingly abrupt and typically takes place within 1–2 inches, but this contact has no primary depositional significance. It is not marked by any compositional variation or textural change, other than the change from glassy to crystalline state of the groundmass.

The crystalline tuff (240 ft thick) between the lower vitrophyre and the main lithophysal zone is densely welded and pale grayish red. It appears homogeneous from a distance, but several thin vapor-phase and lithophysal zones can be recognized between flow units within it. The lower and upper contacts of the main lithophysal zone are both gradational over 30–50 feet. The lowest lithophysal cavities are small (<1 in. in diameter) and widely scattered, but cavities become progressively larger (avg. 2 in. in diameter) and more closely spaced toward the center of the zone, so that the rock in the center of the zone resembles Swiss cheese in appearance (fig. 2). The lithophysal rock (approximately 245 ft thick) is mottled pale grayish red and medium light gray. The rock immediately above the lithophysal zone tends to be medium light gray and typically contains pumice in which vapor-phase crystallization is well developed. About 50 feet above its base, this gray vapor-phase rock grades within 10–20 feet into pale-reddish-brown densely welded crystalline tuff. This upward gradation is accompanied by a considerable progressive increase in phenocrysts and by a gradual chemical change from rhyolite to quartz latite. The reddish-brown crystal-rich quartz latitic zone (40 ft) is more resistant to erosion than the underlying rhyolitic tuff and typically forms a prominent bluff (fig. 3) or caprock. Although not strictly a lithologic name, caprock is a useful term to describe this distinctive zone which, because of its gradational lower contact, ranges in com-

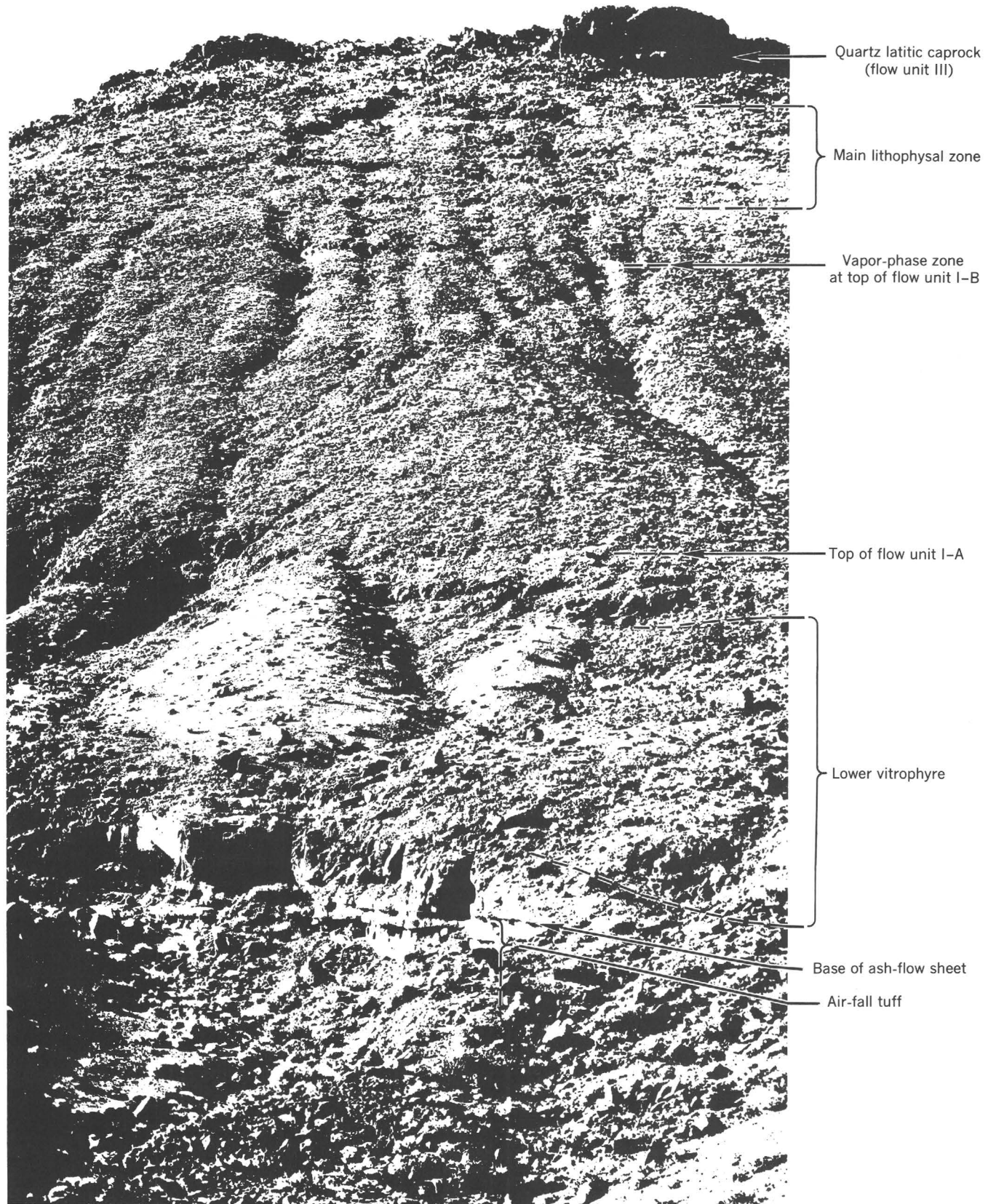


FIGURE 3.—Thick stratigraphic section of Topopah Spring Member, east side of Busted Butte. Apparent relative thicknesses of units within the ash-flow sheet are misleading because of extreme foreshortening in the photograph.

position from low-silica rhyolite to quartz latite. The caprock contains large light-gray eutaxitic collapsed pumice lapilli (fig. 5) which display distinct vapor-phase crystallization near the top but not near the base. Thus, in the upper part of the cooling unit, there are two vapor-phase zones which are separated by the lower part of the caprock.

The transition from crystallized caprock to the upper vitrophyre is as abrupt as the basal contact between glass and crystalline rock. The upper vitrophyre is only 10 feet thick; the lower 7 feet is black, but the upper 3 feet is moderate red owing to oxidation of magnetite crystallites to hematite. The vitrophyre grades upward into yellowish-gray and pinkish-gray partly welded glassy tuff (5 ft) and nonwelded glassy tuff (10 ft).

The main welding and crystallization zones of the Busted Butte section, particularly the thick densely welded crystallized interior surrounded by glassy less welded rocks, demonstrate that the ash-flow tuffs form a single cooling unit, but several features of the zonation indicate that the cooling history of the unit was not simple. Compound cooling is indicated by the repetition of vapor-phase and lithophysal zones and by the presence of densely welded zones overlying porous vapor-phase zones. Other sections of the Topopah Spring Member, as at Yucca Mountain (fig. 11) and Fluorspar Canyon (fig. 17), also contain multiple lithophysal zones and an upper vitrophyre above a vapor-phase zone. Further diagnostic evidence of compound cooling is found in a small area near Prospector Pass where the upper part of the cooling unit consists of alternating densely welded and slightly welded glassy tuffs that locally contain distinct bedding (fig. 16). These features indicate numerous interruptions in both welding and crystallization of the cooling unit.

Furthermore, the progression of vertical welding changes in the Topopah Spring differs from that characteristic of simple cooling units, wherein the densest welded material occurs in the lower part of the unit, and the lower zone of lesser welding is much thinner than the upper zone (Smith, 1960a, p. 826-827; Smith, 1960b, pl. 20). In the Topopah Spring, the lower nonwelded zone is everywhere as thick or thicker than the upper nonwelded zone (figs. 4, 6, 7, 10, 11, 12, 15, 17; pl. 1), and the degree of flattening of pumice lenses indicates that the caprock near the top of the ash-flow sheet is the most densely welded part. These features indicate a general progressive increase in emplacement temperature during eruption of the Topopah Spring Member. The changing emplacement temperature probably resulted in part from increasing magma temperature as progressively lower parts of the magma chamber were drained

during eruption, but they may also reflect more efficient heat conservation during eruption and emplacement of the later ash flows.

VERTICAL COMPOSITIONAL VARIATIONS

The welding and crystallization zones in the Topopah Spring Member are superimposed across zones that contain significant vertical and lateral variations in mineralogy, chemistry, and primary texture. The upward increase in phenocryst content and the upward chemical change from rhyolite to quartz latite have already been mentioned briefly and will now be considered in more detail, along with variations in distribution of pumice and lithic inclusions. These variations are described by reference to 8 measured sections (see fig. 1 for locations), selected from among 23 available, because they provide especially fine documentation of the major compositional variations. Complete descriptions are not given for every section as most have numerous features in common. Rather, attention is focused on the distinctive features of the individual sections. Discussion of the nature of the vertical variations is followed by description of the lateral variations.

BUSTED BUTTE SECTION

The Busted Butte section, for which the welding and crystallization zones were described in the preceding paragraphs, also provides a good introduction to the primary compositional variations because of the completeness of the analytical data. In figure 4, modal analyses of phenocrysts in eight specimens from the measured section, as well as chemical analyses of major oxides and minor elements from six specimens, are plotted against vertical position in the cooling unit. Modes generally have not been determined from nonwelded and partly welded tuffs because variations in compaction introduce uncertainties in interpretation of the phenocryst variations.

The phenocryst content within the densely welded zone of the Topopah Spring Member at Busted Butte increases systematically from about 1 percent near the base to more than 20 percent near the top (fig. 4A). Although the counted modes are rather widely spaced, they should closely approximate the actual variation in phenocryst content; the trend of the phenocryst variation is very evident in the field, and any sizable local deviations would have been noticed. The modal determinations are less precise for the lower part of the section than for the more crystal-rich upper parts because of the relative scarcity of phenocrysts, and the modal contrasts between the lower vitrophyre and the immediately overlying devitrified tuff are with the determina-

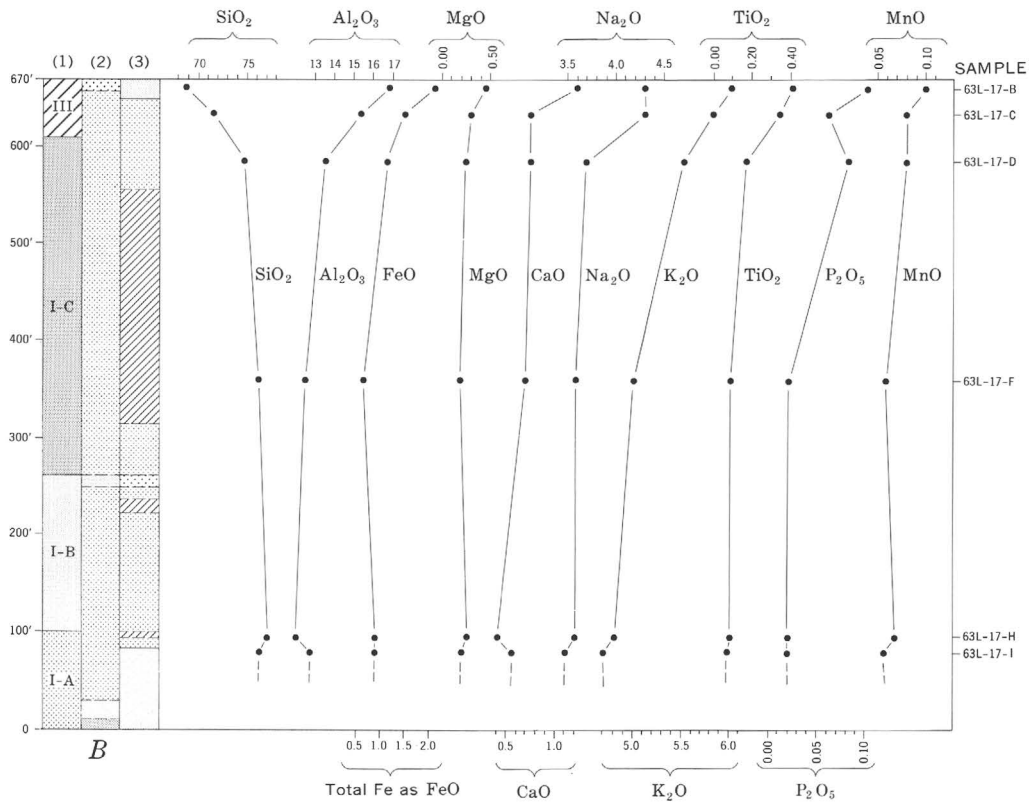
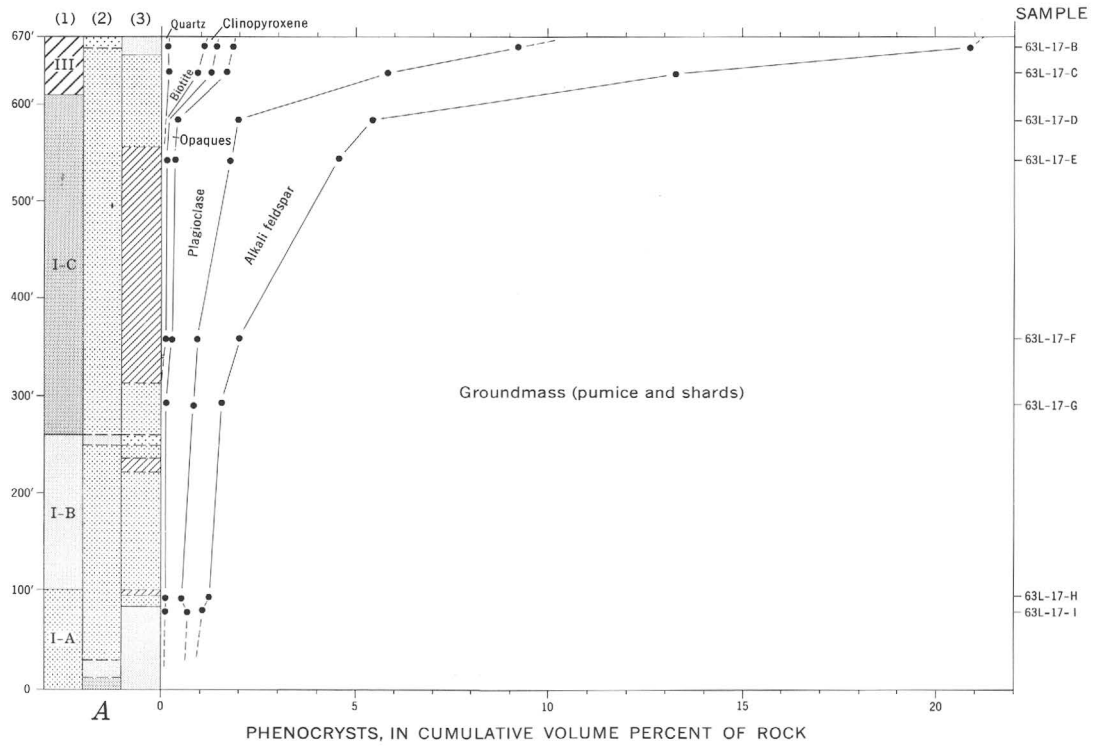
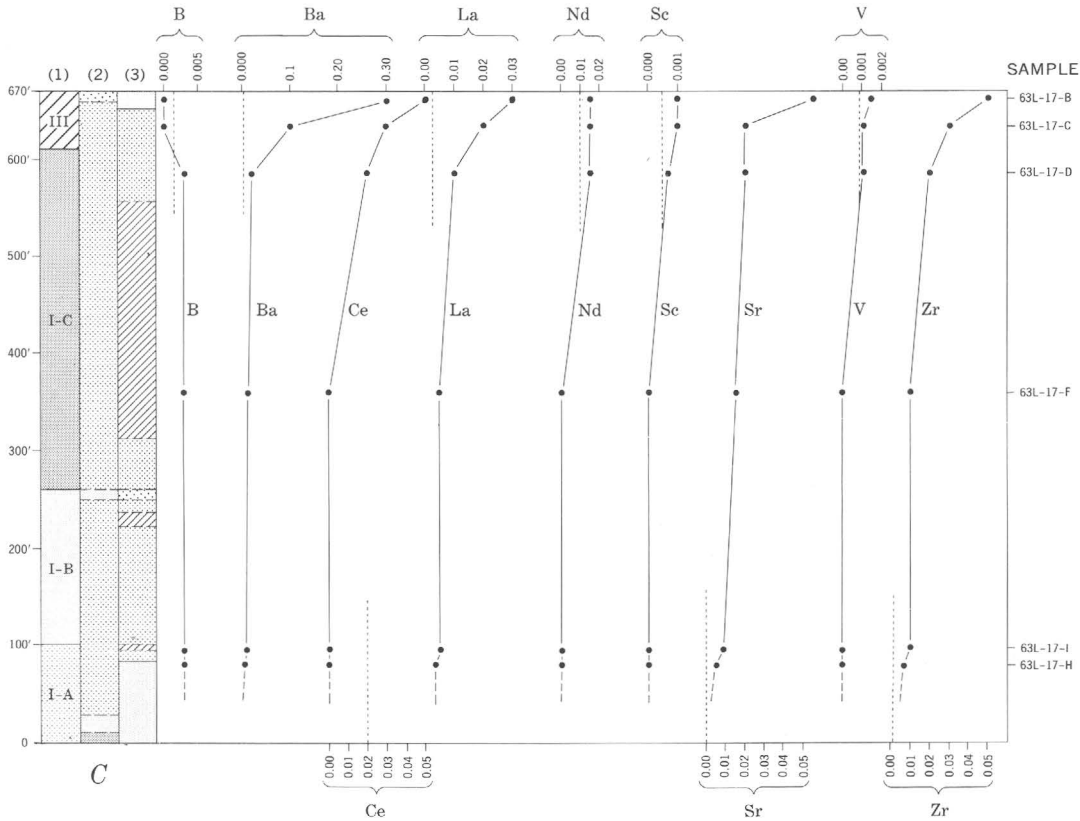


FIGURE 4.—Measured section of the Topopah Spring Member at Busted Butte, showing variations in depositional units, weld-indicate gradational contact. A, Modal phenocryst variations, in volume percent. B,



EXPLANATION

| | | |
|---|---------------------------------|------------------------------|
| (1) DEPOSITIONAL UNITS | (2) WELDING ZONES | (3) CRYSTALLIZATION ZONES |
| Crystal-rich quartz latitic caprock | Nonwelded | Glassy |
| Crystal-poor rhyolite <i>Locally recognized flow units</i> | Partly welded | Crystalline |
| | Nonwelded and partly welded | Vapor phase |
| | Densely welded | Lithophysal |

NOTE: Dashed lines in columns indicate gradational contacts. Dotted lines represent normal threshold of detectability, shown on part C only.

ing zones, and crystallization zones. Analytical data from table 2. Dashed lines in columns in this and other similar figures Major-oxide variations, in weight percent. C, Minor-element variations, in weight percent.

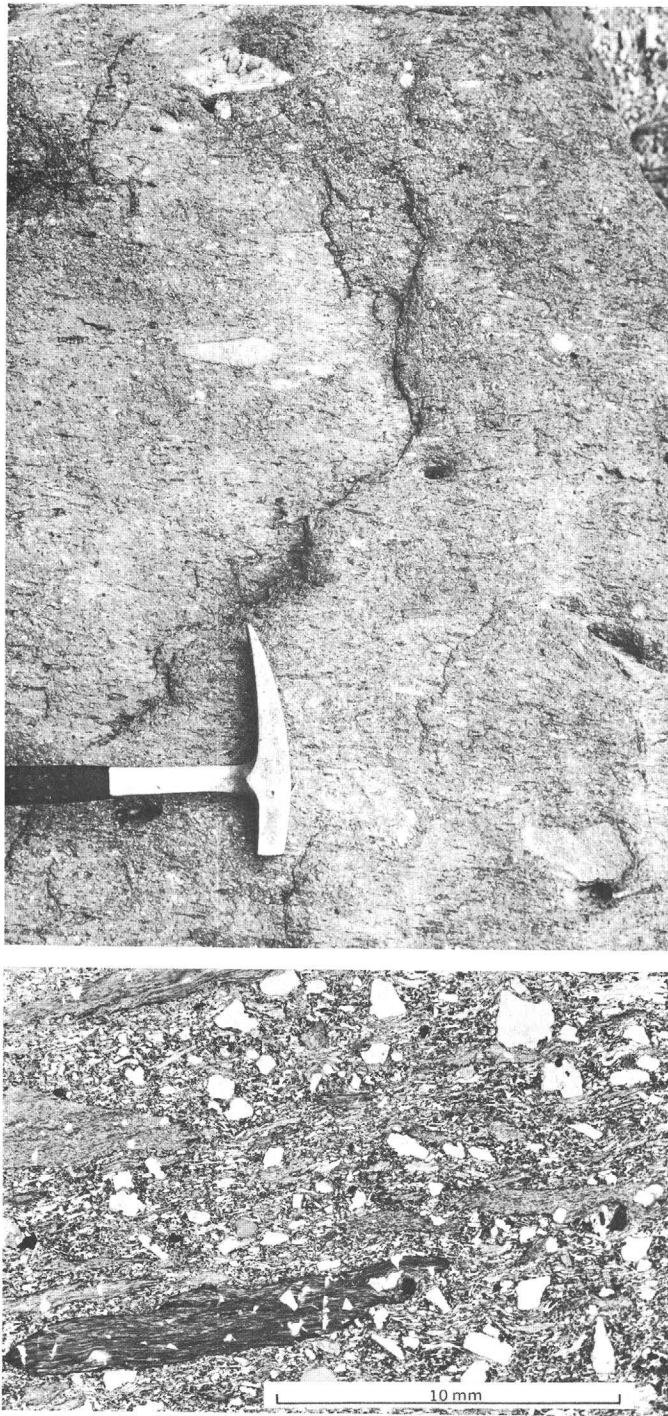


FIGURE 5.—Crystal-rich quartz latitic caprock of the Topopah Spring Member. *Upper.*—Densely welded crystallized caprock, Black Glass Canyon area. Three medium-size (3–5 in. long) lithic inclusions are aligned parallel to the eutaxitic foliation defined by smaller collapsed pumice lapilli. *Lower.*—Photomicrograph (plane-polarized light) of caprock vitrophyre, 311 Wash section. Phenocrysts are mainly sanidine and plagioclase. Matrix consists of deformed shards and collapsed pumice lapilli. Compare size and abundance of phenocrysts and pumice with those of basal rhyolitic vitrophyre shown in figure 194.

tive error. The phenocryst content increases uniformly upward to about the 600-foot level, where it is approximately 6 percent. At about this level (near the base of the caprock) the rate of increase in phenocrysts changes abruptly, and within 75 feet the phenocryst content increases to almost 21 percent. No discontinuity in phenocryst content or in other physical aspects of the tuffs is evident from field examination of this interval, and the changes appear entirely gradational.

Concurrent with the upward increase in total phenocrysts in the Busted Butte section are systematic variations in types and proportions of phenocrysts. In the lower part of the section, plagioclase and alkali feldspar are subequal in amount and are accompanied by relatively minor amounts of opaque minerals and only traces of biotite. Both feldspars increase upward in amount, but the ratio between them gradually changes; near the top of the section, alkali feldspar is almost twice as abundant as plagioclase. The mafic minerals also increase upward. Biotite content at the top of the section is almost 100 times that at the base, and clinopyroxene, absent in the lower part of the cooling unit, is a significant constituent of the caprock. Opaque minerals increase only slightly. A little quartz is present in the caprock, whereas quartz is generally absent in the lower part of the section.

Although not plotted in figure 4, the amount and size of pumice also vary vertically in the Busted Butte section. These variations help identify some of the partings between flow units, a few of which can be correlated between stratigraphic sections. In the basal 15 feet of the cooling unit, a concentration of pumice blocks as much as 12 inches across constitutes 10–20 percent of the tuff. This basal concentration may be due to rafting of the largest pumice toward the front of the advancing ash flow, where it was deposited and overridden by the bulk of the flow. From this basal zone the size and quantity of pumice decrease upward in an interval of about 10 feet, approximately coincident with the inception of welding. The collapsed pumice in the lower vitrophyre is mostly lapilli size and constitutes about 4–8 percent of the rock. About 15 feet above the lower glass-crystalline interface, the pumice decreases again, abruptly, to small lapilli size and to 3–4 percent of the rock. In the overlying rock, pumice is consistently smaller and less abundant than in the underlying rock. This change, which coincides with the top of a thin lithophysal zone, appears to mark the contact between two flow units which can be correlated in several sections (fig. 4; flow units I-A and I-B). Another flow-unit contact was recognized about 150 feet higher in the cooling unit. At this level the lower flow unit (I-B) contains a thin gray vapor-phase zone above a slightly

thicker zone of faint lithophysal crystallization. Coincident with the top of the vapor-phase zone is a pumice swarm 1–2 feet thick that marks the contact between the flow units. The overlying flow unit (I–C) contains slightly larger and more abundant pumice blocks than the unit below (I–B). Thus, in the Busted Butte section there are at least three separate flow units of petrographically similar crystal-poor rhyolite. Depositional breaks are particularly difficult to locate within zones of dense welding, and other flow units probably are present in the Busted Butte section but have not been recognized.

The transition from crystal-poor rhyolite to crystal-rich quartz latitic caprock, which appears to be completely gradational in the Busted Butte section, is also accompanied by variation in the abundance and size of pumice fragments. Collapsed pumice lenses constitute about 10 percent of the crystal-rich zone and average about 5 inches in length; some lenses are as long as 12 inches.

The major-oxide analyses (fig. 4B) show that the phenocryst variations reflect a fundamental chemical zonation. SiO₂ decreases from 77 percent near the base of the section to less than 69 percent near the top, and the other oxides show correspondingly significant variations. The lower part of the cooling unit is silicic rhyolite, and the upper part is silicic quartz latite. As was found in the modal data, the most pronounced chemical change occurs near the base of the caprock.

Of the 18 minor elements for which semiquantitative determinations are available, the 9 that show the largest variations have been plotted in figure 4C; this plot also consistently indicates a major chemical change near the base of the caprock.

311 WASH SECTION

The only additional chemical data with close stratigraphic control are a series of eight semiquantitative spectrographic analyses from the 311 Wash section (fig. 6; table 2, cols. 15–22), the thickest measured section of the Topopah Spring Member. Most of the section is crystal-poor rhyolite that shows little variation in either phenocryst or minor-element compositions. At the gradation to the thin caprock the compositional variations are similar to those found in the Busted Butte section, but modal and spectrographic data indicate that the 311 Wash caprock does not become as mafic.

The Busted Butte and the 311 Wash sections are both exceptionally thick but otherwise exemplify the most common and widespread features of vertical compositional variation in the Topopah Spring Member. With these two sections as standards for comparison, it will

now be worthwhile to consider briefly several additional measured sections which, though representative of relatively small areas, show some instructive contrasts.

BLACK GLASS CANYON SECTION

The Black Glass Canyon section (fig. 7) is strikingly different from the Busted Butte section, although the two are only 8 miles apart. In the Black Glass Canyon section, the crystal-poor rhyolite is much thinner and the quartz latitic caprock is thicker; between them there is an additional flow unit characterized by abundant xenoliths.

The Black Glass Canyon section is along the north edge of the Topopah Spring ash-flow sheet, where it laps against a pile of older rhyolitic lava flows. The nonwelded basal ash-flow material is separated from the older lava flows by 15–30 feet of reworked tuff breccia that contains abundant rubble from the lava flows, and the nonwelded to partly welded base of the ash-flow sheet contains about 10–20 percent of rhyolitic lithic inclusions derived locally from the underlying rubble. The entire interval of crystal-poor rhyolite, which is only 90 feet thick in this section, is considered to be correlative with the lowermost flow unit (I–A) at the Busted Butte section because of similarities in amounts and sizes of pumice, but it has no basal concentration of blocky pumice such as that in the Busted Butte section.

The crystal-poor rhyolitic tuff is abruptly overlain by a distinctive flow unit, not present in the Busted Butte or 311 Wash sections, that contains extremely abundant xenoliths in a matrix of crystal-poor rhyolitic tuff similar to that of the underlying flow unit. The xenoliths, which constitute about half the rock volume, are packed so closely that they resemble a surficial rubble (fig. 8). They consist predominantly of light-purplish-gray crystal-poor welded tuff, less abundant blocks of flow-laminated rhyolite, and sparse fragments of unaltered medium-grained quartz monzonite. The xenoliths, which are mostly subequant, average about 4 inches in diameter, but some are as large as several feet (fig. 9). No local source is evident for any of the xenoliths, but the dominant welded tuffs closely resemble those in a thick welded unit exposed about 9 miles to the northwest. The welded-tuff inclusions are abundant throughout the xenolithic flow unit but are especially concentrated in the lower half. The upper part of the xenolithic unit, which contains relatively more flow-laminated rhyolite and quartz monzonite and less welded tuff, coincides approximately with the zone of lithophysal crystallization.

Where the lower contact of the xenolithic unit is visible, it is generally sharp and depositional. The

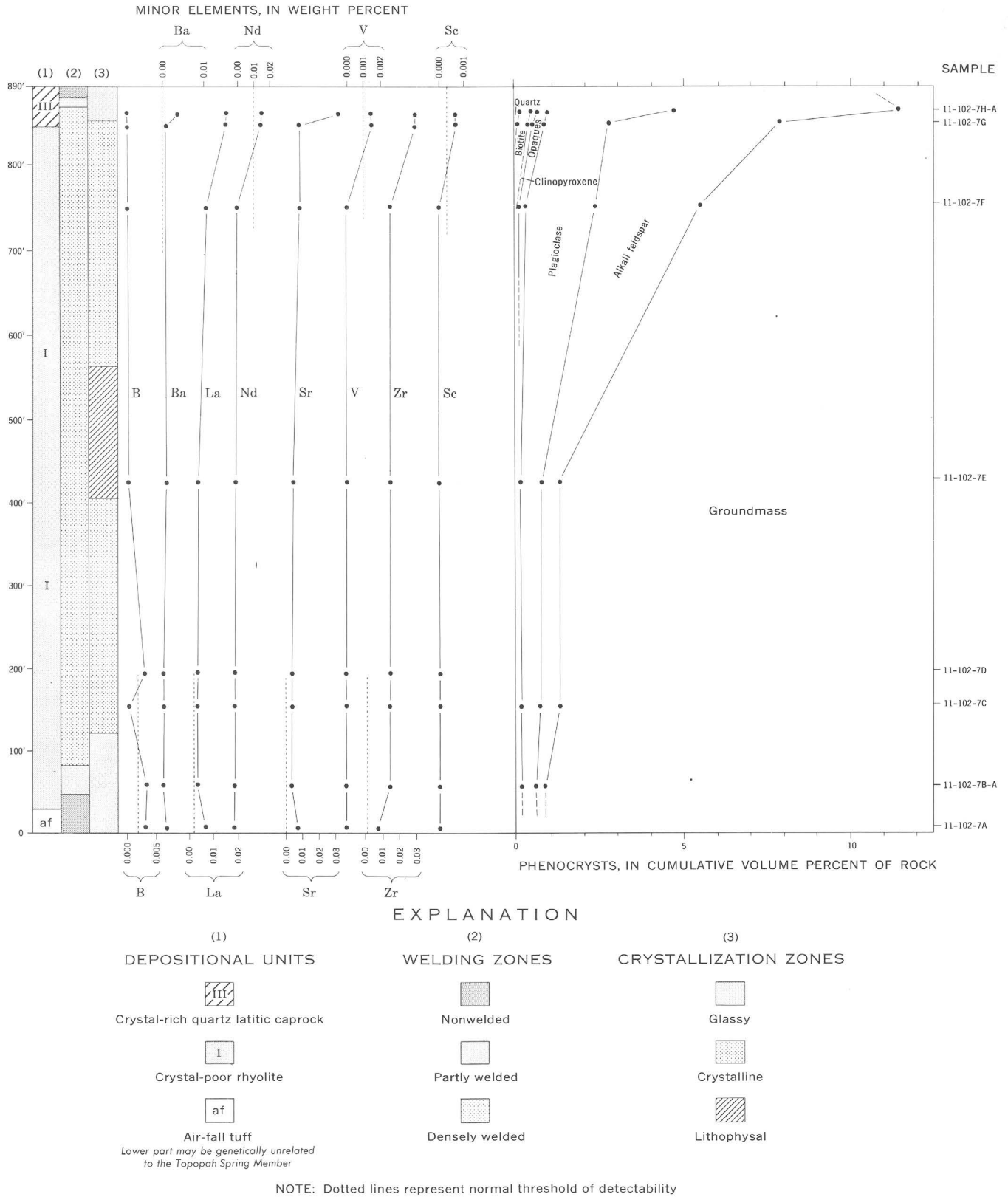
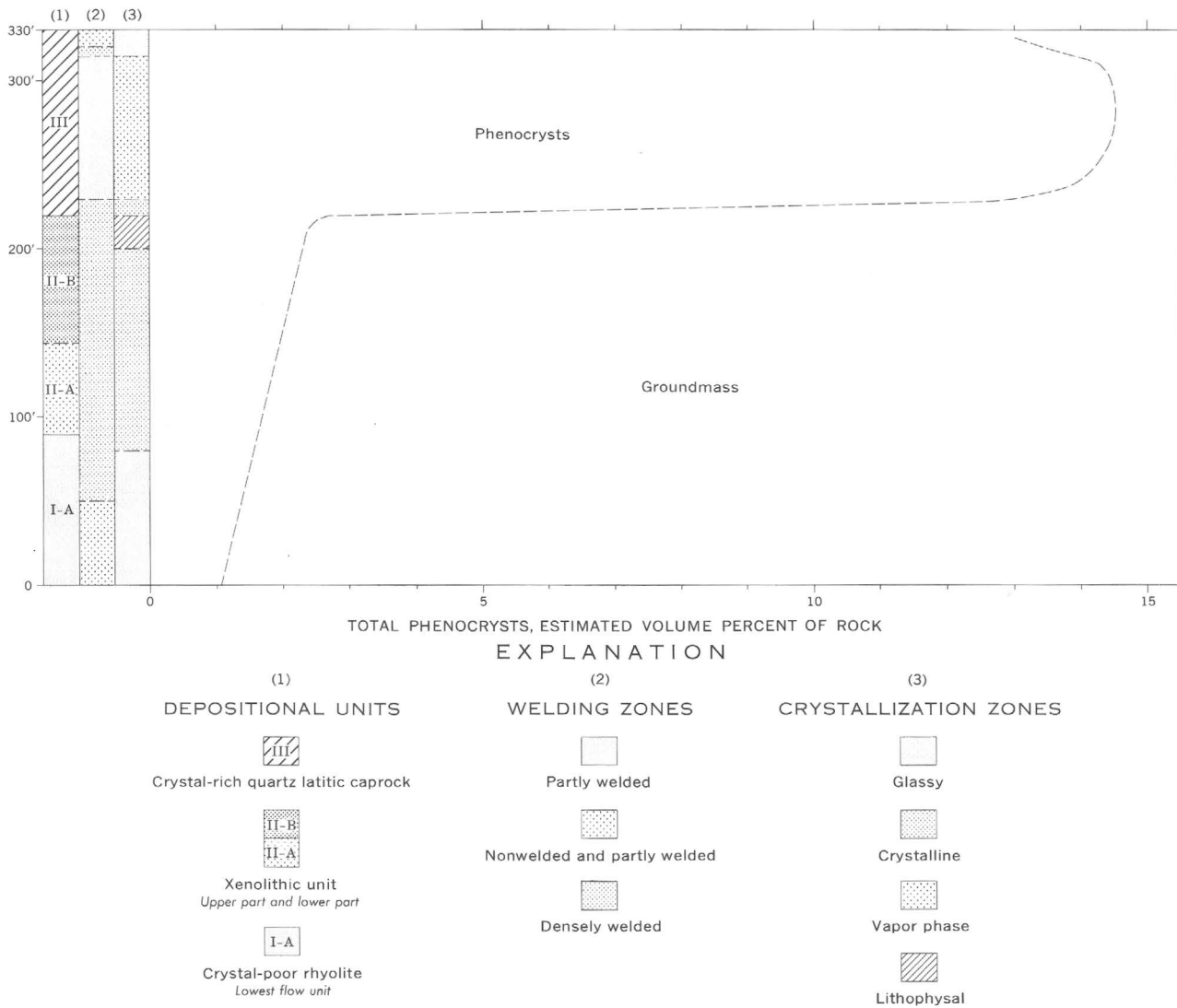


FIGURE 6.—Measured section of the Topopah Spring Member at 311 Wash, showing variations in depositional units, welding zones, crystallization zones, minor-element content (weight percent), and modal phenocryst content (volume percent). Section measured by F. A. McKeown and W. P. Williams, U.S. Geological Survey. Analytical data from table 2.



NOTE: Dashed lines in columns indicate gradational contacts

FIGURE 7.—Measured section of the Topopah Spring Member at Black Glass Canyon, showing variations in depositional units, welding zones, crystallization zones, and estimated total phenocryst content.

contact between the xenolithic unit and the overlying caprock changes laterally. In places, it is marked by a knife-edge depositional contact between crystal-rich quartz latite and xenolithic rock in a crystal-poor rhyolitic matrix (fig. 9). In other places the matrix in the upper 10–20 feet of the xenolithic unit is a mechanical intermixture of crystal-poor rhyolite and crystal-rich quartz latite.

Thus, at least three depositional subunits are sharply defined by abrupt changes in mineralogy, chemistry, and primary texture in the Black Glass Canyon section: the basal crystal-poor rhyolite, the xenolithic unit, and the crystal-rich quartz latitic caprock. Significantly, the xenolithic unit occurs at a horizon which in the Busted

Butte section is characterized by compositional gradation. The upper part of the crystal-poor rhyolite recognized at the Busted Butte section (flow units I–B and I–C) is absent in the Black Glass Canyon section.

PAH CANYON SECTION

The Pah Canyon section ² (fig. 10) is generally similar to the Black Glass Canyon section, except that the caprock is somewhat thinner and the rhyolitic lower part is considerably thicker. In thickness and character of depositional units, this section is intermediate between the Black Glass Canyon and Busted Butte sections.

² O'Connor (1963) gave the location of this measured section as "Spring Canyon," a preliminary topographic name for Pah Canyon.

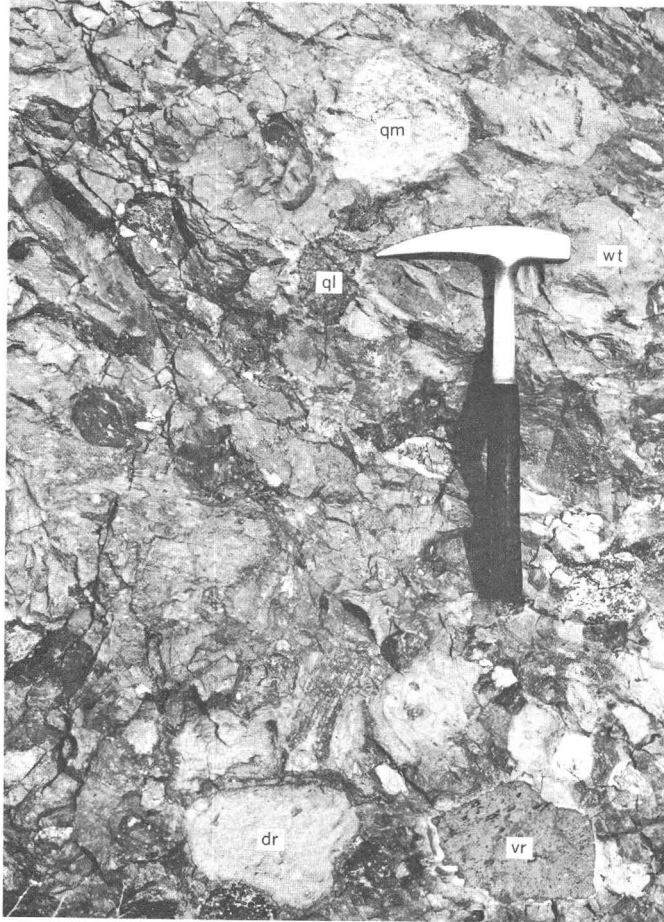


FIGURE 8.—Outcrop in Black Glass Canyon showing typical appearance of the xenolithic unit in the Topopah Spring Member. The xenoliths are subequant and slightly rounded, fairly uniform in size, and heterogeneous in rock type. Among the more conspicuous inclusions are quartz monzonite (qm), crystal-rich quartz latitic welded tuff (ql), crystal-poor rhyolitic welded tuff (wt), vesicular flow-banded rhyolitic lava (vr), and dense crystallized flow-banded rhyolitic lava (dr). The many other inclusions are difficult to discern from the matrix; total inclusion content is greater than 50 percent.

The modal data show vertical variations in phenocryst proportions and contents that are generally similar to those of the 311 Wash and Busted Butte sections. The decrease in phenocryst content at the top of the upper vitrophyre probably reflects settling and accumulation of a winnowed shard-rich ash from which most of the crystals had been separated. Field observations suggest that similar decreases in phenocryst content occur in the nonwelded to partly welded upper parts of several other sections, but the phenocryst variations in this interval cannot be determined precisely without special techniques because of the concurrent changes in welding.

YUCCA MOUNTAIN SECTION

The Yucca Mountain section (fig. 11), 3 miles west of the Black Glass Canyon section, contains the same three depositional units and is approximately as thick as that section; but the relative thicknesses of the depositional units differ. In particular, the crystal-poor rhyolite (I) is much thicker and the crystal-rich caprock (III) is thinner. Two flow units were recognized within the crystal-poor rhyolite tuff, and an additional lithophysal zone is present at the top of the lower flow unit (I-A). This lower unit probably corresponds to the entire thickness of rhyolitic tuff at Black Glass Canyon, and the parting between the two rhyolitic flow units in the Yucca Mountain section probably correlates with the break between the lower two flow units recognized at Busted Butte (I-A and I-B).

Although this section is relatively thin, its zonal assemblage of depositional, welding, and crystallization variations is as complex as can be found in any other exposure of the Topopah Spring Member.

LATHROP WELLS SECTION

In the Lathrop Wells section, which is near the south edge of the Topopah Spring ash-flow sheet, the cooling unit is about 200 feet thick and is glassy throughout (fig. 12). Although this section is rather thin, it shows an



FIGURE 9.—Contact between xenolithic and caprock flow units in Black Glass Canyon. Caprock is more resistant to erosion than closely fractured xenolithic unit and overhangs slightly. Contact is sharp in this area and planar on large scale. Matrix of xenolithic unit remains crystal poor to contact. Note two large blocks of quartz monzonite just below contact in lower right of the photograph. The larger block, which is approximately 4 feet in diameter, is the largest that has been observed in the xenolithic unit.

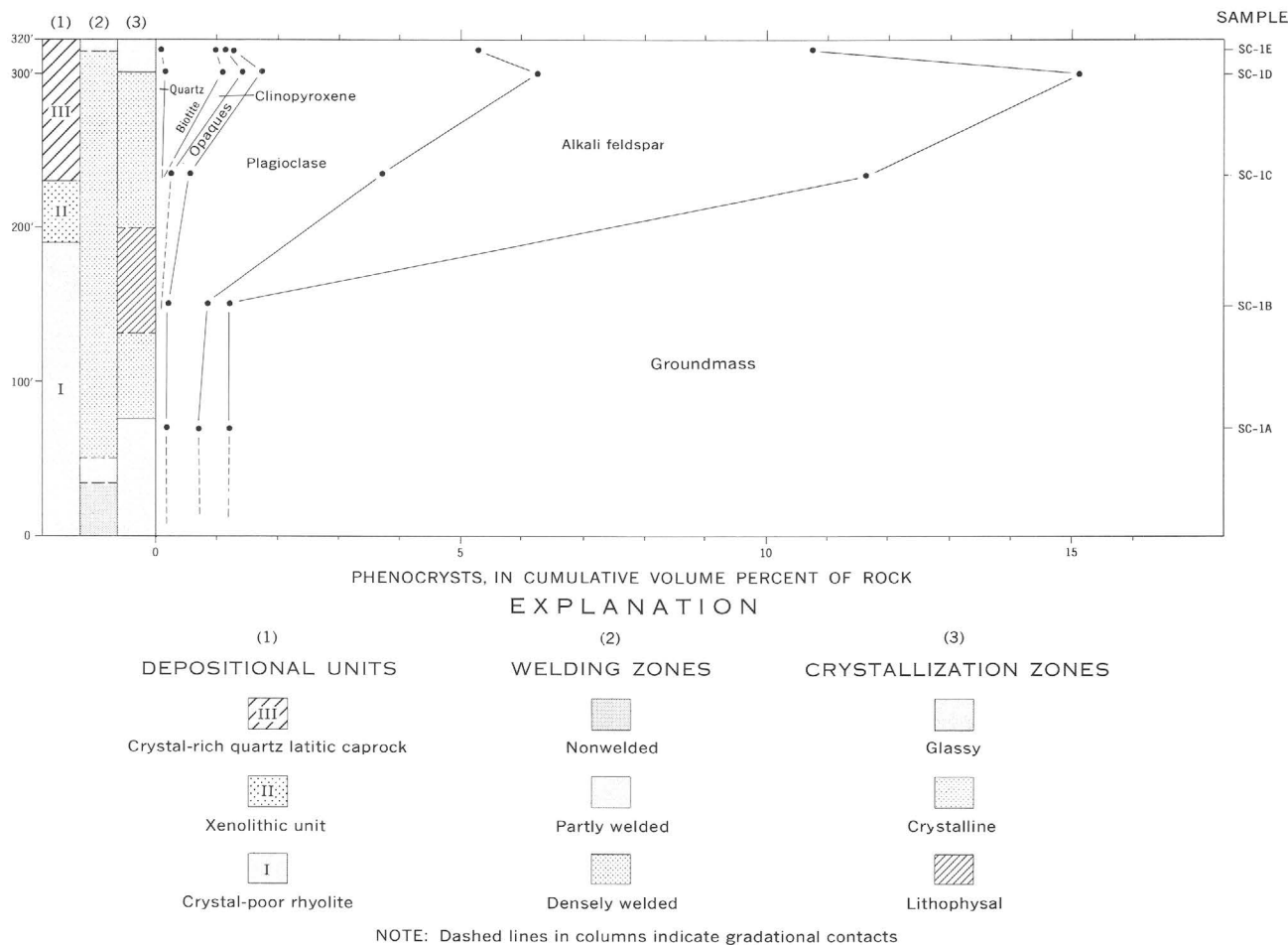


FIGURE 10.—Measured section of the Topopah Spring Member in Pah Canyon, showing variations in depositional units, welding zones, crystallization zones, and modal phenocryst content.

upward increase in phenocryst content similar to that of the thicker sections farther north. The upper part of the section contains a maximum of about 14 percent phenocrysts, however, and is less mafic than the typical caprock farther north.

An unusual feature of the Lathrop Wells section is the variable distribution and composition of the pumice. The base of the cooling unit averages about 40 percent of rhyolitic pumice blocks as much as 12 inches long (fig. 13), but this concentration of large pumice ends abruptly about 10 feet above the base and is overlain sharply by tuff that contains pumice dominantly of lapilli size. This basal pumice zone may be correlative with the pumiceous lower part of the cooling unit at Busted Butte, but the pumice fragments are larger and more concentrated in the Lathrop Wells area, perhaps as a result of more effective rafting toward the edges of the ash-flow sheet (Ross and Smith, 1961, p. 21-22).

The pumice lapilli higher in the Lathrop Wells section are mostly crystal-poor rhyolite whose refractive index is similar to that of the shard matrix (about 1.49), but there are scattered lapilli of crystal-rich pumice (refractive index about 1.50) that appear to be similar to the caprock lithology. The crystal-rich pumice is most evident in the transition zone from partly welded to densely welded tuff; here the crystal-rich collapsed pumice is jet black, whereas both rhyolitic collapsed pumice and the shard matrix are light brown. In the lower part of the ash-flow sheet the crystal-rich pumice is sparse (about 1 percent), but about 80 feet from the base of the section this pumice increases abruptly in size and abundance and forms a swarm about 10 feet thick (fig. 14) that is very conspicuous because the black collapsed pumice contrasts with the light-brown matrix below and above. The pumice (table 2, col. 6) is chemically and mineralogically indistinguishable from fairly

mafic caprock (table 2, col. 5), whereas the matrix in the swarm (table 2, col. 8) is identical with typical crystal-poor rhyolite of the lower part of the cooling unit (table 2, col. 9-14). Because glassy tuffs commonly show the effects of appreciable leaching during secondary hydration (Lipman, 1965), the analyzed samples of collapsed pumice and matrix were collected from a thicker section containing crystallized rock about 1 mile farther north. In the interior of the swarm the collapsed pumice constitutes about 75 percent of the rock. Individual eutaxitic blocks average 10 inches in length, and blocks 30 inches long are fairly common. Lower and upper boundaries of the swarm are gradational over intervals of 2-3 feet.

For about 15 feet above the top of the swarm, the collapsed pumice is of lapilli size and the phenocryst content of the matrix remains low, although not as low as below the swarm. Higher in the section the size of the pumice again increases, as at the base of the swarm.

This second increase in pumice size is accompanied by a gradual increase in the phenocryst content of the shard matrix, and within a few feet the matrix is as crystal rich and as black as the pumice. The resulting dense and uniformly black vitrophyre in the upper part of the cooling unit is almost as mafic as the caprock at Busted Butte. Within the vitrophyre the boundaries between pumice and groundmass are obscure, but in contrast with the underlying swarm the average length of the eutaxitic pumice is less (about 4-6 in.). Incompletely compacted pumice in partly welded tuff above the vitrophyre averages only 2-3 inches in length.

A final change in the pumice distribution occurs in the nonwelded zone at the top of the cooling unit. The uppermost 10 feet of the section contains abundant blocky pumice and sharply overlies the small-pumice tuff just described. This upper pumiceous zone closely resembles the basal zone of large blocky pumice, and

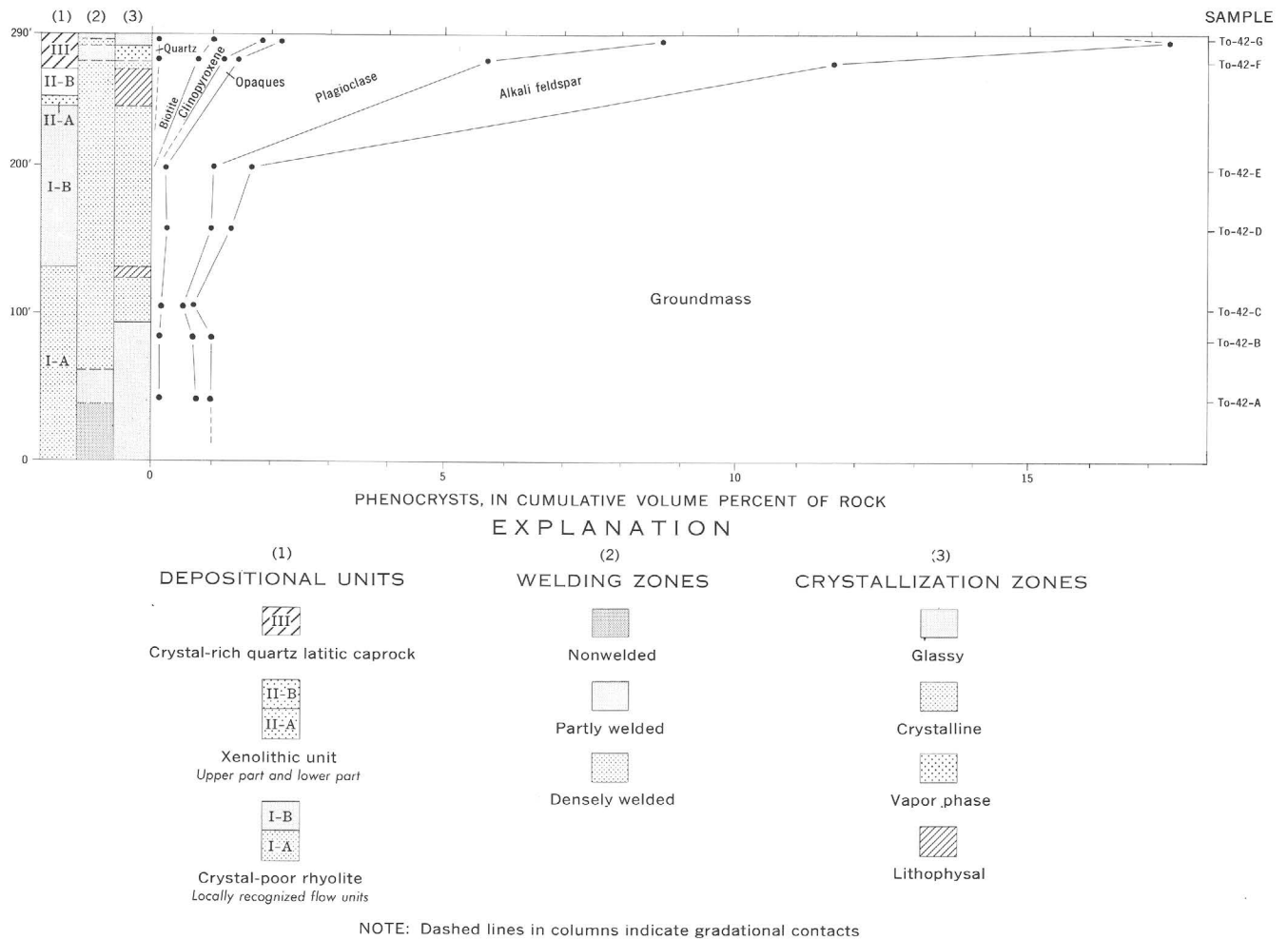


FIGURE 11.—Measured section of the Topopah Spring Member at the northeast end of Yucca Mountain, showing variations in depositional units, welding zones, crystallization zones, and modal phenocryst content.

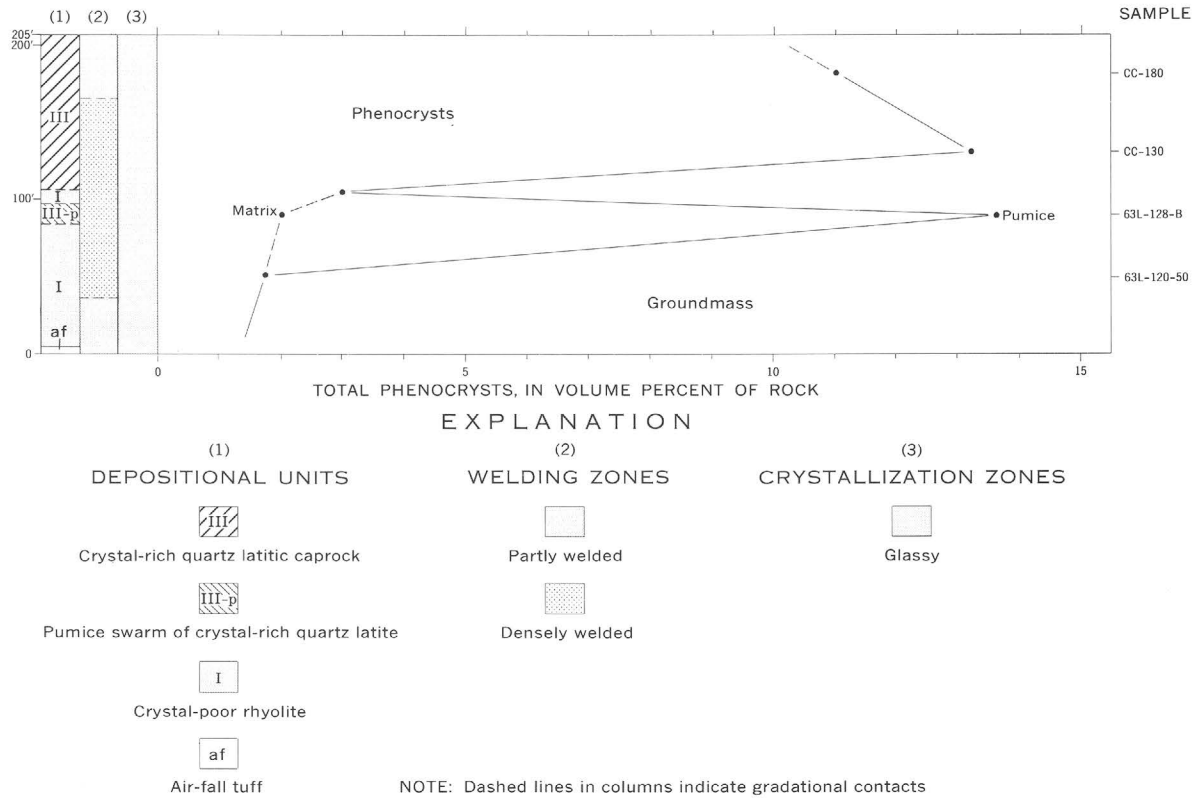


FIGURE 12.—Measured section of the Topopah Spring Member near Lathrop Wells, showing variations in depositional units, welding zones, crystallization zones, and modal phenocryst content.

both probably represent an envelope of rafted pumice around the edge of the ash-flow sheet.

PROSPECTORS PASS SECTION

The section at Prospectors Pass (fig. 15), 7 miles west of the Yucca Mountain section, is an example of a thick cooling unit (460 ft) near both the depositional edge of the ash-flow sheet and the probable source area near Oasis Valley.

Except for the absence of large pumice blocks, the base of this section resembles other thick sections of the Topopah Spring Member. The upper part, however, which is stratigraphically equivalent to the caprock lithology elsewhere, is distinctively bedded and shows many alternations in degree of welding, crystallization, and phenocryst content (fig. 16). The base shows the normal gradational sequence from nonwelded glassy tuff to densely welded black vitrophyre and then to crystallized grayish-red welded tuff, all uniform rhyolite having low pumice and phenocryst contents. However, at 235 feet the crystallized tuff passes upward into a second black vitrophyre which, unlike the upper vitrophyres of the other described sections, remains low in phenocrysts (1.5 percent) and collapsed pumice (<5

percent). This vitrophyre is about 50 feet thick and is overlain by medium-light-gray partly to densely welded vapor-phase crystallized tuff that shows distinct bedding defined by vertical variations in amounts of phenocrysts and pumice (fig. 16B). The contact between the bedded gray tuff and underlying vitrophyre is gradational over 4 or 5 inches.

The gray tuff is the lower part of a welded bedded sequence that constitutes the upper 160 feet of the cooling unit. Individual beds range in thickness from less than an inch to several feet (fig. 16B). There are several hundred lithologically homogeneous beds. The phenocryst content of the bedded tuff ranges from 2 to 30 percent or more, and the pumice content, from 5 to 25 percent. In addition to the variations in quantities of phenocrysts and pumice, some stratification is defined by size variations (fig. 16C). In any individual bed, phenocrysts and pumice are moderately well sorted, but from bed to bed the average diameter of phenocrysts ranges from about 0.1 to 1.0 mm, and the average length of eutaxitic pumice, from 5 to 50 mm. In general, large phenocrysts occur in the same beds in which large pumice occurs. Some beds also show concentrations of small angular light lithic inclusions that average about 0.5 cm in diameter.

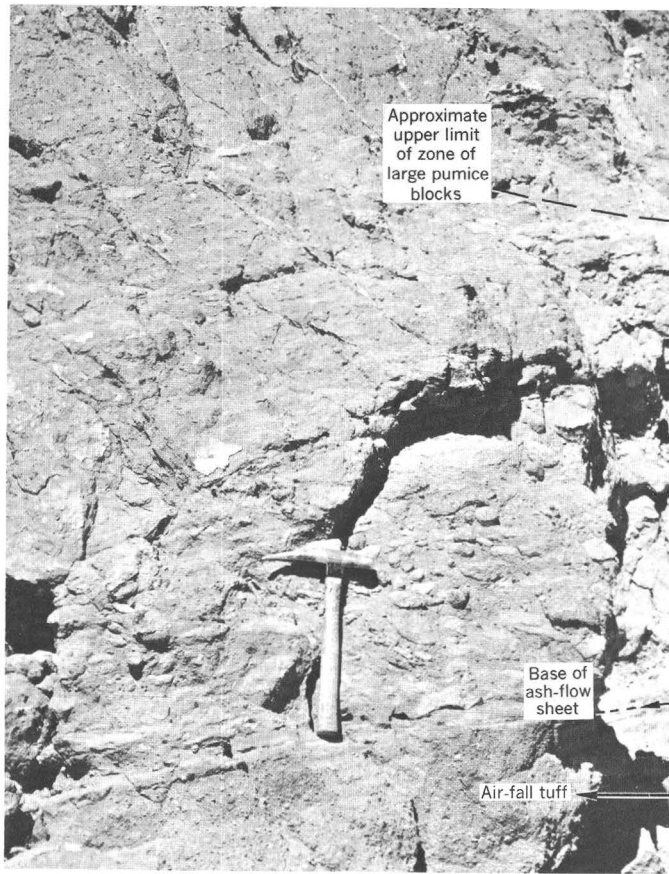


FIGURE 13.—Base of ash-flow sheet of Topopah Spring Member at Lathrop Wells, showing underlying air-fall tuff, basal concentration of large blocky pumice, and upward gradation into welded bluff-forming tuff.

Within the bedded interval are four main zones of densely welded ledge-forming reddish-brown and black vitrophyre (fig. 16A). Between the vitrophyres are slightly to moderately welded tuffs; some are still glassy, but others have undergone vapor-phase crystallization. Bedding is as distinct in the densely welded vitrophyre zones as in the intervening less welded tuffs. The sequence of welding and crystallization zones is shown fairly precisely in figure 15, but the variations in phenocryst content from bed to bed are indicated only diagrammatically because precise determination of the mineralogical fluctuations in the hundreds of beds would require many modal counts spaced at several-foot intervals up the section.

The high phenocryst and pumice contents of most bedded rocks in the section suggest that this interval is correlative with the crystal-rich caprock lithology in other sections of the Topopah Spring Member. The unusual features of this interval are probably related to the location of the section, which is near both the depositional edge of the ash-flow sheet and the source area. In

such a position voluminous partly sorted ash-fall material that had cooled only slightly might have interfingered with thin pulsating lobes of ash-flow material without having been swept entirely away, and the resulting deposit would possess characteristics of both ash-fall and ash-flow origin. Partly welded air-fall deposits that resemble the Prospectors Pass rocks are known at several young volcanic centers in Japan, including Towada caldera, Mashu caldera, and a small vent in southern Kyushu (Aramaki, 1964).

FLUORSPAR CANYON SECTION

The measured section nearest the probable source in the Oasis Valley area is the Fluorspar Canyon section (fig. 17), whose striking feature is its great thickness of uniformly crystal-poor tuff. No increase in crystal content could be detected in the field up to about 30 feet from the top of the zone of dense welding, and even at this level the increase is small in comparison with other sections. A maximum of 10 percent phenocrysts is reached in the upper part of a 5–10-foot vitrophyre zone, above which the phenocryst content decreases in partly welded tuff. Clinopyroxene is absent in this interval, and the caprock lithology is only incipiently formed. The upper part of this section correlates more closely with the gradational transition to crystal-rich caprock than with the typical caprock lithology of sections to the east. As in the Prospectors Pass section, there is no concentration of large blocky pumice at the base; as in the Busted Butte and Yucca Mountain sections, there are several lithophysal zones.

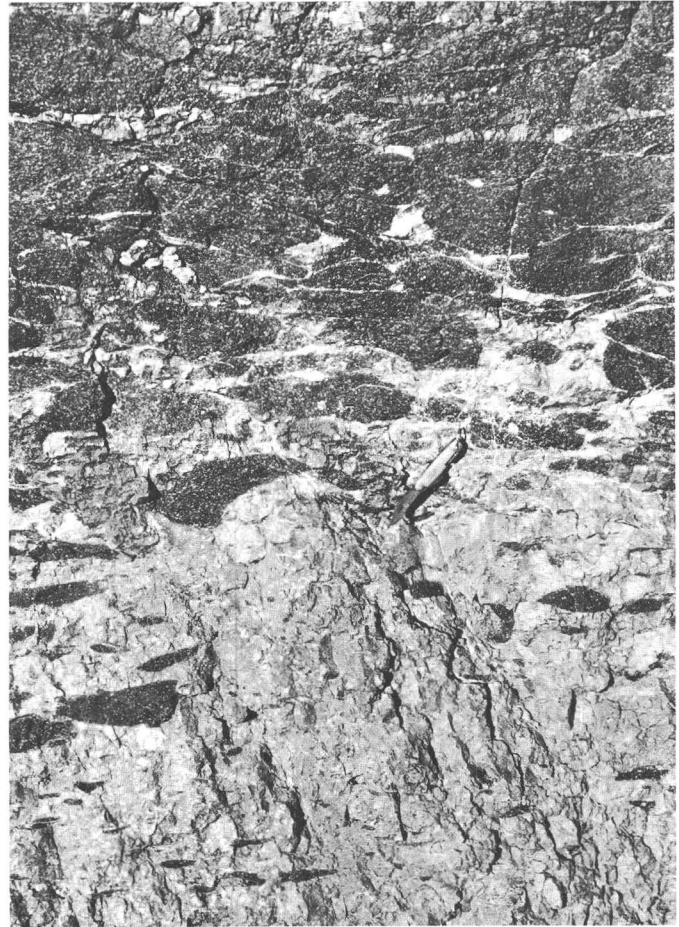
LATERAL COMPOSITIONAL VARIATIONS

The differences among the measured sections just described reflect lateral compositional variations resulting from the presence of many ash flows within a single cooling unit. The distribution of the various subunits is independent of total thickness of the cooling unit. Depositional subunits that have sharp contacts in some sections may have gradational contacts in nearby sections and may be absent in others. The most significant compositional subunits, each representing one or more flow units, are (1) the crystal-poor pumice-poor rhyolite, (2) the crystal-rich quartz latitic caprock, (3) the basal zone of large pumice blocks, (4) the unit that contains abundant xenoliths, (5) the swarm of crystal-rich quartz latitic pumice blocks, and (6) the bedded equivalent of the caprock. The differences between these subunits probably reflect interactions of two processes: (1) progressive change in the chemical and mineralogical composition of the erupted magma, and (2) sorting, mixing, and other mechanical modifications related to interruptions and pulsations during the processes of eruption

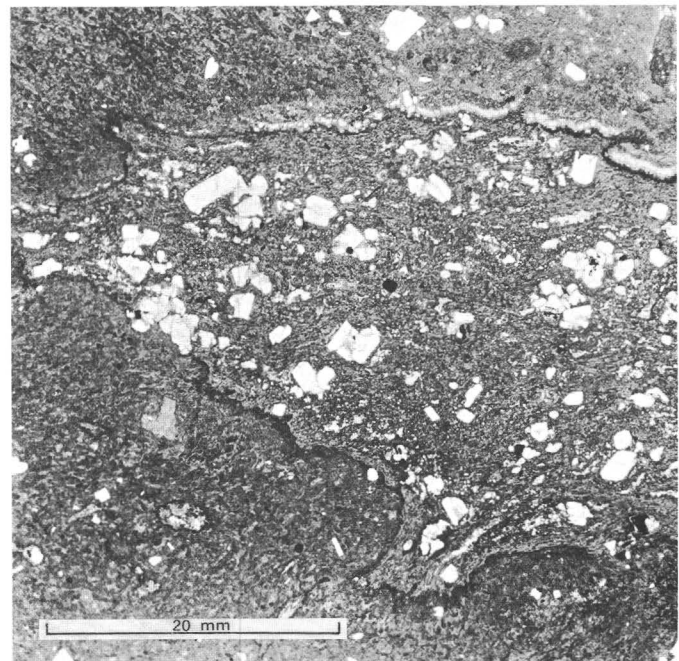


A

FIGURE 14.—Swarm of quartz latitic pumice in rhyolitic shard matrix. Lathrop Wells section. *A*, Upper part of dark pumice swarm, overlying light-colored rhyolitic tuff and dark capping quartz latite. Size and abundance of collapsed pumice decrease abruptly upward at the top of the swarm. Scale is given by white sample sack, which is about 1 foot high, and by penknife. *B*, Detail of basal contact of pumice swarm, about 15 feet below the upper contact of the swarm shown in *A*. The interior of the swarm consists almost entirely of compacted crystal-rich pumice blocks separated by thin films of light crystal-poor rhyolitic tuff. *C*, Crystal-rich collapsed pumice block surrounded by welded shard matrix of lower crystal content.



B



C

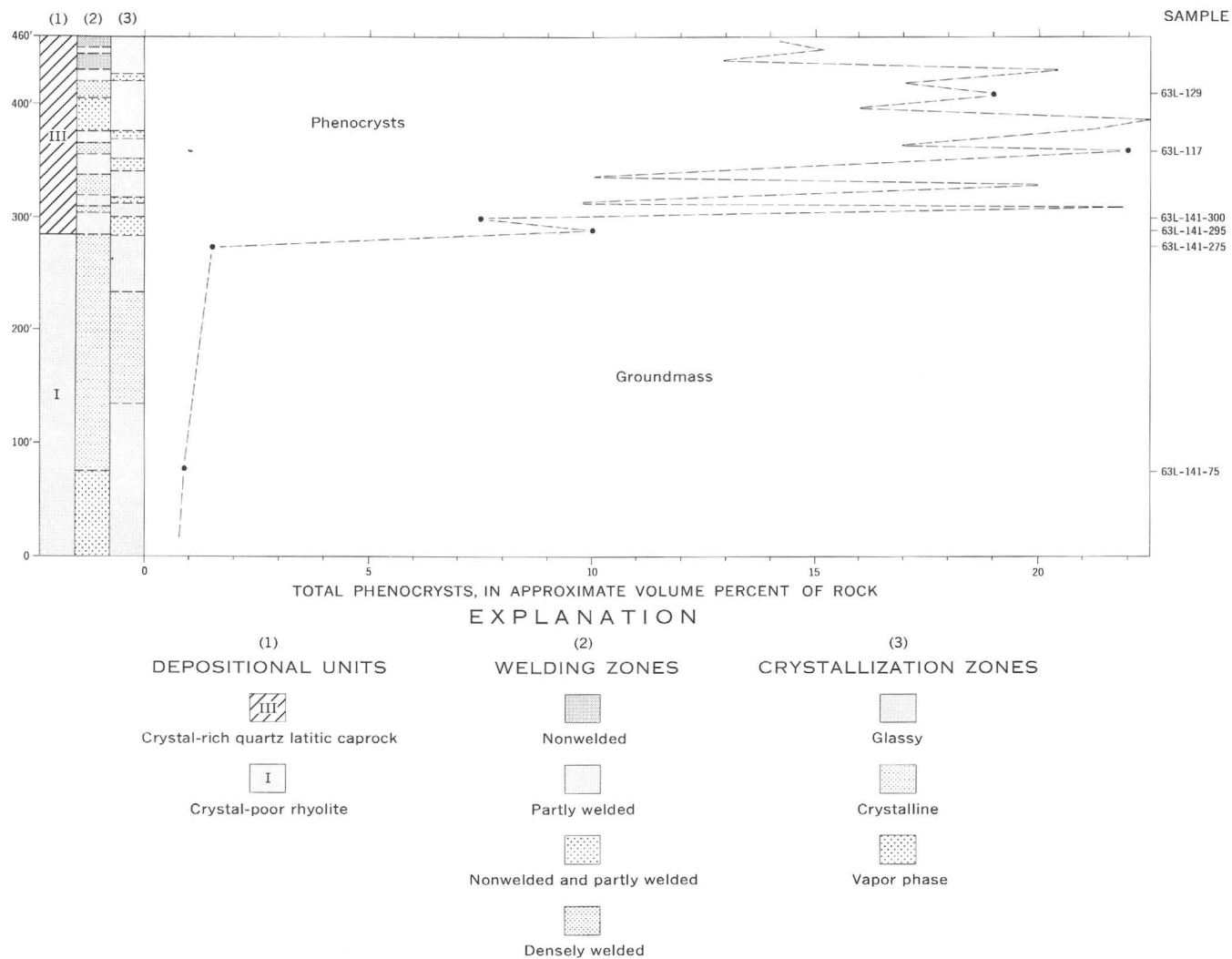
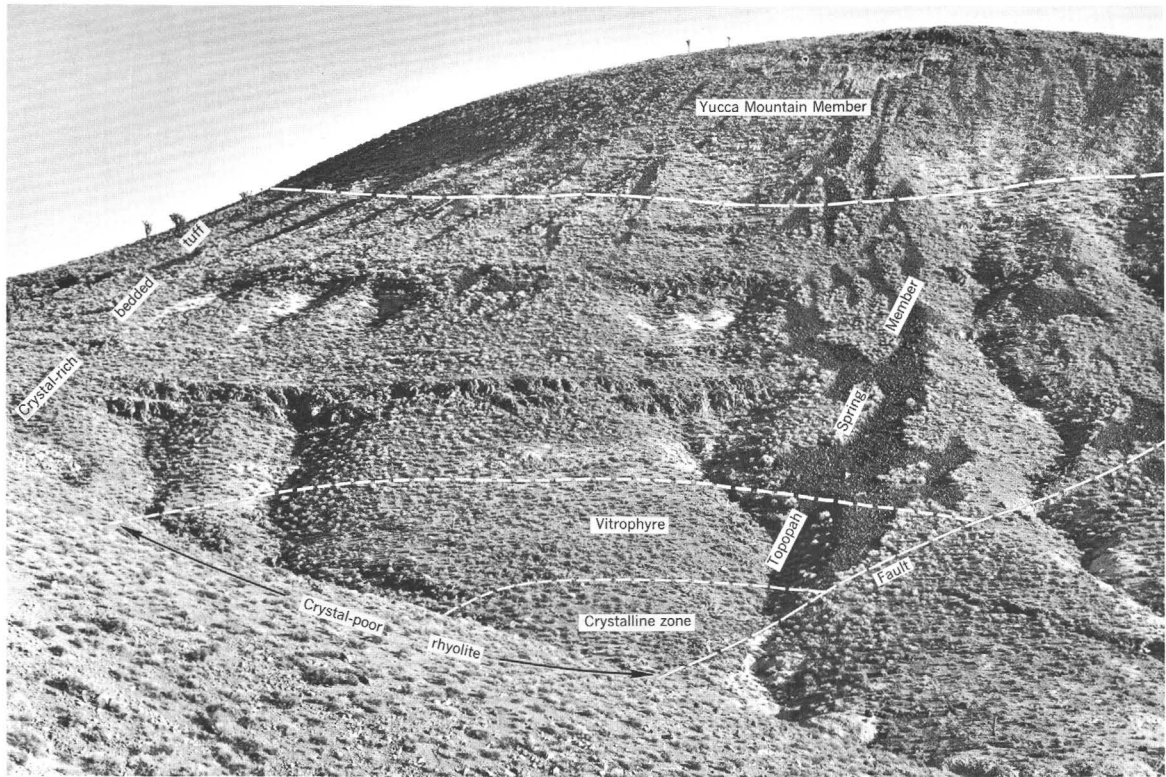


FIGURE 15.—Measured section of the Topopah Spring Member at Prospectors Pass, showing variations in depositional units, welding zones, crystallization zones, and total phenocryst content.

and emplacement. Interpretations of the changes in magma composition are deferred to the section on petrology. The present section reviews salient features and describes the lateral extent of the various subunits, and presents interpretations of the origin of those units that apparently formed primarily through mechanical processes operative during emplacement of the ash-flow sheet. Reconstruction of the distribution of the subunits is based on 23 measured sections, including the 8 just described, and on numerous observations made during detailed mapping.

The crystal-poor pumice-poor rhyolitic tuff represents the normal lithology of the lower part of the cooling unit. It is present in almost every mapped area of the Topopah Spring Member, but its thickness variations are great. This is illustrated by a series of exposures from Lathrop Wells to Black Glass and Paintbrush

Canyons (pl. 1) that provides a cross section through the ash-flow sheet. At Black Glass Canyon the rhyolitic tuff is only 90 feet thick; at Busted Butte, 7 miles to the south, it is nearly 600 feet thick (pl. 1). At the north end of Paintbrush Canyon, where the ash-flow sheet laps onto older lava flows, the rhyolitic tuff is absent and the entire thickness of the section, about 40 feet, is crystal-rich caprock (pl. 1). The maximum known thickness of the crystal-poor rhyolite, in the 311 Wash section (fig. 6), is approximately 800 feet. Because this rock type forms the bulk of most sections, especially the thick ones, the isopach map for the entire member (fig. 1) also provides a qualitative approximation of lateral thickness variation in the rhyolite unit. As many as three flow units have been recognized within this unit, but many more have probably gone unrecognized because of poor exposures, low initial pumice content, and dense



A

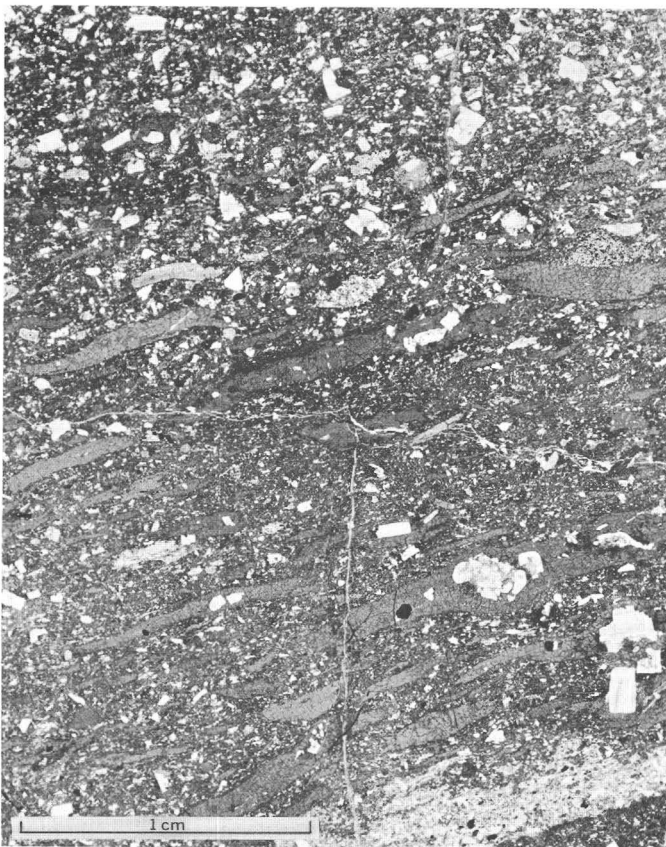


B

FIGURE 16 A, B. See next page for explanation and parts C and D.



C



D

FIGURE 16.—Bedded welded tuff in upper part of ash-flow sheet of Topopah Spring Member. Prospectors Pass section. *A* (preceding page), General view. Layered appearance of upper part of ash-flow sheet as seen in this photograph results mainly from alternation of welding zones (fig. 15); bedding not visible at this distance. Approximately the upper two-thirds of the ash-flow sheet is visible; the basal part is concealed as a result of faulting. *B* (preceding page), Closer view of a densely welded zone showing stratification due to variations in size and abundance of pumice lapilli and phenocrysts. Partings in lower right half of photograph are in densely welded crystallized tuff and follow concentrations of eutaxitic pumice lapilli which have been preferentially weathered out. Darker layer behind hammer is vitrophyre in which phenocryst and pumice contents are similar to those of underlying crystallized tuff. Thin light-colored layers above hammer head are beds in which phenocryst and pumice contents are lower than average. *C*, Bedded vitrophyre showing gradational variations in the crystal and pumice content. The dark zone (1) at the top has relatively large pumice and an intermediate crystal content. The lighter colored underlying layer 2 has more phenocrysts and more abundant smaller pumice. Zone 3 contains only sparse small phenocrysts and pumice. Layer 4 has much more abundant phenocrysts and slightly more pumice. In the lowest layer (5) the phenocryst content is about the same, but the pumice is both larger and more abundant. *D*, Bedded vitrophyre, showing variations in size and abundance of phenocrysts and pumice. At top, phenocrysts are abundant and pumice is scarce. In the middle, pumice is abundant and large; phenocrysts are large but scarce. The thin light-colored layer at lower right consists of shards and fairly abundant small phenocrysts; pumice and large phenocrysts are absent. The basal contact is sharp. In the underlying rock small pumice and moderately large phenocrysts are both abundant. Plane-polarized light.

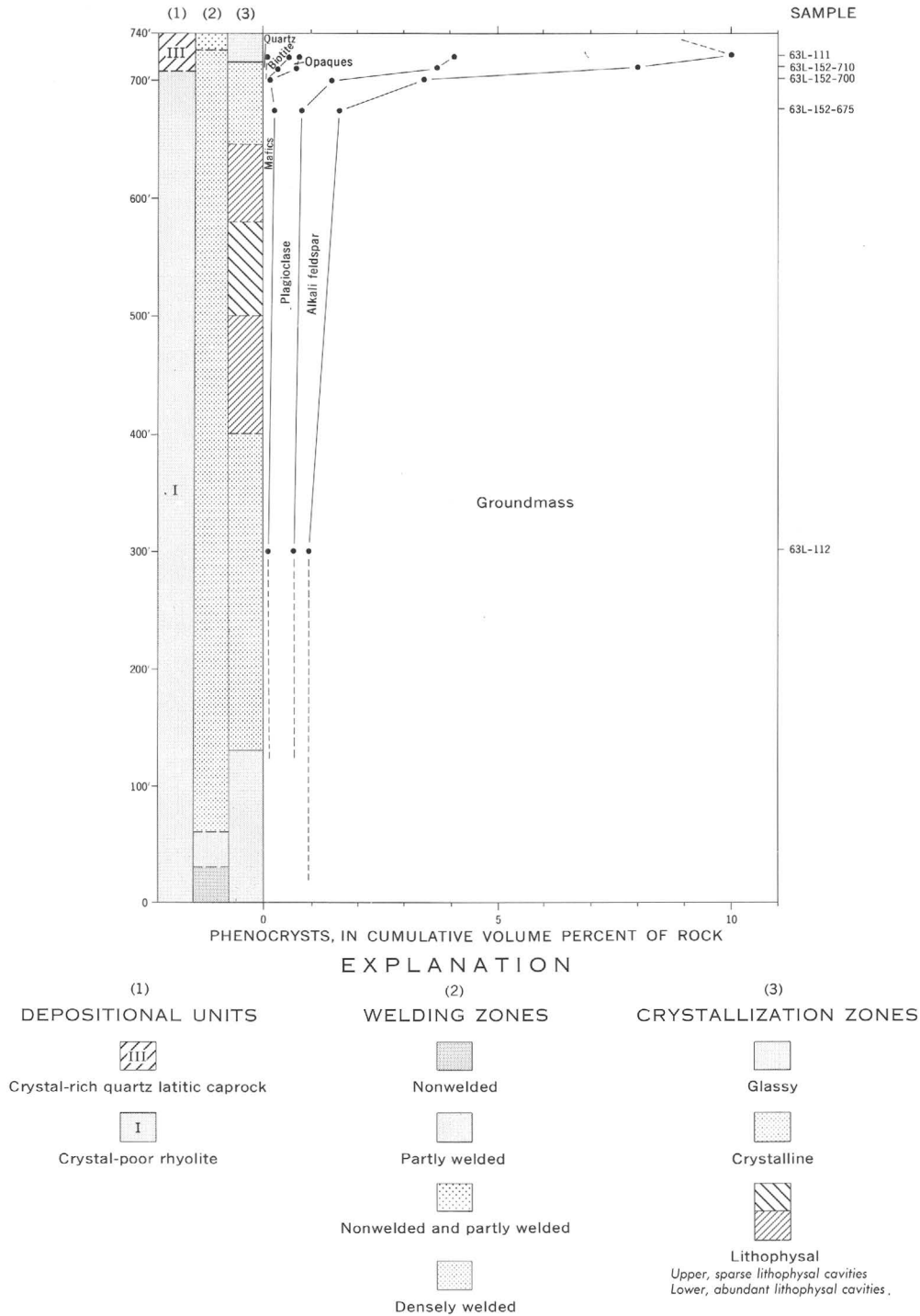


FIGURE 17.—Measured section of the Topopah Spring Member in Fluorspar Canyon, showing variations in depositional units, welding zones, crystallization zones, and modal phenocryst content.

welding. As a result, the distribution of most individual flow units is known only over small areas. Some probable correlations between flow units are shown on plate 1. The recognition of more than one flow unit within a major lithologic subunit of the Topopah Spring Member is essential to interpretation of the compositional variations. These variations are most readily explained in terms of successive emplacement of numerous small flow units, most of which are lithologically similar, even though many have not been recognized because of crystallization and dense welding.

The crystal-rich quartz latite is the normal rock type of the upper part of the cooling unit and, just as the rhyolitic lower part, is present over nearly the entire area of the ash-flow sheet. Its thickness, however, is even more variable and is virtually independent of the thickness of the cooling unit. The compositional gradation at the base of this unit presents a potential ambiguity in determination of thickness. Because the topographic change from slope-forming rhyolite to cliff-forming caprock is generally more abrupt than the compositional gradation and commonly occurs at a phenocryst content of about 10 percent, this number is used as a compositional minimum for the base of the caprock lithology. By this criterion the thickness of the caprock ranges from 10 to 200 feet. Caprock thicknesses of 20–40 feet are common over large areas, especially in the eastern part of the sheet, but thicker sections occur only in small areas. Caprock more than 50 feet thick (fig. 18B) occurs along the northern and southern margins of the ash-flow sheet, midway between the probable source area and the farthest traveled edge of the sheet. The northern area is roughly coincident with the area of the xenolithic unit, the southern area with that of the swarm of crystal-rich pumice. Although no definite depositional breaks were recognized within the caprock, emplacement of this unit in several separate ash flows is probably indicated by the compositional zonation at the base and within the unit. In this respect the differences in chemical composition and phenocryst content between the middle and upper parts of the caprock at Busted Butte are particularly significant (table 2, col. 1, 5; also see variation diagrams, fig. 4). It seems improbable that such a zonation would originate or be preserved during emplacement of a single enormous ash flow. Together with the ubiquitous upward gradation from rhyolite to quartz latite, this relation suggests formation of the ash-flow sheet by eruption of successive ash flows whose compositions changed progressively from rhyolite to quartz latite.

The distribution of the basal zone of large pumice blocks is best known along the geologic section on plate 1, although it is not shown there. Along this section

the basal pumice zone thickens and the blocks coarsen from the interior toward the south edge of the ash-flow sheet, and the zone is absent from the westernmost and northernmost parts of the sheet. The pumice in this basal concentration is crystal poor, very much like the bulk rock composition of the rhyolitic lower part of the cooling unit. The western edge of the zone, which must be in the vicinity of Crater Flat and the western side of Yucca Mountain, cannot be located precisely because of inadequate exposures of the basal part of the Topopah Spring. Concentrations of pumice blocks at the base, and locally at the top, of the ash-flow sheet have been noted in the Skull Mountain area, at French Peak, and at Nye Canyon; all these localities are near the edge of the sheet. As noted previously, the blocky pumice probably was concentrated by rafting toward the top and front of advancing ash flows. The basal zone formed where the frontal concentration was overridden by the interior of a flow. The less common (less widely preserved?) upper pumice zone represents rafted pumice that was not overridden but was swept toward the distal downslope edges of the sheet. The variation from sharp to gradational contacts indicates local turbulent intermixing during formation of the pumice concentrations. The absence of the basal zone in the northwestern part of the ash-flow sheet suggests that the velocity of flow was too great in this area for the frontal accumulation of pumice to form or be deposited, which would be in accord with the inference of a source area to the northwest.

The unit that contains abundant xenoliths occurs only in a small area along the north edge of the ash-flow sheet (fig. 18A). The thickness of this unit is commonly less than 50 feet; its known maximum is 135 feet. Throughout its extent the unit occurs stratigraphically between the crystal-poor rhyolite and the crystal-rich quartz latite. The matrix between the inclusions generally resembles the crystal-poor rhyolitic tuff although in some sections the matrix near the top of the xenolithic unit contains patchy zones of both crystal-poor rhyolite and crystal-rich quartz latite. Such patchy zones probably represent turbulent intermixing between the xenolithic unit and an overriding ash flow of the caprock composition. The source of the xenoliths probably lay to the west, where the distinctive crystal-poor tuff that constitutes the dominant inclusion type occurs widely. The xenoliths may represent surface detritus that was picked up and incorporated in the turbulent ash flow, but unambiguous examples of this process, such as that already described at the base of the Black Glass Canyon section, show much less extreme concentrations of inclusions even very close to the source of the rubble. A more probable interpreta-

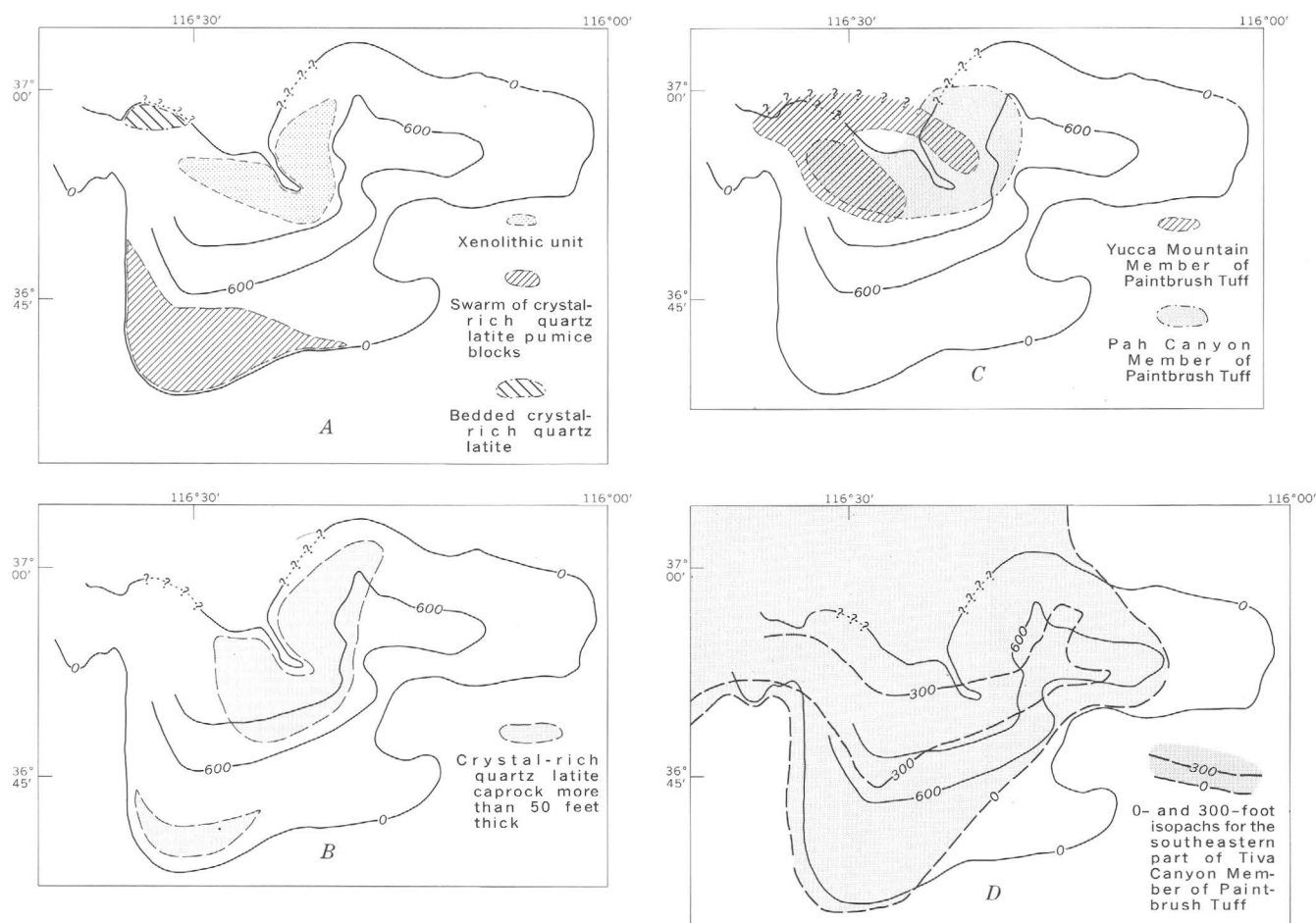


FIGURE 18.—Distribution of depositional subunits of the Topopah Spring Member and of the other major ash-flow members of the Paintbrush Tuff. The 0- and 600-foot isopachs shown in figure 1 give location.

tion is that the xenoliths were derived from a block of wallrock that shattered and collapsed into the magma chamber or the vent during eruption. Such subsurface source would explain the presence of the granitic inclusions, for granite is nowhere exposed on the pre-eruption surface. The nonuniform distribution of the inclusions, blocks of crystal-poor tuff concentrated in the lower part and flow-laminated rhyolite in the upper part of the unit, might suggest that the unit consists of two separate ash flows erupted in rapid succession. On the other hand, this dual distribution may represent successively collapsed parts of the magma chamber or vent walls during a single eruption. Whichever interpretation is correct, the lithic-rich unit represents a significant eruptive episode for which evidence is entirely lacking over much of the area of the ash-flow sheet.

The swarm of crystal-rich pumice occurs only in a small area near Lathrop Wells (fig. 18A), and the top of the swarm is everywhere 10–15 feet below the base of the caprock. The swarm has a maximum observed thickness of about 15 feet, so its volume is small. To-

gether with the small volume, the relatively abrupt lower and upper contacts (fig. 14A, B) indicate that the swarm was emplaced as a single ash flow. The pumice in the swarm is chemically and mineralogically indistinguishable from the local caprock, whereas the matrix is identical with the typical crystal-poor rhyolite of the lower part of the cooling unit. These features demonstrate the hybrid character of this zone and suggest at least two hypotheses for its origin. First, the swarm may have originated before emplacement: some of the underlying quartz latitic magma could have risen into the lower part of the rhyolitic magma column during eruption, and this batch of mixed magma would then have been emplaced as a single ash flow. The rhyolitic fraction would have vesiculated extensively and burst into shards, whereas the quartz latitic fraction, perhaps because of lower volatile content, would have vesiculated less intensely and remained as pumice. Alternatively, rhyolitic shards and quartz latitic pumice might have been erupted simultaneously from separate vents

within the caldera, and pumice and shards might have been mixed during surficial flowage.

The bedded equivalent of the caprock is exposed only over a small area at the northwest edge of Crater Flat (fig. 18A). At the Prospectors Pass measured section this interval is 180 feet thick; it is nearly as thick in the adjacent area, but complex structure has obscured the pattern of lateral variation. The nature of the transition from the bedded interval to the massive caprock farther east is obscure because of limited exposures. Available exposures suggest that neither bedded nor massive caprock accumulated to appreciable thickness in the area between Prospectors Pass and the main part of Yucca Mountain, along the central flowage path of the ash-flow sheet. Probably, after deposition of the rhyolitic tuffs smoothed the initially irregular topography, the later more mafic pulses tended to bypass the Crater Flat area and deposit the bulk of their loads farther from the source. The bedded interval, which apparently is stratified because of nearness to the source area, could probably accumulate only along the edge of the ash-flow sheet. Any similar material deposited along the main flowage path across Crater Flat presumably was scoured out or incorporated by later ash-flow pulses. The variations in sorting, welding, and crystallization in the bedded interval provide significant additional evidence for interruptions or pulsations during eruption of the crystal-rich part of the ash-flow sheet.

In summary, comparison of the distribution patterns of the various lithologic subunits provides additional insight into the manner of emplacement of the ash-flow sheet. The voluminous early rhyolitic pulses flowed much farther than most of the subsequent flow units and accumulated to maximum thickness along the east-west axis of the sheet. In contrast, all later flow units mainly accumulated at intermediate distances along the flow axis, and they thin both toward the east edge of the sheet and toward the inferred source area in Oasis Valley. Despite the great accumulation of the early rhyolitic tuff in the Fluorspar Canyon area, only minor deposition appears to have occurred in this area after the initial topography was smoothed.

The late flow units largely bypassed the area and were deposited farther east. These late flow units are thickest along the flanks of the ash-flow sheet rather than along the axis of maximum accumulation of the early rhyolitic tuff (pl. 1). In this respect the separate flow units are shingled and asymmetrically distributed like successive mudflows on an alluvial fan.

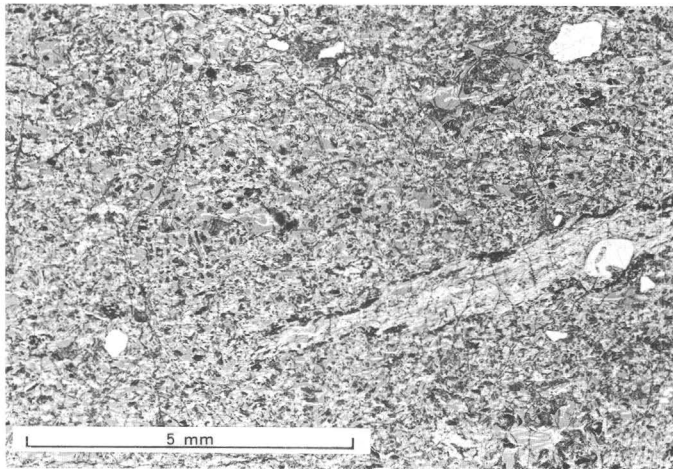
The distribution of the four main ash-flow sheets of the Paintbrush Tuff is similarly asymmetrical, although the general east-west zone of maximum accumulation of

the basal sheet, the Topopah Spring Member, is followed by the subsequent ash-flow sheets. The zones of maximum accumulation of the second and third major sheets, the Pah Canyon and Yucca Mountain Members, are displaced to the north, approximately coincident with the areas of maximum thickness of the xenolithic and caprock flow units of the Topopah Spring Member (fig. 18C). Eruption of the Pah Canyon and Yucca Mountain Members further smoothed the topography, for the last ash-flow sheet of the Paintbrush Tuff, the Tiva Canyon Member, covers a much larger area and is more uniform in thickness. Although this unit is closely related in petrology and in time of eruption to the underlying Yucca Mountain Member, its zone of maximum accumulation is farther south, only slightly north of the axis of the Topopah Spring Member (fig. 18D).

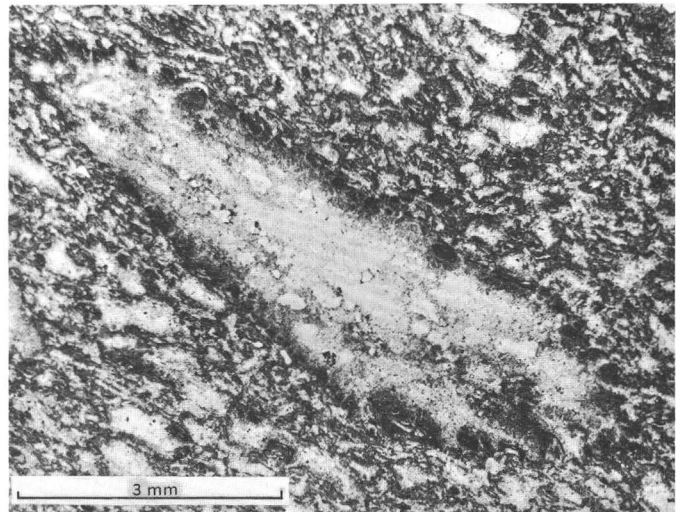
This shingled distribution pattern, both within flow units of the Topopah Spring Member and among ash-flow sheets of the Paintbrush Tuff, might suggest that the primary dip on the upper surface of each flow unit or ash-flow sheet, although possibly very slight, was sufficient to influence the depositional position of the succeeding flow. Formation of slight primary dips would appear to be possible regardless of the fact that the upper surfaces of ash-flow sheets are widely observed to be planar (Marshall, 1935; Gilbert, 1938; Smith, 1960a). This possibility suggests the additional hypothesis that the momentum of the early voluminous ash flows of the Topopah Spring, as they moved along their arcuate course, may have caused the tuffs to be deposited with a slight northward slope toward the inside of the arc. In a similar manner, the surface of a river flowing around a meander slopes inward. The later, less voluminous flow units of the Topopah Spring Member and the ash flows of the Pah Canyon and Yucca Mountain Members, also relatively limited in volume, accordingly may have tended to follow the topographic low and to accumulate along an axis farther north. On topography smoothed and leveled by preceding flows, the Tiva Canyon Member (equal to or greater in volume than the Topopah Spring Member) was able to cover a larger area than the Topopah Spring and to accumulate to maximum thickness along an axis almost as far south.

PETROLOGY

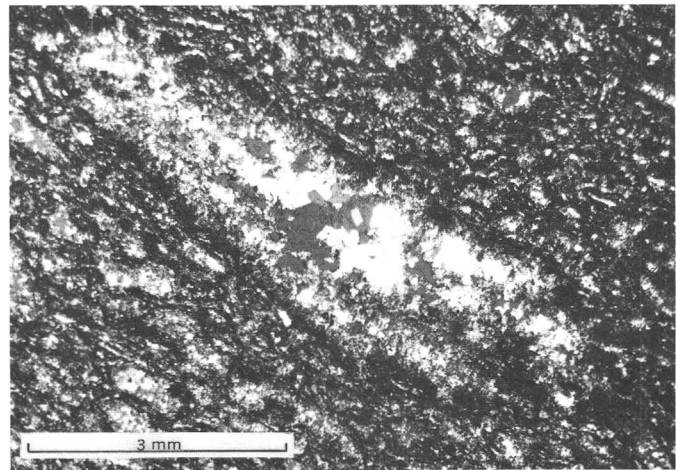
Some features of the chemistry and phenocryst mineralogy of the Topopah Spring Member have been summarized in the general descriptions of vertical and lateral compositional zonations. This section considers the petrographic and chemical variations in more detail to provide a basis for interpreting the origin of the compositional zonations.



A



B



C

FIGURE 19.—Crystal-poor rhyolitic tuff of the Topopah Spring Member, 311 Wash section. *A*, Basal vitrophyre, showing outlines of distorted shards and compacted pumice. Phenocrysts are very scarce. Compare with crystal-rich quartz latite shown in figure 5. Plane-polarized light. *B*, Densely welded crystallized tuff from the 400-foot level. Shard and pumice outlines are easily recognized, although slightly obscured by crystallization. Plane-polarized light. *C*, Same view as *B*; nicols oblique at about 60°. Crystallization products are quartz and alkali feldspar. Flattened pumice lapillus has localized coarse-grained intergrowth.

GROUNDMASS MINERALOGY AND TEXTURE

The groundmass mineralogy and texture of ash flows result from pyroclastic eruption, turbulent emplacement, and welding and crystallization after emplacement. The groundmass petrography of the Topopah Spring Member closely resembles that of other described ash-flow tuffs (for example, Marshall, 1935; Enlows, 1955; Ross and Smith, 1961); accordingly these features are only briefly described here.

At its base and top the Topopah Spring Member consists of typically vitroclastic tuff that has been neither welded nor crystallized and accordingly provides some indication of the original character of the erupted material. The base is a distinctively uniform shard tuff that contains some pumice but only minor phenocrysts and lithic inclusions. The refractive index of clear glass shards from this level is about 1.490–1.495, but in many samples the shards are charged with fine opaque dust and the refractive index cannot be determined reliably.

The nonwelded glassy top of the cooling unit contains greater proportions of phenocrysts and pumice lapilli; the refractive index of clear glass from this level averages about 1.500–1.505. The porous nonwelded to partly welded glassy rocks are locally yellowish and altered to the zeolite clinoptilolite.

In the upper and lower vitrophyres all primary porosity has been destroyed by compaction and welding, but the contorted vitroclastic outlines of shards and pumice are easily recognized in thin section (fig. 19A).

In the zone of crystallization the outlines of shards are obscured but are everywhere recognizable, even in the thickest stratigraphic sections. The groundmass crystallization products have not been studied in detail, but X-ray determinations indicate that alkali feldspar and cristobalite are the dominant minerals in most specimens. These minerals are typically less than 0.05 mm in diameter, but collapsed pumice lapilli in the interiors of thick stratigraphic sections commonly crystallize to

intergrowths of alkali feldspar and quartz as much as 1.0 mm in diameter (granophyric crystallization described by Smith (1960b, p. 152, 153)). In these thick sections the crystallization products of the matrix are also quartz and alkali feldspar, but they are finer grained (fig. 19B). Distinctive spherulitic crystallization commonly occurs in collapsed pumice lapilli in the basal 10–20 feet of devitrified tuff overlying the lower vitrophyre; apparently these collapsed lapilli remained glassy after crystallization of the surrounding matrix and devitrified as spherulites at a later stage.

PHENOCRYST MINERALOGY

The main phenocryst constituents of the Topopah Spring Member are alkali feldspar, plagioclase, biotite, clinopyroxene, opaque oxides, and quartz. Apatite, zircon, brown hornblende, and allanite are present as very minor accessories, mainly in the quartz latitic caprock. Most phenocrysts have well-formed crystal faces, but broken crystals are common. Rounded and embayed crystal faces, presumably resulting from resorption, are also notable, especially in plagioclase in the upper part of the cooling unit. Some plagioclase phenocrysts are mantled by alkali feldspar (fig. 20). Most phenocrysts occur individually, but sparse glomeroporphyritic clots, hypidiomorphic-equigranular in texture, contain as many as 10 grains. In any one specimen the grain size of phenocrysts tends to be uniform, but the average grain size increases from about 0.5–1.0 mm at the base of the ash-flow sheet to about 1.0–2.0 mm at the top.

The feldspar phenocrysts of the Topopah Spring Member show intricate compositional variations that are only partly understood. Most grains are obviously alkali feldspar ($n_z \leq 1.53$; $2V_x$ moderate to small; Carlsbad twinning only) or obviously plagioclase ($n_x \geq 1.54$; $2V_x$ large; prominent albite twinning), but the optical properties of a few grains in every thin section are intermediate between those of alkali feldspar and those of plagioclase. Such grains appear to be transitional between the two types. Some of these are probably anomalously sodic (and potassic?) plagioclase (albite twinning, $n_z \approx 1.54$, $2V_x$ intermediate); others appear to be anomalously sodic alkali feldspar, probably anorthoclase ($n_z \approx 1.53$, $2V_x$ moderate, faint quadrille twinning in a few grains).

The limited available optical and X-ray data indicate that the dominant alkali feldspar phenocrysts of the Topopah Spring Member are soda-rich sanidine cryptoperthite. Compositions determined by X-ray measurements of $(\bar{2}01)$ spacings of thermally homogenized alkali-feldspar separates by the method of Bowen and Tuttle (1950) vary from $Or_{60}Ab_{40}$ to $Or_{47}Ab_{53}$; no consistent difference was detected between rhyolitic base

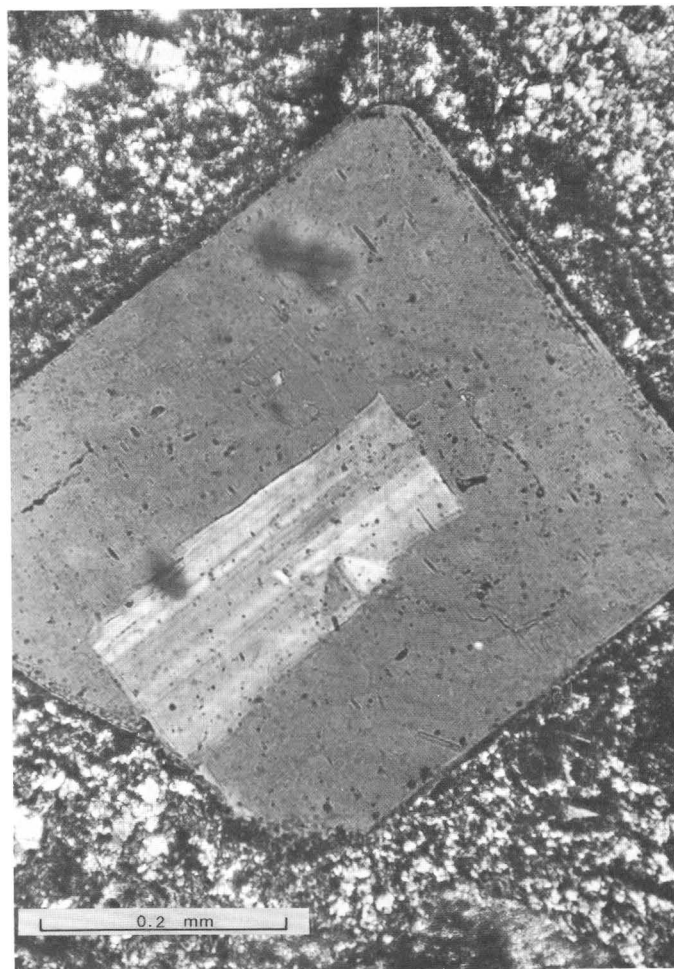


FIGURE 20.—Phenocryst of plagioclase mantled by alkali feldspar, in crystal-poor rhyolitic tuff from Busted Butte measured section. Nicols oblique at about 75°.

TABLE 1.—Partial analysis of alkali feldspar from quartz latitic caprock of Topopah Spring Member

[Major-oxide analysis by flame photometer by Wayne Mountjoy. Minor-element analysis by semiquantitative spectrographic methods by Nancy Conklin; Ag, As, Au, B, Be, Bi, Cd, Ce, Co, Cr, Ge, Hf, Hg, In, La, Li, Mo, Nb, Ni, P, Pd, Pt, Re, Sb, Sc, Sn, Ta, Te, Th, Tl, U, V, W, Y, Yb, Zn looked for but below determinative threshold. Field No. AGE-2B-2; lab. No. 302656. Analysis of rock from which feldspar was separated is given in table 2, col. 2]

| Major oxides, in weight percent | | | | | |
|-----------------------------------|-------|-------|------|-------|-------|
| CaO | ----- | | 0.4 | | |
| Na ₂ O | ----- | | 5.22 | | |
| K ₂ O | ----- | | 7.87 | | |
| Minor elements, in weight percent | | | | | |
| Ba | ----- | 0.07 | Mn | ----- | 0.002 |
| Cu | ----- | .0002 | Pb | ----- | .002 |
| Fe | ----- | .2 | Sr | ----- | .01 |
| Ga | ----- | .003 | Ti | ----- | .01 |
| Mg | ----- | .02 | Zr | ----- | .001 |

(2 samples) and quartz latitic caprock (6 samples). Most of the X-ray peaks are fairly sharp and should provide good average compositions. Partial chemical analysis of an alkali feldspar from the quartz latitic caprock (table 1; whole rock analysis: table 2, col. 2) indicates a composition of $Or_{48}Ab_{49}An_3$, in good agreement with the X-ray determination for this specimen ($Or_{51}Ab_{49}$). The optic angles of the alkali feldspar average about $35^\circ-40^\circ$ (—) but show a sizable range (fig. 21). Individual crystals are only slightly zoned and few show more than a few degrees of variation in optic angle, but variations of $10^\circ-25^\circ$ have been found between adjacent grains in a thin section. The magnitude of this variation in optic angle suggests that composition or structural state of individual phenocryst grains may depart markedly from the average although the percentage of anomalous phenocrysts is probably small. Optic angles of alkali feldspars from crystal-poor rhyolitic tuffs at the base of the ash-flow sheet are not consistently different from those of crystal-rich quartz latite at the top. The relations between optic axial angles and X-ray compositions of six Topopah Spring alkali feldspars, interpreted by the determinative diagram of Tuttle (1952), indicate that the six are near the sanidine-anorthoclase series in structure but deviate consistently toward the more ordered orthoclase-low albite series.

Plagioclases, as estimated by refractive indices and maximum extinction angles using the high-temperature curves of Tröger (1956) and Deer, Howie, and Zussman (1963), are mostly oligoclase and sodic andesine. More precise determinations for some plagioclases, as made on the universal stage by extinction-angle measurements in the plane normal to (010) and (001), are plotted in figure 21. This plot shows that the average plagioclase composition changes from about An_{20} for crystal-poor rhyolites in the lower part of the ash-flow sheet to about An_{25-30} for the crystal-rich rocks in the upper part. Individual samples show a considerable compositional range between separate grains. Zoned crystals are sparse in the lower part of the ash-flow sheet, and although many grains in the caprock show distinct oscillatory zoning, the compositional range is small, typically less than 5 percent anorthite content.

In the quenched glassy rocks, the biotite is transparent and pleochroic (red brown to straw yellow), but in crystallized specimens it is generally cloudy (bronze colored in hand specimen) and in places nearly opaque from fine-grained magnetite(?) dust. The clinopyroxene phenocrysts are very pale green and slightly pleochroic. The optic angle ($2V_z$) of one specimen is $59 \pm 4^\circ$ and N_x is 1.687 ± 0.002 , indicating a composition

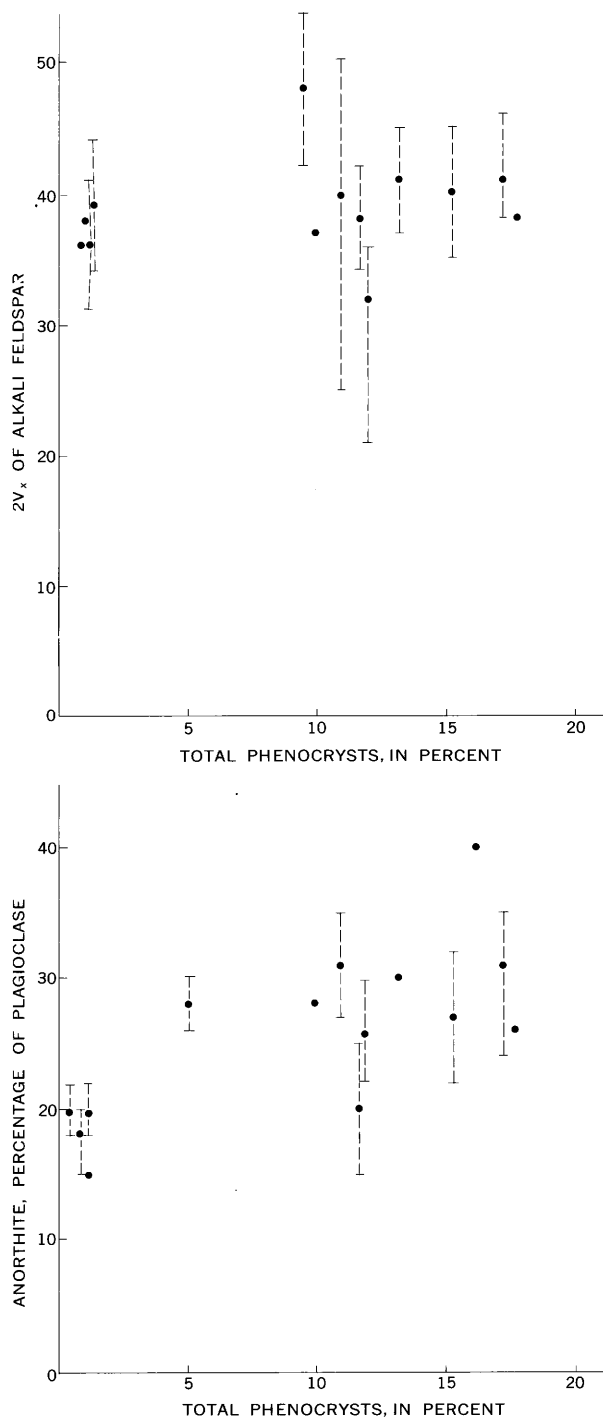


FIGURE 21.—Variations in plagioclase compositions (as determined by extinction-angle and refractive-index measurements) and in $2V_x$ of alkali feldspars, tuffs of the Topopah Spring Member. Dashed line indicates range of determinations; dot indicates average value for each specimen studied.

of $En_{38}Fs_{13}Wo_{49}$ (Hess, 1949). The sparse hornblende is light brown.

Quartz occurs throughout the ash-flow sheet as sparse

fragments and deeply embayed small bipyramidal phenocrysts.

Although it has been suggested that the so-called phenocrysts in many rhyolitic volcanic rocks may actually be xenocrysts resulting from incomplete melting at the time of magma generation (for example, Peterson and Roberts, 1963, p. 120-121), several features indicate that most crystals in the Topopah Spring tuffs are true phenocrysts that crystallized from a magmatic liquid. Most crystals are euhedral, and many plagioclase grains have distinct oscillatory zoning, features considered indicative of igneous origin. The alkali feldspar is sodic, a feature typical of rhyolitic volcanic rocks but relatively uncommon in plutonic rocks, most of which contain subsolvus feldspars. As will be discussed in a following section, crystals in the Topopah Spring Member show a systematic order of formation that agrees well with the theoretical sequence of crystallization for igneous rocks of this composition. Also, variations in crystal constituents are closely related to chemical variations in bulk-rock and groundmass compositions.

Although most crystals are therefore thought to be true phenocrysts, all thin sections contain a few possible xenocrysts. Particularly conspicuous are plagioclase crystals whose compositions, determined by extinction-angle methods, differ from the dominant plagioclase of the rock by 10 percent An or more.

Much of the variability in optical properties probably results from mechanical mixing of phenocrysts from rhyolitic and quartz latitic pumices. Some crystal-poor rhyolitic tuffs contain small amounts of crystal-rich pumice (as described in the Lathrop Wells section), and a little crystal-poor pumice also occurs in some crystal-rich quartz latites. Partial disintegration of these atypical pumices during flowage would have introduced minor amounts of anomalous phenocrysts into the bulk-rock modal compositions.

Some variability in optical properties of the phenocrysts may also result from modification of phenocryst contents and proportions by density sorting during emplacement of the ash flows. That such a process operated in the Aso ash flows of Japan has been documented by K. Ono (oral commun., 1964) and by one of us (Lipman, unpub. data). In the Aso tuffs, winnowing of shards from the ash matrix during flowage produced a concentration of crystal fragments relative to shards near the caldera and a concentration of shards relative to crystals near the distal end of the ash-flow sheet. Also, the denser mafic crystals are concentrated near the caldera, and the lighter feldspar crystals are concentrated near the distal end of the ash-flow sheet. At Aso only the pumice represents the original composition of the flow. This raises the possibility that some varia-

tions in the bulk-rock phenocryst contents of the Topopah Spring Member are due to sorting processes rather than to differences in crystal content of the erupted magma. Although this interpretation appears likely on a small scale for variations near the edges of the ash-flow sheet, it cannot explain the major variations. Phenocryst percentages in the matrix and in the predominant pumice type are very nearly alike in most Topopah Spring specimens.

CHEMISTRY

The Topopah Spring Member varies significantly in chemical composition, as has been shown for the Busted Butte and 311 Wash measured sections (fig. 4*B*, *C*; fig. 6). Table 2 contains 14 major-oxide analyses and 22 minor-element analyses from these and other sections. Norms are given as calculated from the major-oxide analyses, and modes are given for the chemically analyzed samples where available.

The analyses are listed in order of increasing SiO₂ content. This order corresponds in a general way to a downward sequence in stratigraphic section, but the detailed relations are more complex owing to the irregular distribution of individual ash flows and flow units. In areas where the uppermost mafic ash flows were not deposited, the glassy top of the cooling unit may be considerably more silicic than crystallized interior parts in areas where the depositional sequence is more complete.

MAJOR OXIDES

Rhyolitic volcanic rocks contain at most a few tenths of a percent of water at cooling as shown by Ross and Smith (1955) and Ross (1964), and secondary hydration has evidently modified many of the analyzed samples from the Topopah Spring Member, especially the glassy rocks. Accordingly, the major-oxide analyses have been recalculated free of volatiles in order to facilitate comparisons. All the tuffs high in CO₂ show appreciable secondary carbonate in thin section, and CO₂ has been calculated out as CaCO₃.

SiO₂-variation diagrams (fig. 22) for the recalculated volatile-free analyses show linear trends having very little scatter. The analyzed rocks range from silicic rhyolite in the basal part of the ash-flow sheet to silicic quartz latite in the caprock. As compared with average rocks of similar types (Nockolds, 1954), the Topopah Spring rocks are rich in SiO₂, Al₂O₃, and total alkalis; the Na₂O:K₂O is high; and total iron, MgO, CaO, TiO₂, and P₂O₅ contents are low.

SiO₂ in the recalculated analyses ranges from 68.8 to 77.4 percent. All the other oxides decrease as SiO₂ increases, but the proportional decrease is lower for the alkalis than for the other abundant oxides. Thus, al-

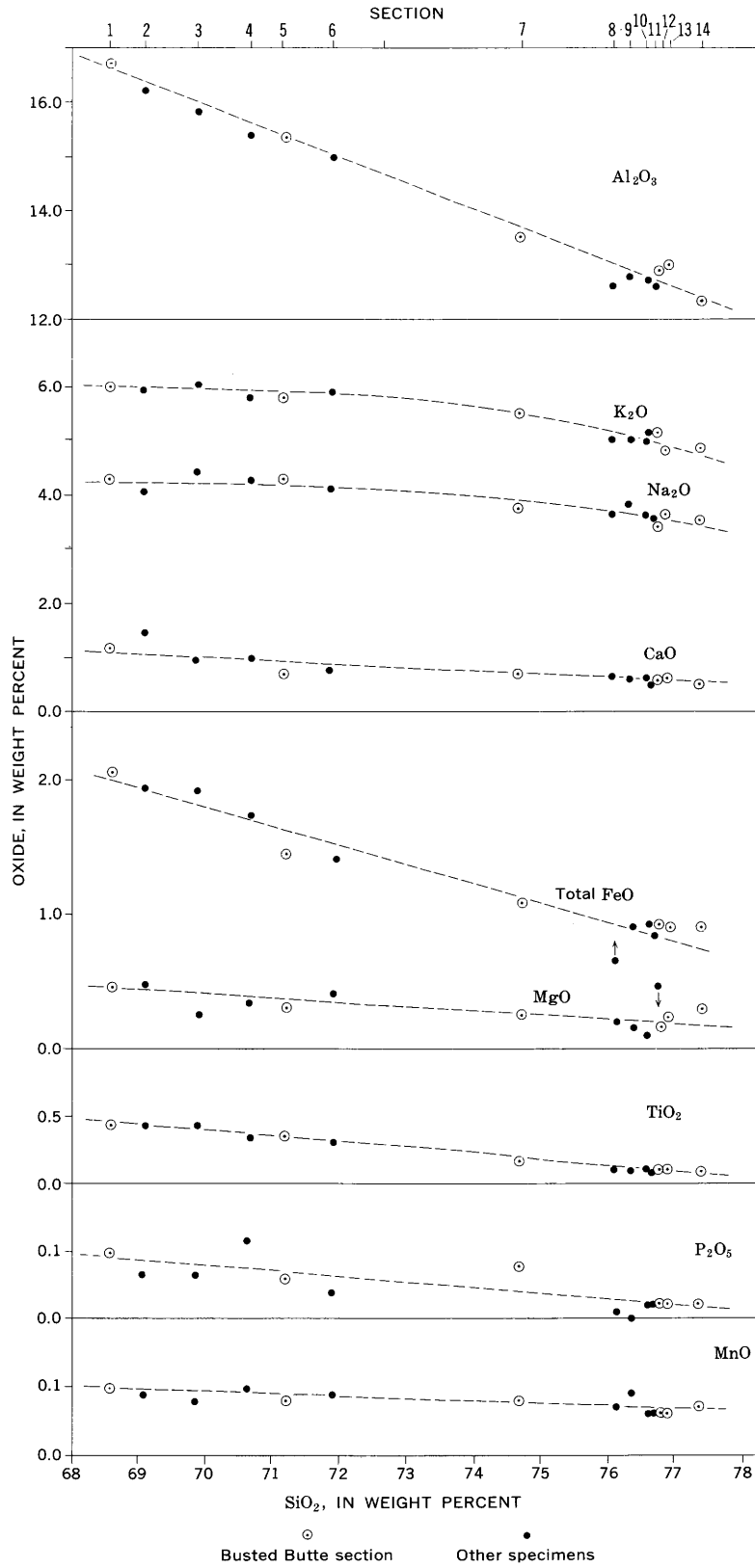


FIGURE 22.—SiO₂-variation diagrams for weight percent of major oxides of tuffs of the Topopah Spring Member, free of volatiles. Data are from table 2.

TABLE 2.—Composition of tuffs of the Topopah Spring

[Major-oxide analyses 1, 4-9, 12-14 made by P. L. D. Elmore, S. Botts, G. Chloe, L. Artis, and H. Smith; by rapid methods described by Shabiro and Brannock (1962); by J. C. Hamilton and reported as midpoint values of logarithmic 3d divisions. Comparison with quantitative analyses indicates that the same class interval is assigned Re, Rh, Ru, Sb, Sn, Sm, Ta, Tb, Te, Th, Tl, Tm, U, W, Zn]

| Location No. (see fig. 1) | Upper vitrophyre | Densely welded crystallized tuff | Upper vitrophyre | Densely welded crystallized tuff | Densely welded crystallized pumice | Densely welded crystallized tuff | | | Lower vitrophyre | |
|------------------------------|------------------|----------------------------------|------------------|----------------------------------|------------------------------------|----------------------------------|----------|-------------|------------------|--------|
| | Quartz latite | | | Rhyolite—quartz latite | | | Rhyolite | | | |
| | 1 | 2 | 3 | 4 | 5 | 6 | 7 | 8 | 9 | 10 |
| Field No. | 63L-17-B | AGE-2B | AGE-2A | 160ENH35 | 63L-17-C | 63L-128-B-2 | 63L-17-D | 63L-128-B-1 | 160ENH32 | TO-41C |
| Chemical lab. No. | 161293 | 13848 | 13847 | 158092 | 161294 | 162826 | 161295 | 162825 | 158091 | I4192 |
| Spectrographic lab. No. | D110781W | 13848 | 13847 | ----- | D110782W | D112927W | D110783W | D112926W | ----- | I4192 |

Major oxides (weight percent), recalculated

| | | | | | | | | | | |
|--------------------------------------|-------|--------|--------|-------|-------|-------|-------|-------|-------|--------|
| SiO ₂ | 68.8 | 69.09 | 69.91 | 70.8 | 71.5 | 71.8 | 74.8 | 76.4 | 76.66 | 76.6 |
| Al ₂ O ₃ | 16.8 | 16.25 | 15.79 | 15.4 | 15.3 | 14.9 | 13.6 | 12.8 | 12.94 | 12.7 |
| Fe ₂ O ₃ | 1.4 | 1.50 | 1.95 | 1.2 | 1.5 | 1.3 | 1.0 | .82 | .65 | .86 |
| Sum as FeO..... | 2.0 | 1.94 | 1.93 | 1.7 | 1.4 | 1.4 | 1.1 | .9 | .90 | .84 |
| FeO..... | .74 | .59 | .18 | .63 | .08 | .20 | .14 | .16 | .32 | .07 |
| MgO..... | .45 | .48 | .25 | .35 | .30 | .43 | .25 | .17 | .09 | .49 |
| CaO..... | 1.1 | 1.45 | .94 | .96 | .72 | .7 | .72 | .6 | .62 | .6 |
| Na ₂ O..... | 4.3 | 4.07 | 4.41 | 4.3 | 4.3 | 4.2 | 3.7 | 3.9 | 3.55 | 3.4 |
| K ₂ O..... | 6.0 | 5.99 | 6.00 | 5.8 | 5.8 | 6.0 | 5.5 | 5.0 | 4.98 | 5.1 |
| TiO ₂ | .41 | .42 | .42 | .36 | .34 | .31 | .18 | .10 | .10 | .10 |
| P ₂ O ₅ | .10 | .07 | .07 | .12 | .06 | .04 | .08 | .00 | .01 | .02 |
| MnO..... | .10 | .09 | .08 | .10 | .08 | .09 | .08 | .09 | .07 | .06 |
| Total..... | 100.0 | 100.00 | 100.00 | 100.0 | 100.0 | 100.0 | 100.0 | 100.0 | 100.0 | 100.00 |

Minor elements

| | | | | | | | | | | |
|---------|--------|--------|--------|--------|--------|--------|--------|--------|--------|--------|
| B..... | <.002 | <.002 | <.002 | 0.0015 | <.002 | <.002 | 0.003 | <.002 | 0.0015 | <.002 |
| Ba..... | .3 | .15 | .15 | .15 | .1 | .02 | .02 | .01 | .007 | .007 |
| Be..... | .0002 | <.0001 | <.0001 | .00015 | .0002 | .0003 | .0003 | .0003 | .0003 | .0005 |
| Ce..... | .05 | .03 | .03 | .03 | .03 | .03 | .02 | .015 | <.02 | <.02 |
| Cr..... | <.0001 | .0001 | .0001 | <.0001 | .00015 | <.0001 | <.0001 | <.0001 | <.0001 | .0002 |
| Cu..... | .0015 | .0003 | .0015 | .0007 | .0007 | .001 | .001 | .0007 | .0003 | .0002 |
| Ga..... | .003 | .002 | .002 | .0015 | .003 | .003 | .003 | .003 | .0015 | .003 |
| La..... | .03 | .015 | .02 | .015 | .02 | .015 | .01 | .007 | .003 | .005 |
| Mo..... | .0007 | <.0005 | <.0005 | <.0005 | <.0005 | <.0005 | <.0005 | .0005 | <.0005 | .0007 |
| Nb..... | .001 | <.001 | <.001 | .0015 | .0015 | .002 | .002 | .002 | .0015 | .003 |
| Nd..... | .015 | .015 | .015 | .015 | .015 | .015 | .015 | <.01 | <.01 | <.01 |
| Pb..... | .003 | .0015 | .002 | .003 | .003 | .005 | .003 | .005 | .007 | .003 |
| Sc..... | .001 | .0005 | .0005 | .0007 | .001 | .0007 | .0007 | <.0005 | <.0005 | <.0005 |
| Sr..... | .05 | .02 | .03 | .03 | .015 | .007 | .015 | .005 | .003 | .003 |
| V..... | .0015 | .001 | .001 | <.001 | .0015 | .0015 | .001 | <.001 | <.001 | <.001 |
| Y..... | .003 | .002 | .003 | .003 | .003 | .005 | .003 | .002 | .002 | .003 |
| Yb..... | .0003 | .0003 | .0003 | .0003 | .0003 | .0005 | .0003 | .0003 | .0003 | .0003 |
| Zr..... | .05 | .02 | .02 | .03 | .03 | .02 | .02 | .01 | .007 | .01 |

CIPW norms (weight percent).

| | | | | | | | | | | |
|-------------------|-------|-------|-------|-------|-------|-------|-------|-------|-------|-------|
| Quartz..... | 17.88 | 19.19 | 19.30 | 21.43 | 22.29 | 22.74 | 30.47 | 33.08 | 34.86 | 35.85 |
| Orthoclase..... | 35.27 | 35.36 | 35.45 | 34.52 | 34.41 | 35.32 | 32.38 | 29.58 | 30.27 | 29.34 |
| Albite..... | 36.56 | 34.14 | 37.16 | 36.41 | 36.52 | 35.14 | 31.48 | 32.84 | 29.18 | 29.75 |
| Anorthite..... | 4.94 | 6.35 | 3.86 | 3.98 | 3.19 | 3.35 | 3.05 | 2.64 | 2.98 | 2.63 |
| Corundum..... | 1.29 | .79 | .65 | .52 | .69 | .36 | .38 | .00 | .34 | .80 |
| Enstatite..... | 1.13 | 1.20 | .63 | .87 | .75 | 1.06 | .62 | .43 | 1.22 | .23 |
| Ferrosillite..... | .00 | .00 | .00 | .00 | .00 | .00 | .00 | .00 | .00 | .01 |
| Magnetite..... | 1.53 | .99 | .00 | 1.31 | .00 | .04 | .23 | .53 | .14 | .94 |
| Hematite..... | .38 | .82 | 1.95 | .33 | 1.51 | 1.29 | .88 | .45 | .76 | .00 |
| Ilmenite..... | .78 | .80 | .56 | .68 | .34 | .60 | .33 | .19 | .20 | .20 |
| Rutile..... | .00 | .00 | .12 | .00 | .16 | .00 | .00 | .00 | .00 | .00 |
| Apatite..... | .24 | .17 | .17 | .29 | .14 | .10 | .20 | .00 | .05 | .02 |
| Total..... | 100 | 100 | 100 | 100 | 100 | 100 | 100 | 100 | 100 | 100 |

Minerals

| | | | | | | | | | | |
|----------------------|-------|-------|-------|-------|-------|-------|-------|-------|-------|-------|
| Quartz..... | 0.1 | 0.1 | Trace | ----- | 0.1 | Trace | Trace | ----- | ----- | Trace |
| Alkali feldspar..... | 11.6 | 11.0 | 9.6 | ----- | 7.1 | 8.0 | 3.2 | 0.9 | ----- | 0.3 |
| Plagioclase..... | 7.3 | 5.1 | 5.1 | ----- | 4.3 | 4.2 | 1.6 | 1.2 | ----- | 1.4 |
| Biotite..... | .9 | .8 | .7 | ----- | .8 | .7 | Trace | Trace | ----- | Trace |
| Clinopyroxene..... | .4 | .1 | .2 | ----- | .3 | .2 | .2 | ----- | ----- | ----- |
| Hornblende..... | Trace | Trace | Trace | ----- | ----- | ----- | ----- | ----- | ----- | ----- |
| Sphene..... | .1 | Trace | Trace | ----- | ----- | ----- | ----- | ----- | ----- | ----- |
| Opaque minerals..... | .4 | .3 | .5 | ----- | .3 | .5 | .3 | Trace | ----- | .1 |
| Groundmass..... | 79.2 | 82.6 | 83.9 | ----- | 87.0 | 86.4 | 94.8 | 97.8 | ----- | 98.2 |
| Points counted..... | 2892 | 2351 | 2809 | ----- | 3006 | 2500 | 2855 | 5000 | ----- | 6970 |

See footnotes at end of table.

Member (locations of analyzed specimens shown in fig. 1)

2, 3, 11 by standard methods by D. F. Powers; 10 by standard methods by C. L. Parker. Minor-element analyses made by semiquantitative spectrographic methods in about 30 percent of the samples. Elements looked for but not found—Ag, As, Au, Bi, Cd, Co, Dy, Er, Eu, Gd, Ge, Hf, Hg, Ho, In, Ir, Li, Lu, Ni, O, Pd, Pr, Pt,

| Densely welded crystallized tuff | Lower vitrophyre | Densely welded crystallized tuff | | Upper vitrophyre | Densely welded crystallized tuff | | | | | | Partly welded glassy tuff | Nonwelded glassy tuff |
|----------------------------------|--------------------------------|----------------------------------|--------------------------------|-----------------------------------|-----------------------------------|----------------------------------|----------------------------------|----------------------------------|----------------------------------|------------------------------------|----------------------------------|-----------------------|
| Rhyolite—Continued | | | | Rhyolite-quartz latite | Rhyolite | | | | | | | |
| 11 | 12 | 13 | 14 | 15 | 16 | 17 | 18 | 19 | 20 | 21 | 22 | |
| SC-1B I4069 I4069 | 63L-17-I 161298 D110786W | 63L-17-F 161296 D110784W | 63L-17-H 161297 D110785W | ² 11-102-7-H 287481 | ² 11-102-7-G 287480 | ² 11-102-7F 287479 | ² 11-102-7E 287478 | ² 11-102-7D 287477 | ² 11-102-7C 287476 | ² 11-102-7B-A 287475 | ² 11-102-7A 287474 | |

without H₂O, F, Cl, and CO₂ as CaCO₃

| | | | | | | | | | | | |
|--|--|--|--|-------|-------|-------|-------|-------|-------|-------|-------|
| 76.76 12.88 .98 }.91 | 76.9 13.0 .66 }.89 | 77.0 12.7 .61 }.63 | 77.4 12.3 .85 }.89 | ----- | ----- | ----- | ----- | ----- | ----- | ----- | ----- |
| .03 .14 .53 3.36 5.14 .10 .02 .06 | .30 .23 .55 3.5 4.7 .09 .02 .06 | .08 .20 .59 3.6 5.0 .10 .02 .06 | .13 .29 .40 3.6 4.8 .10 .02 .07 | ----- | ----- | ----- | ----- | ----- | ----- | ----- | ----- |
| 100.0 | 100.0 | 100.0 | 100.0 | ----- | ----- | ----- | ----- | ----- | ----- | ----- | ----- |

(weight percent)

| | | | | | | | | | | | |
|--|--|--|--|---|--|---|---|--|---|--|--|
| <0.003 .005 .0002 <.02 <.0001 .0003 .002 .005 <.0005 .002 <.01 .003 <.0005 .003 <.001 .002 .0003 .007 | 0.003 .005 .0005 <.02 <.0001 .0007 .003 .003 .007 .002 <.01 .003 <.0005 .0015 <.001 .002 .0003 .002 .007 | 0.003 .01 .0003 <.02 <.0001 .0002 .003 .005 <.0005 .002 <.01 .003 <.0005 .01 <.001 .002 .0002 .01 | 0.0003 .007 .0003 <.02 .0007 .0007 .003 .003 .007 .0015 <.0005 .0015 .015 .003 .0007 .003 .0015 .003 .0003 .0002 .01 | <0.003 .03 .00015 <.02 <.0001 .0003 .003 .015 <.0005 .0015 .015 .003 .0007 .007 .0015 .003 .0003 .0003 .0003 .03 | <0.003 .007 .00015 <.02 <.0001 .00015 .0007 .003 .003 <.0005 .0015 <.01 .003 <.0005 .007 .003 <.001 .0015 .003 .0003 .0015 | <0.003 .007 .0003 <.02 <.0001 .0007 .003 .003 <.0005 .007 .0015 <.01 .007 <.0005 .007 .003 <.001 .003 .0003 .015 | <0.003 .007 .0003 <.02 <.0001 .0007 .003 .003 <.0005 .007 .0015 <.01 .007 <.0005 .003 .007 <.001 .003 .0003 .015 | 0.003 .003 .0003 <.02 <.0001 .0007 .003 .003 <.0005 .007 .0015 <.01 .003 <.0005 .003 .007 <.001 .003 .0003 .015 | <0.003 .003 .0003 <.02 <.0001 .0003 .003 .003 <.0005 .0015 <.01 .003 <.0005 .003 .007 <.001 .003 .0003 .015 | 0.003 .003 .0003 <.02 <.0001 .0015 .003 .003 <.0005 .003 .003 <.001 .003 .003 .003 .015 | 0.003 .007 .0003 <.02 <.0001 .0003 .003 .007 .0015 <.01 .003 <.0005 .007 .003 <.001 .003 .0003 .015 |
|--|--|--|--|---|--|---|---|--|---|--|--|

from recalculated analyses

| | | | | | | | | | | | |
|--|--|---|---|-------|-------|-------|-------|-------|-------|-------|-------|
| 36.43 30.34 28.30 2.26 1.00 .35 .00 .00 .98 .19 .00 .05 | 37.07 27.59 29.84 2.59 1.17 .57 .00 .90 .04 .18 .00 .05 | 34.93 29.86 30.77 2.78 .26 .50 .00 .17 .49 .19 .00 .05 | 36.62 28.54 30.64 1.86 .41 .73 .00 .36 .60 .19 .00 .05 | ----- | ----- | ----- | ----- | ----- | ----- | ----- | ----- |
| 100 | 100 | 100 | 100 | ----- | ----- | ----- | ----- | ----- | ----- | ----- | ----- |

(volume percent)

| | | | | | | | | | | | |
|-----------------------------|-----------------------------|---------------------------|--------------------------|-------------------------------|-------------------------------|-------------------------|-----------------------|-------|----------------------------|--------------------|-------|
| Trace 0.4 .7 Trace | Trace 0.4 .5 Trace | 0.1 1.1 .7 Trace | 0.1 .7 .5 Trace | 0.2 6.7 3.5 .5 .2 | 0.1 5.2 1.9 .3 .2 | 0.1 3.2 2.1 .1 | 0.1 .5 .6 .1 | ----- | Trace .6 .6 Trace | 0.3 .4 Trace | ----- |
| Trace 98.9 6500 | .1 99.0 6000 | .1 98.0 5671 | Trace 98.7 6000 | .4 88.4 3000 | .3 92.0 2500 | .2 94.4 3400 | .1 98.7 3500 | ----- | .1 98.7 3500 | .1 99.2 3400 | ----- |

See footnotes at end of table.

TABLE 2.—Composition of tuffs of the Topopah Spring Member

| Location No. (see fig. 1) | Upper vitrophyre | Densely welded crystallized tuff | Upper vitrophyre | Densely welded crystallized tuff | Densely welded crystallized pumice | Densely welded crystallized tuff | | | Lower vitrophyre | |
|--------------------------------------|------------------|----------------------------------|------------------|----------------------------------|------------------------------------|----------------------------------|-------------|----------|------------------|----------------------|
| | Quartz latite | | | Rhyolite—quartz latite | | | Rhyolite | | | |
| | 1 | 2 | 3 | 4 | 5 | 6 | 7 | 8 | 9 | 10 |
| | Field No. | 63L-17-B | AGE-2B | AGE-2A | ¹ 60ENH35 | 63L-17-C | 63L-128-B-2 | 63L-17-D | 63L-128-B-1 | ¹ 60ENH32 |
| Chemical lab. No. | 161293 | I3848 | I3847 | 158092 | 161294 | 162826 | 161295 | 162825 | 158091 | 14192 |
| Spectrographic lab. No. | D110781W | I3848 | I3847 | ----- | D110782W | D112927W | D110783W | D112926W | ----- | I4192 |
| Major oxides (weight | | | | | | | | | | |
| SiO ₂ | 66.7 | 65.73 | 69.02 | 69.0 | 71.2 | 70.9 | 72.3 | 74.7 | 73.2 | 74.16 |
| Al ₂ O ₃ | 16.2 | 15.46 | 15.60 | 15.0 | 15.0 | 14.7 | 13.1 | 12.5 | 12.1 | 12.51 |
| Fe ₂ O ₃ | 1.4 | 1.43 | 1.93 | 1.2 | 1.5 | 1.3 | 1.0 | .80 | .82 | .63 |
| FeO..... | .72 | .56 | .18 | .61 | .05 | .20 | .14 | .16 | .07 | .31 |
| MgO..... | .44 | .46 | .25 | .34 | .30 | .42 | .24 | .17 | .47 | .09 |
| CaO..... | 1.3 | 1.39 | .94 | .94 | .72 | 1.1 | 2.2 | 1.1 | 2.6 | .61 |
| Na ₂ O..... | 4.2 | 3.88 | 4.36 | 4.2 | 4.3 | 4.1 | 3.6 | 3.8 | 3.3 | 3.45 |
| K ₂ O..... | 5.8 | 5.70 | 5.93 | 5.7 | 5.8 | 5.9 | 5.3 | 4.9 | 4.9 | 4.81 |
| H ₂ O+..... | 2.7 | 3.61 | .31 | }2.8 | .52 | .43 | .56 | .51 | }70 | 2.77 |
| H ₂ O..... | .10 | .70 | .22 | | .23 | .05 | .15 | .17 | | .19 |
| TiO ₂ | .40 | .40 | .41 | .35 | .34 | .31 | .17 | .10 | .10 | .10 |
| P ₂ O ₅ | .10 | .07 | .07 | .12 | .06 | .04 | .08 | .00 | .02 | .01 |
| MnO..... | .10 | .09 | .08 | .10 | .08 | .09 | .08 | .09 | .06 | .07 |
| CO ₂ | .15 | .01 | .01 | <.05 | <.05 | .30 | 1.2 | .37 | 1.6 | .01 |
| Cl..... | ----- | .04 | .02 | ----- | ----- | ----- | ----- | ----- | ----- | .05 |
| F..... | ----- | .05 | .05 | ----- | ----- | ----- | ----- | ----- | ----- | .05 |
| Subtotal..... | ----- | 99.58 | 99.38 | ----- | ----- | ----- | ----- | ----- | ----- | 99.82 |
| Less O..... | ----- | .03 | .02 | ----- | ----- | ----- | ----- | ----- | ----- | .03 |
| Total..... | 100 | 99.55 | 99.36 | 100 | 100 | 100 | 100 | 99 | 100 | 99.79 |
| Powder density..... | 2.48 | ----- | ----- | ----- | 2.52 | ----- | 2.55 | ----- | ----- | ----- |

¹ Sample collected and submitted for analysis by E. Neal Hinrichs, U.S. Geological Survey.

though Na₂O and K₂O show decreases of about 15–20 percent of the total constituent, Al₂O₃ decreases more than 25 percent, total iron more than 50 percent, and CaO more than 60 percent.

MINOR ELEMENTS

The minor elements also show systematic variations when plotted against SiO₂ (fig. 23). The considerable scatter in this plot probably results mainly from the limited precision of the semiquantitative techniques; the six simultaneously analyzed samples from the Busted Butte section (large dots) define trends having much less scatter than is evident in the more randomly obtained data. The most striking variations are shown by barium, cerium, lanthanum, strontium, and zirconium, all of which decrease as silica increases.

The decrease in barium is paralleled by a decrease in K₂O, as is usual (Rankama and Sahama, 1950, p. 471). A much greater range of variation is shown by barium (6,000 percent) than by K₂O (20 percent), however, and the cause of this difference is not clear. Preferential incorporation of barium into early formed alkali feldspar apparently causes large decreases in barium concentration in the silicic parts of some igneous-rock series (Nockolds and Mitchell, 1948, p. 570). This process does not appear to have operated in the Topopah Spring rocks, as the alkali feldspar phenocrysts of the high-

barium quartz latitic caprock apparently are lower in barium than the entire rock (table 1; table 2, col. 2). Also the barium content of the analyzed glassy groundmass (table 4) is almost as high as the bulk-rock analysis and would plot very close to the barium curve in figure 23.

The rare earths lanthanum and cerium are more abundant in the Topopah Spring Member, especially in quartz latitic caprock tuffs, than in most silicic igneous rocks. Average values for lanthanum, cited by Turekian and Wedepohl (1961), are 0.0045 percent in "high-calcium granitic rocks" (approximately granodiorites) and 0.0055 percent in "low-calcium granitic rocks" (approximately true granites). The lanthanum content of the rhyolitic base of the Topopah Spring Member is similar to the average values but is three to five times greater in the quartz latitic caprock. The average values for cerium, 0.0081 percent in "high-calcium granitic rocks," are also three to five times lower than the concentration of this element in the caprock of the Topopah Spring Member. Cerium in the rhyolitic base is below the threshold of detectability (0.02 percent) for the present analyses, as are the average values computed by Turekian and Wedepohl. The high rare-earth content of the quartz latitic caprock is expressed mineralogically by the presence of accessory allanite.

(locations of analyzed specimens shown in fig. 1)—Continued

| Densely welded crystallized tuff | Lower vitrophyre | Densely welded crystallized tuff | Upper vitrophyre | Densely welded crystallized tuff | | | | | | Partly welded glassy tuff | Nonwelded glassy tuff |
|----------------------------------|--------------------------------|----------------------------------|--------------------------------|-----------------------------------|-----------------------------------|----------------------------------|----------------------------------|----------------------------------|----------------------------------|------------------------------------|----------------------------------|
| Rhyolite—Continued | | | | Rhyolite-quartz latite | Rhyolite | | | | | | |
| 11 | 12 | 13 | 14 | 15 | 16 | 17 | 18 | 19 | 20 | 21 | 22 |
| SC-1B 14069 14069 | 63L-17-I 161298 D110786W | 63L-17-F 161296 D110784W | 63L-17-H 161297 D110785W | ² 11-102-7-H 287481 | ² 11-102-7-G 287480 | ² 11-102-7F 287479 | ² 11-102-7E 287478 | ² 11-102-7D 287477 | ² 11-102-7C 287476 | ² 11-102-7B-A 287475 | ² 11-102-7A 287474 |

percent), original analyses

| | | | | | | | | | | | |
|-------|------|------|------|--|--|--|--|--|--|--|--|
| 75.73 | 74.1 | 76.1 | 76.9 | | | | | | | | |
| 12.70 | 12.5 | 12.6 | 12.2 | | | | | | | | |
| .97 | .64 | .60 | .84 | | | | | | | | |
| .03 | .29 | .08 | .13 | | | | | | | | |
| .14 | .22 | .20 | .29 | | | | | | | | |
| .54 | .53 | .68 | .40 | | | | | | | | |
| 3.32 | 3.4 | 3.6 | 3.6 | | | | | | | | |
| 5.07 | 4.5 | 5.0 | 4.8 | | | | | | | | |
| .53 | 2.9 | .52 | .51 | | | | | | | | |
| .52 | .38 | .28 | .22 | | | | | | | | |
| .10 | .09 | .10 | .10 | | | | | | | | |
| .02 | .02 | .02 | .02 | | | | | | | | |
| .06 | .06 | .06 | .07 | | | | | | | | |
| .02 | <.05 | .16 | <.05 | | | | | | | | |
| .02 | | | | | | | | | | | |
| .03 | | | | | | | | | | | |
| 99.80 | | | | | | | | | | | |
| .01 | | | | | | | | | | | |
| 99.79 | 100 | 100 | 100 | | | | | | | | |
| | 2.40 | 2.50 | 2.51 | | | | | | | | |

² Sample collected and submitted for analysis by F. A. McKeown, U.S. Geological Survey.

The strontium content of the Topopah Spring Member varies by a factor of 10 and decreases with increasing SiO₂. The variations in strontium tend to follow those of CaO, as is typical.

Zirconium, which also shows a well-defined trend, ranges from below the granitic-rock averages of Turekian and Wedepohl (0.0140–0.0175 percent) in the basal rhyolite to slightly higher than average in the quartz latitic caprock. The zirconium content of these tuffs appears to correlate closely with presence of the mineral zircon, which is scarce in the basal rhyolite but is a conspicuous accessory mineral in the caprock.

Smaller but nevertheless distinct variations are also shown by neodymium, scandium, and vanadium, which decrease as SiO₂ increases; in contrast, boron and beryllium slightly increase as SiO₂ increases.

RELATIONS BETWEEN BULK-ROCK AND GROUNDMASS CHEMISTRY

It is well known that the groundmass compositions of porphyritic volcanic rocks tend to be more silicic and rhyolitic than corresponding bulk-rock compositions. Accordingly, to interpret the significance of the compositional variation between the crystal-rich quartz latitic caprock and the crystal-poor rhyolitic base of the Topopah Spring Member, it is necessary to determine what part is due to differences in phenocryst content

and what part is due to differences in groundmass composition.

Using the modal data of table 2 and optical, X-ray, and chemical determinations of mineral compositions, the total-phenocryst compositions have been calculated and subtracted from the bulk-rock analyses for the three analyzed rocks having the highest crystal and the lowest SiO₂ contents (table 2, cols. 1–3). The resultant calculated groundmass compositions (table 3) differ only slightly from the bulk-rock analyses. All the groundmasses are higher in SiO₂, but the largest increase is only 2.4 percent. To check the reliability of this maxi-

TABLE 3.—Calculated groundmass composition of tuffs of the Topopah Spring Member, in weight percent

(Column numbers as in table 2. A, calculated groundmass compositions; B, net change from bulk-rock analysis (table 2))

| | 1 | | 3 | | 5 | |
|--------------------------------------|------|------|------|------|------|------|
| | A | B | A | B | A | B |
| SiO ₂ | 71.0 | +2.2 | 72.1 | +2.2 | 73.9 | +2.4 |
| Al ₂ O ₃ | 15.8 | -1.0 | 15.1 | -7 | 14.7 | -6 |
| Fe ₂ O ₃ | .9 | -5 | 1.3 | -7 | .6 | -9 |
| FeO..... | .4 | -3 | .0 | -2 | .0 | -1 |
| MgO..... | .3 | -1 | .1 | -1 | .1 | -2 |
| CaO..... | .8 | -3 | .5 | -4 | .3 | -4 |
| Na ₂ O..... | 4.0 | -3 | 4.2 | -2 | 4.2 | -1 |
| K ₂ O..... | 6.4 | +4 | 6.3 | +3 | 5.9 | +1 |
| TiO ₂ | .4 | | .4 | | .3 | |
| Total..... | 100 | | 100 | | 100 | |
| Volume percent phenocrysts..... | 20.8 | | 16.1 | | 13.0 | |

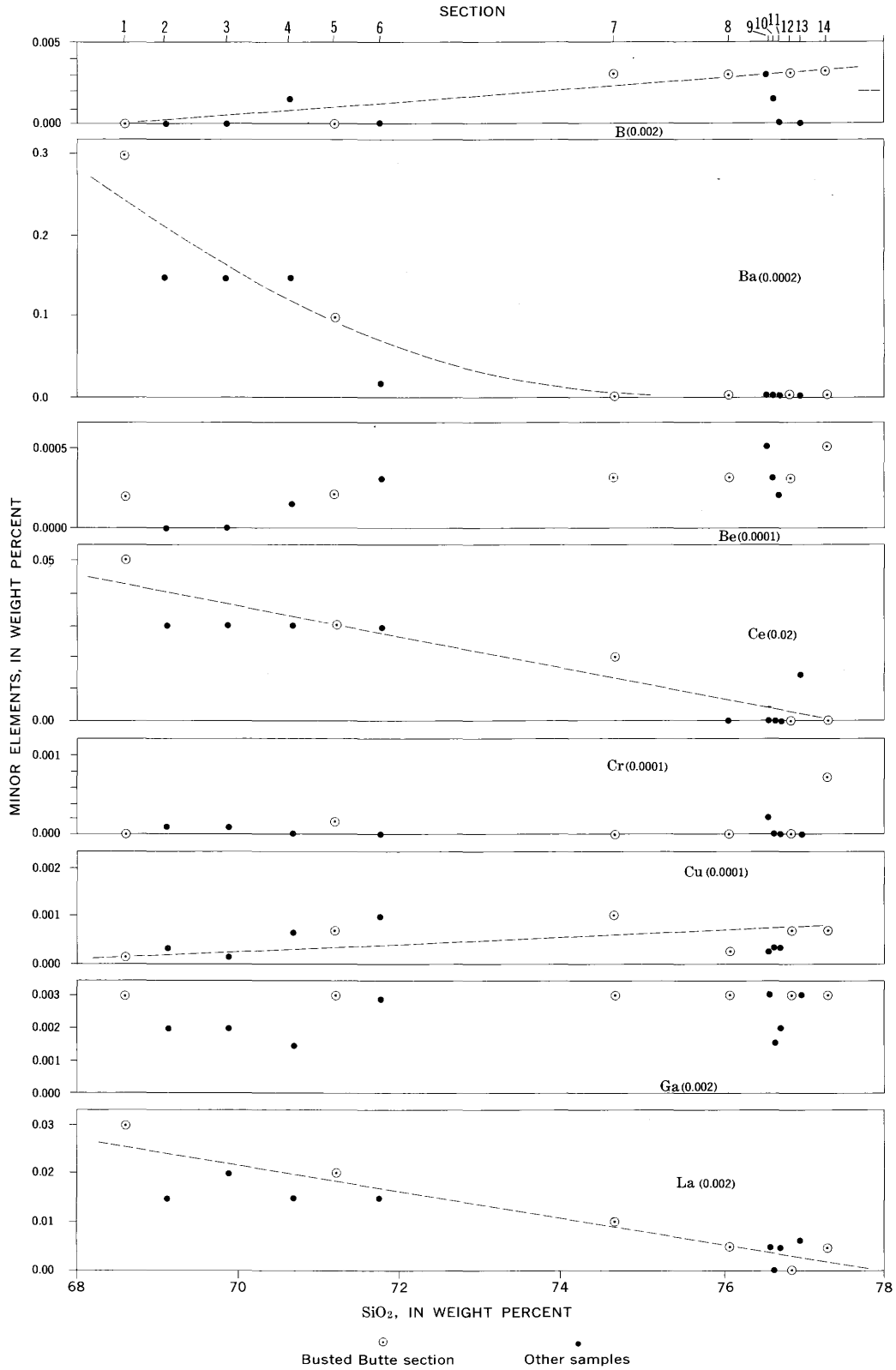


FIGURE 23.—SiO₂-variation diagrams for minor elements in tuffs of the Topopah Spring Member. Data are from threshold determinations are plotted arbitrarily as zero. A few values below the ordinary threshold were

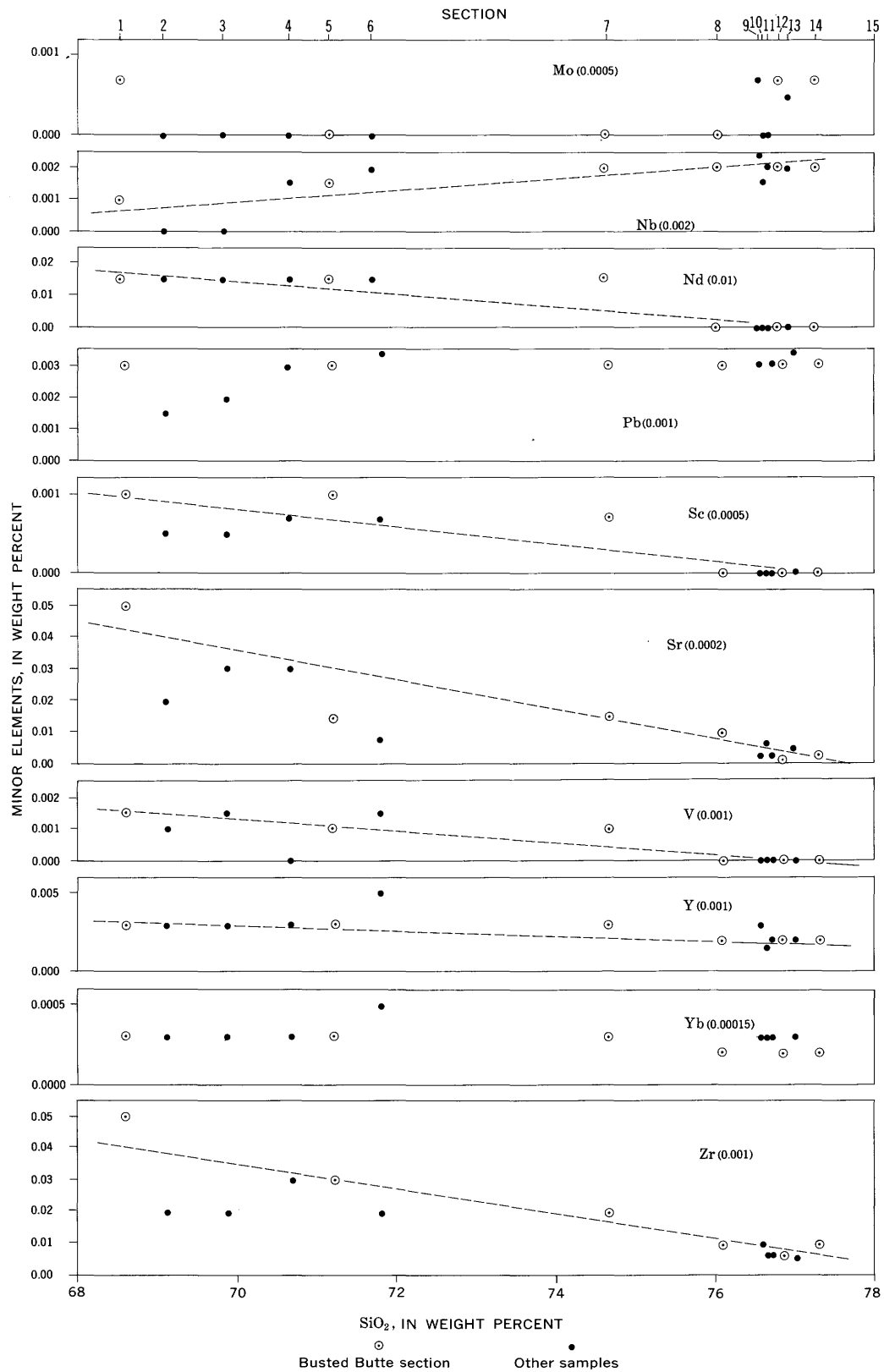


table 2. Ordinary threshold limits of detection indicated for individual elements in parentheses; less-than-determined under particularly favorable conditions. SiO_2 values from analyses recalculated volatile free.

mum calculated value, the groundmass glass of one sample, which also has the highest crystal and the lowest SiO₂ contents among the analyzed rocks, was separated from the phenocrysts in heavy liquids and analyzed (table 4). The analyzed groundmass composition

TABLE 4.—Analysis of glassy groundmass of quartz latitic tuff from the Busted Butte section

[Major-oxide analysis by P. L. D. Elmore, S. Botts, G. Chloe, L. Artis, and H. Smith by X-ray fluorescence supplemented by rapid methods described by Shapiro and Brannock (1962); lab. No. 162824; minor-element analysis by J. C. Hamilton by semiquantitative spectrographic methods, lab. No. D112925W. Field No. 63L-17-B; bulk-rock analysis listed in table 2, col. 1.]

| Major oxides | 1 | 2 | 3 | Minor elements † | |
|--------------------------------------|------|------|-------|------------------|-------|
| SiO ₂ | 67.3 | 69.7 | +0.9 | Ba..... | 0.15 |
| Al ₂ O ₃ | 15.1 | 15.6 | -1.2 | Be..... | .0003 |
| Fe ₂ O ₃ | 1.1 | 1.1 | - .3 | Ce..... | .03 |
| FeO..... | .56 | .58 | - .16 | Cu..... | .0005 |
| MgO..... | .62 | .64 | + .19 | Ga..... | .003 |
| CaO..... | 1.1 | 1.1 | None | La..... | .02 |
| Na ₂ O..... | 4.0 | 4.1 | - .2 | Nb..... | .0015 |
| K ₂ O..... | 6.4 | 6.6 | + .6 | Nd..... | .015 |
| H ₂ O+..... | 2.9 | | | Pb..... | .003 |
| H ₂ O-..... | .41 | | | Sc..... | .0007 |
| TiO ₂ | .37 | .38 | - .03 | Sr..... | .015 |
| MnO..... | .08 | .08 | - .02 | V..... | .001 |
| P ₂ O ₅ | .08 | .08 | - .02 | Y..... | .003 |
| CO ₂ | <.05 | | | Yb..... | .0003 |
| Sum..... | 100 | 100 | | Zr..... | .03 |

† Minor elements looked for but not detected; Ag, As, Au, B, Bi, Cd, Co, Cr, Ge, Hf, Hg, In, Li, Mo, Ni, Pd, Pt, Re, Sb, Sn, Ta, Te, Th, Tl, U, W, Zn, Pr, Sm, Eu.

1. Original analysis.
2. Analysis recalculated free of H₂O.
3. Not change between volatile-free groundmass analysis (col. 2) and bulk-rock analysis (table 2, col. 1).

closely agrees with the calculated values, although the calculated SiO₂ content appears to be slightly high and the values for MgO and CaO slightly low. In addition to the higher SiO₂ content, the groundmasses of the quartz latitic tuffs are clearly higher in K₂O and lower in Na₂O, Al₂O₃, Fe₂O₃, and FeO than the corresponding bulk rocks.

Groundmass compositions have not been determined separately by either calculation or analysis for the crystal-poor rhyolitic tuffs, because the very low crystal content of these rocks precludes sizable difference between bulk-rock and groundmass compositions. The variation in phenocryst content, although striking, accounts for only a small part of the range in bulk-rock compositions because most phenocrysts are feldspars similar to the groundmass in composition. Accordingly, most of the compositional variation between the rhyolitic basal tuff and the quartz latitic caprock of the Topopah Spring Member must be due to variation in groundmass compositions. The maximum observed range in chemical composition of analyzed rocks of the Topopah Spring Member, 8.6 percent SiO₂ content, occurs within a single vertical section (Busted Butte; table 2, col. 1, 14); almost three-fourths of this range is due to variations in groundmass composition.

RELATIONS BETWEEN CHEMICAL AND MINERALOGICAL COMPOSITIONS

It has already been shown that the phenocryst content of the Topopah Spring Member increases from less than 1 percent at the base of the sheet to more than 20 percent at the top. Concurrently, SiO₂ content decreases upward from more than 77 percent to less than 69 percent. The general aspects of this parallelism between modal and chemical trends are already obvious from plots for the measured sections (figs. 4, 6).

The close relation between modal and chemical compositions is indicated more precisely by figure 24, in which total phenocrysts in volume percent are plotted against weight percent SiO₂ for the 12 chemically analyzed rocks for which modal data are available. The trend of this plot is linear with only small deviations. This relation suggests that the volume percent of phenocrysts should provide a fairly precise compositional index for those densely welded rocks of the Topopah Spring Member for which chemical analyses are not available.

Amounts of the major phenocrysts—alkali feldspar, plagioclase, quartz, biotite, clinopyroxene, and opaque oxides—all increase as total phenocryst content increases (figs. 4, 6, 10, 11, 12, 17). In order to consider another aspect of the phenocryst variation—the changes in relative proportions of phenocryst minerals with bulk-rock compositional variations—the phenocryst contents of 38 Topopah Spring rocks for which modal compositions were determined have been recalculated to total 100 percent and plotted against total phenocryst content of the rock (fig. 25). Plots on this diagram show considerable scatter, mainly as a result of inherent limitations of precision in the modal counts and subsequent recalculations. A major cause of the scatter is the low phenocryst contents of many of the rocks, especially those of rhyolitic composition. Additional scatter probably results from density sorting during emplacement and from contamination by anomalous pumices and their disintegration products, as described earlier. Despite the scatter, most of the plots show fairly well defined trends that are considered significant.

The low-phenocryst rhyolites have lower proportions of alkali feldspar and higher proportions of plagioclase than the high-phenocryst quartz latites; thus the ratio of alkali feldspar to plagioclase decreases as SiO₂ and CaO increase. This relation is the opposite of that to be expected if bulk-rock composition were the dominant control on variations in feldspar composition. This matter will be discussed further in the section on petrogenesis, but it can be stated that the relation is consistent with a more advanced state of crystallization of

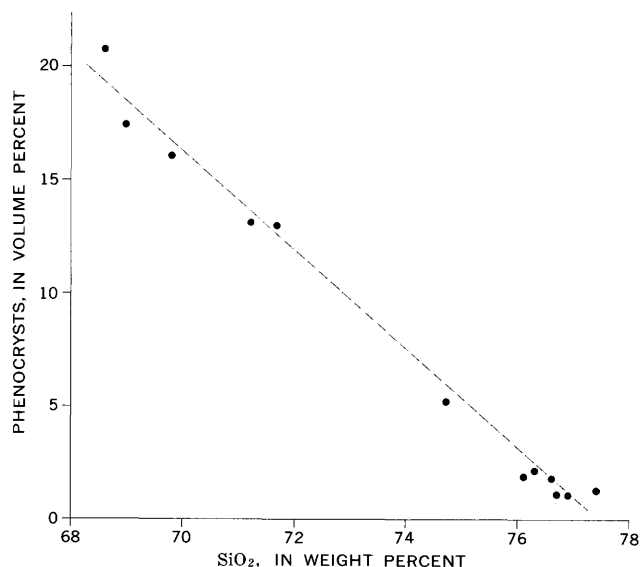


FIGURE 24.—Relation between SiO_2 and total phenocryst contents of 12 analyzed rocks of the Topopah Spring Member. SiO_2 contents from analyses recalculated volatile free.

the quartz latite than the rhyolite. Thin sections of the crystal-poor rhyolites typically contain only a few grains each of quartz and the mafic minerals, and plots for these minerals scatter widely. The proportion of quartz phenocrysts possibly increases slightly as total phenocrysts decreases (increasing SiO_2), although the total quartz content is higher in the more crystal-rich tuffs. The proportions of biotite and clinopyroxene appear lower in the crystal-poor rhyolitic rocks, but the proportion of opaque oxides appears to increase slightly as phenocryst content decreases. The proportion of total mafic minerals appears to decrease as phenocryst content decreases, but there is much scatter at the low-phenocryst rhyolitic end of the trend. The total content of mafic phenocrysts is much lower in the crystal-poor rhyolitic tuffs than in the crystal-rich quartz latitic rocks.

COMPOSITIONAL ZONATIONS IN OTHER ASH-FLOW SHEETS

Although most ash-flow sheets have been described as homogeneous, the compositional variations in the Topopah Spring Member are not unique. Similar zonations in ash-flow tuffs from various parts of the world have been reported by Howel Williams (1942), Katsui (1963), and Ratté and Steven (1964); nine examples in addition to the Topopah Spring Member have thus far been recognized in southern Nevada by us and by our colleagues with the U.S. Geological Survey. The observation that such compositional zonations are widespread features of ash-flow tuffs is essential to in-

terpretation of the Topopah Spring Member, and accordingly, some significant features of the other southern Nevada zoned ash-flow sheets are briefly outlined.

The other extensive ash-flow sheet in the Paintbrush Tuff, the Tiva Canyon Member (Hinrichs and Orkild, 1961), is so similar to the Topopah Spring Member that the two tuffs can be mistaken in the field. The Tiva Canyon Member was erupted after the Topopah Spring Member, and other ash-flow units had filled irregularities in the topography; although volumes of the two units are similar, the Tiva Canyon Member spread over a larger area and shows smaller variations in thickness. Like the Topopah Spring Member, the Tiva Canyon Member is a compound cooling unit that contains several recognized flow units. Contacts between individual flow units are sharp in places but become gradational as traced laterally. The Tiva Canyon Member grades from crystal-poor rhyolite at its base (2–3 percent phenocrysts; 76–77 percent SiO_2) upward into a crystal-rich quartz latitic caprock (15–20 percent phenocrysts; 68–69 percent SiO_2). For any given SiO_2 content, the Tiva Canyon Member has a slightly higher Na_2O and total phenocryst content and a much higher alkali feldspar-plagioclase ratio than the Topopah Spring Member; otherwise the two units are chemically and petrographically similar.

All voluminous ash-flow sheets in the Timber Mountain Tuff (Orkild, 1965), a post-Paintbrush unit that consists of ash-flow tuffs related in part to the Timber Mountain caldera (Christiansen and others, 1965), show striking compositional zonations. The Pliocene Timber Mountain Tuff is petrologically distinctive as a whole, although small differences (mainly petrographic) have been recognized among individual ash-flow sheets within it. The chemical composition and compositional range of the Timber Mountain Tuff are virtually identical with that of the Topopah Spring Member, but for a given SiO_2 content the Timber Mountain Tuff has a much higher phenocryst content; quartz is a major phenocryst constituent (O'Connor, 1963; Quinlivan and Lipman, 1965). The Rainier Mesa and Ammonia Tanks Members of the Timber Mountain Tuff, both compound cooling units that extend in every direction about 20–30 miles away from the Timber Mountain caldera, have conspicuous compositional zonations. Each member consists of basal moderately crystal-rich rhyolite (76–77 percent SiO_2 ; 20–25 percent phenocrysts with alkali feldspar > quartz > plagioclase > biotite) that grades upward into a very crystal-rich quartz latitic caprock (67–68 percent silica; 35–40 percent phenocrysts with alkali feldspar > plagioclase > quartz > biotite > clinopyroxene). The subsided area included in the Timber Mountain caldera was partly

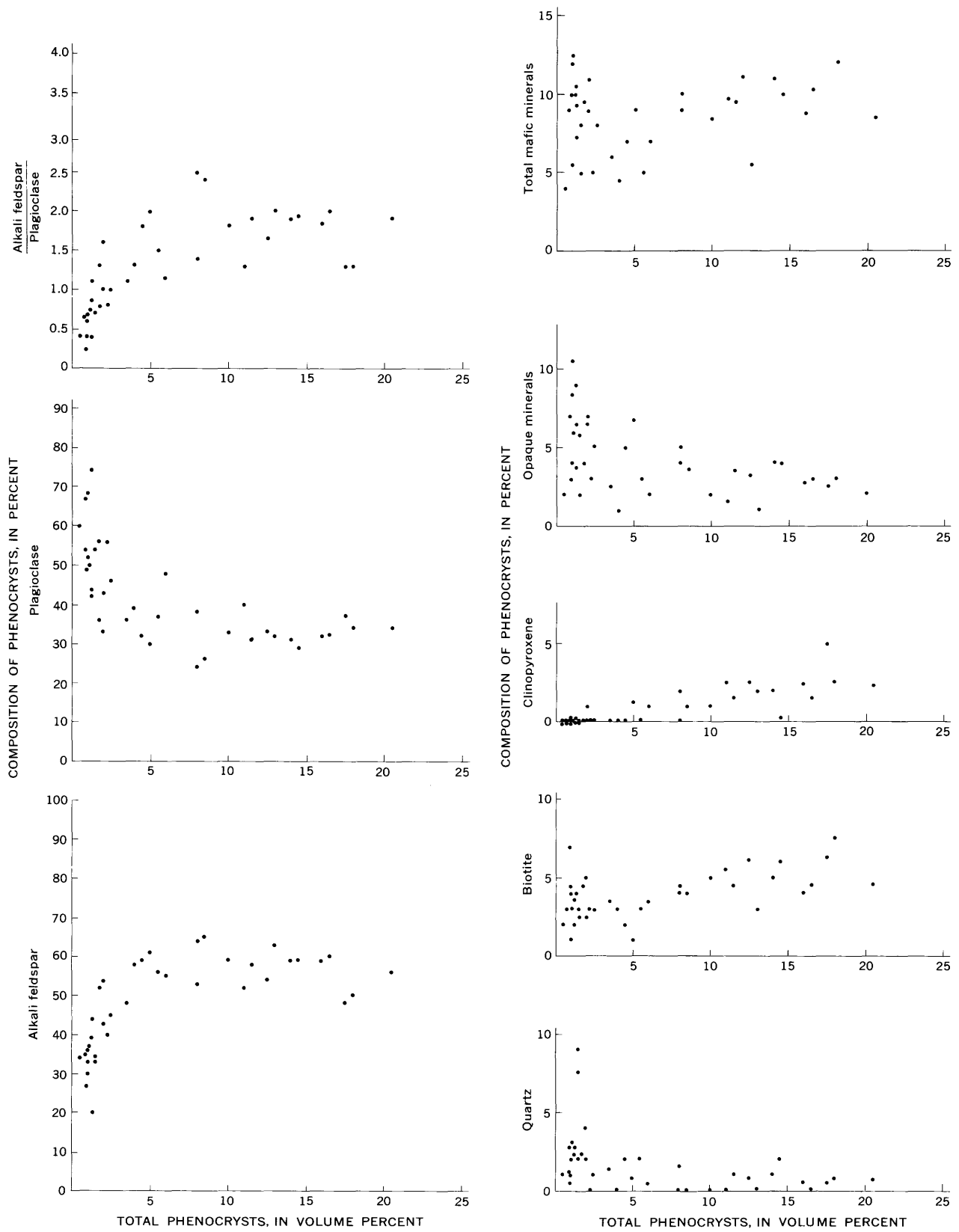


FIGURE 25.—Relations between phenocryst proportions and total phenocryst content of tuffs of the Topopah Spring Member.

filled by the tuff of Cat Canyon, a composite sheet of the Timber Mountain Tuff intermediate in age between the Rainier Mesa and Ammonia Tanks Members. Although the base of the Cat Canyon is not exposed, the visible part contains four separate alternations of rhyolite and quartz latite. Thus, there are at least six repetitions of similar compositional zonations within the Timber Mountain Tuff.

The Pliocene Thirsty Canyon Tuff (Noble and others, 1964)—a sequence of five ash-flow sheets related to the Black Mountain caldera (Christiansen and Noble, 1965)—is mostly rather uniform alkalic rhyolite (70–76 percent SiO_2 ; 10–20 percent phenocrysts). In places, however, both of the most voluminous and widespread ash-flow sheets in the Thirsty Canyon Tuff, the Spearhead and Trail Ridge Members, grade upward into crystal-rich caprocks (66–68 percent SiO_2 ; 35 percent phenocrysts).

These nine examples of compositionally zoned tuffs from southern Nevada include approximately one-third of the ash-flow sheets mapped in the vicinity of the Nevada Test Site, and similar compositional zonations almost certainly occur elsewhere in the voluminous ash-flow tuffs of the Great Basin, although they have not yet been reported. The presence of similar compositionally zoned ash-flow sheets may also be suggested by the data of Peterson and Roberts (1963), who, using published chemical and modal data, noted a general association of crystal-poor rhyolites and crystal-rich quartz latites among ash-flow tuffs of the Great Basin. They did not, however, recognize the contrasted types together in any particular unit.

Other compositionally zoned ash-flow sheets have been recognized in U.S. Geological Survey investigations currently in progress. The Pleistocene Bandelier Tuff, which surrounds the Valles caldera in northern New Mexico, includes several compositionally zoned ash-flow sheets in which upward increase in crystal content correlates with decrease in SiO_2 content (R. L. Smith, 1960a, p. 833; R. L. Smith and R. A. Bailey, oral commun., 1964). The vitric-crystal tuff member of the Pliocene Starlight Formation in southern Idaho contains at least two thin widespread ash-flow sheets that show upward increases in phenocryst content from less than 5 percent at their bases to as much as 40 percent at their tops; the chemistry of these rocks has not been investigated (D. E. Trimble and W. J. Carr, oral commun., 1964).

INTERPRETATION OF MAGMATIC DIFFERENTIATION

The basic petrogenetic problem of the Topopah Spring Member is the origin of the compositional zonation from rhyolite to quartz latite. Fundamental to

subsequent discussion of this problem is the conclusion that the entire compositional sequence is comagmatic and was erupted from a single magma chamber. This interpretation seems required by the systematic gradational variations in mineralogical and chemical composition over the transition from rhyolite to quartz latite, as described in the preceding sections. The gradation within a single cooling unit would perhaps not in itself preclude an alternative hypothesis of two separate sources of magma, one rhyolitic and the other quartz latitic, partly mixed during eruption and emplacement. Such mixing, however, could not reasonably be called upon to explain the similar variation patterns of all the other zoned ash-flow sheets just described. All known examples of compositionally zoned ash-flow sheets show upward increases in phenocryst content and decreases in SiO_2 content. In addition each example has an apparently consanguineous mineralogy from top to bottom; for example, quartz-rich units are quartz rich throughout, plagioclase-poor units are plagioclase poor throughout.

Thus, the sequence of petrologic variations within the Topopah Spring Member and other compositionally zoned ash-flow sheets, together with independent evidence of the rapidity of eruption and emplacement of each sheet, require eruption by progressive emptying of compositionally zoned magma from the source chambers. The sequence of compositional variation in each ash-flow sheet represents in inverted order the compositional zonation that existed in the magma chamber at the time of eruption. In the Topopah Spring magma the original zonation was downward, from crystal-poor rhyolite to crystal-rich quartz latite. Similar interpretations have been advanced for other compositionally zoned ash-flow sheets (Howell Williams, 1942, p. 156; Katsui, 1963, p. 641–642; Ratté and Steven, 1964, p. D52–D53; Smith, 1960a, p. 833).

CORRELATION OF NORMATIVE COMPOSITIONS WITH EXPERIMENTAL DATA

CIPW norms of the tuffs of the Topopah Spring Member (table 2) consist mainly of quartz, orthoclase, and albite, hereafter referred to as Q, Or, and Ab. As the chemical composition of the tuffs varies from quartz latite to silicic rhyolite, the main variation in normative bulk-rock composition is an increase in Q; the Or:Ab ratio remains virtually constant at about 1:1. The sum of Q, Or, and Ab, which is equal to the differentiation index of Thornton and Tuttle (1960) for all the rocks in this study, ranges from 89.7 percent in the most mafic caprock of the Topopah Spring Member (table 2, col. 1) to as much as 95.8 percent in the basal rhyolitic tuff (table 2, col. 14).

Accordingly, the tuffs of the Topopah Spring Member, especially the basal rhyolitic rocks, are closely approximated in composition by the quaternary system Q-Or-Ab-H₂O studied by Tuttle and Bowen (1958). Their study showed that the position of the thermal trough marking the boundary between the quartz and feldspar fields of stability shifts as water pressure varies. Figure 26 (upper diagram) shows positions of the thermal trough and the ternary thermal minimum at various water pressures; each position of the minimum indicates the theoretical composition of the last residual liquid remaining after perfectly fractional crystallization of an ideal rhyolite magma at the given water pressure (Tuttle and Bowen, 1958, p. 75). On this diagram, points for normative Q, Or, and Ab of the Topopah Spring bulk-rock analyses have also been plotted. The points form a well-defined trend that terminates at its rhyolitic end near the thermal trough and ternary minimum for about 600±100 bars water pressure. The rhyolite analyses that are critical in determining the location of the thermal minimum should be good approximations of a magmatic liquid, as the phenocryst contents of these rocks are very low. The quartz latite analyses do not represent the composition of a magmatic liquid as precisely because of the appreciable phenocryst content of those rocks; however, the positions of these points are much less critical in determining the position of the appropriate thermal minimum. If the analyzed and calculated groundmass compositions (tables 3, 4) are plotted for the quartz latitic tuffs instead of the bulk-rock compositions (fig. 26, lower diagram), this end of the trend lies only slightly closer to the Or corner. The point of termination at the thermal minimum is not affected. These trend relations suggest that the prevalent water pressures during differentiation of the Topopah Spring magma were about 600 bars. On the other hand, the scarcity of phenocrystic quartz in the rhyolitic rocks indicates that water pressures were about the same during phenocryst growth. Had water pressures been appreciably higher during phenocryst crystallization, quartz would be abundant.

Figure 26 (lower diagram) also shows isobaric fractionation curves for 600 bars water pressure, interpolated from the experimentally determined fractionation curves for 1000 bars water pressure (Tuttle and Bowen, 1958, p. 65). Although both bulk-rock and groundmass compositional trends follow the experimental fractionation curves fairly closely, the tielines connecting bulk-rock and groundmass compositions for individual specimens do not parallel the fractionation curves. The reason is the high degree of fractionation of liquid from crystals required to produce the principal variation trend. Liquids can follow the fractionation curve

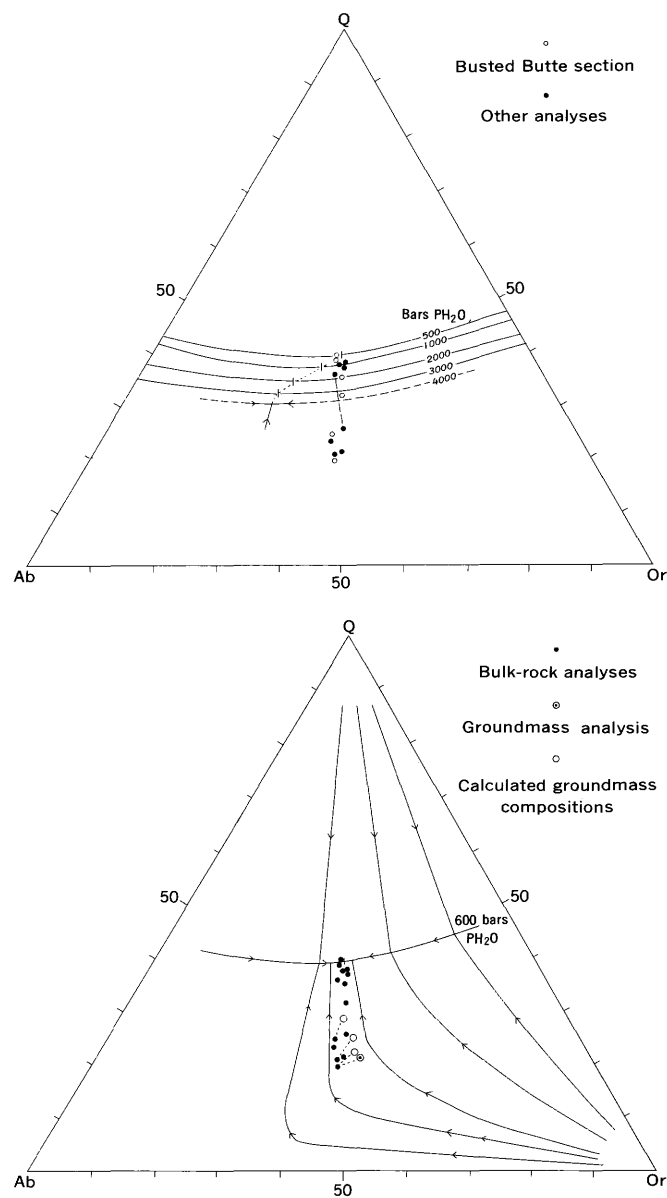


FIGURE 26.—Normative compositions of tuffs of the Topopah Spring Member in the system Q-Or-Ab. *Upper*.—Isobaric lines mark positions of the quartz-feldspar boundary at various water pressures. The position of the thermal minimum along each isobaric line is indicated by a dash or ternary intersection. Modified from Tuttle and Bowen (1958, p. 75). Points are bulk-rock analyses from table 2. Tieline connects compositions of groundmass and pumice from Lathrop Wells section. *Lower*.—Isobaric fractionation curves for 600 bars water pressure, interpolated from Tuttle and Bowen (1958, p. 65). Dashed tielines connect groundmass and bulk-rock compositions of individual specimens.

and be preserved at all stages along it only if they are separated continuously from the crystals. The tielines indicate nonfractional relations between bulk-rock compositions and the liquid phases present at the time of eruption. If projected to the base of the triangle, the

tielines connect the liquid composition with the average compositions of the concurrently stable feldspar phases. The feldspars, remaining in the system rather than being separated from it, can react with the liquid and change in composition as crystallization proceeds. The general trends of the changing phase compositions are illustrated by the work of Tuttle and Bowen (1958, p. 130-137). By combining the results of their experimental work in the system Q-Or-Ab-H₂O with data from natural rocks approximating this composition, they produced a phase equilibrium diagram for the system Or-Ab-An (anorthite). This diagram shows that rocks similar in composition to the Topopah Spring tuffs begin to crystallize by precipitating plagioclase, after which both alkali and plagioclase feldspar crystallize. The path followed by liquids during this crystallization is toward the field boundary between the feldspars and then along it. The direction of this path is consistent with the slope of the tielines in figure 26 (lower diagram).

The parallelism between the trend of compositions of the Topopah Spring tuffs and the experimental isobaric fractionation curve for the liquid line of descent in the system Q-Or-Ab-H₂O (fig. 26, lower diagram) is remarkable. It strongly suggests that the compositional variation of the Topopah Spring Member developed by continuous separation of liquid and crystalline phases under conditions controlled by crystal-liquid equilibrium. Although this parallelism does not in itself prove this origin for the observed relations, it does make various other hypotheses of magmatic differentiation appear less probable. Had some other mechanism such as volatile transfer been the dominant means of differentiation, the observed parallelism between Topopah Spring compositions and the experimental fractionation curves would have to be coincidental. Available experimental evidence indicates that differentiation by volatile transfer, for instance, should produce a divergent compositional trend in which the ratio of Or to Ab increases during fractionation (Orville, 1963).

HYPOTHESIS OF CRYSTAL ACCUMULATION

The phenocryst content of the Topopah Spring quartz latite, higher than that of the rhyolite, immediately suggests a hypothesis of magmatic differentiation by which crystals settled out of the upper part of the erupted magma column and accumulated in the lower part. This mechanism, however, cannot account for the character of variations in phenocryst proportions and in groundmass compositions.

It is rather easily shown that the phenocrysts present in rocks from the upper part of the magma chamber were inadequate as sources for the dominant pheno-

crysts of the lower part of the chamber. Because of the consistent nature of gradational variations in the Topopah Spring ash-flow sheet and the rapidity with which this single cooling unit must have been erupted, the phenocryst proportions determined for various levels in the sheet (fig. 25) should provide a fairly good representation of phenocryst variations in the magma chamber just before eruption. In the phenocryst-poor rhyolites from the upper part of the magma chamber, plagioclase phenocrysts are slightly more abundant than alkali feldspar. Because the specific gravity of plagioclase is greater than that of alkali feldspar, crystal settling should have produced a progressive downward increase in the ratio of plagioclase to alkali feldspar; instead, this ratio is lowest in the crystal-rich rocks from the lower part of the magma chamber.

Although not in accord with the crystal-accumulation hypothesis, the phenocryst proportions are reasonably interpreted as products of progressive crystallization in place. The observed variations in phenocryst types and proportions appear to reflect both more advanced crystallization in the quartz latites than in the rhyolites and also bulk-rock compositional differences between them. Plagioclase appears to have been the first mineral to crystallize. This is consistent with the data of Tuttle and Bowen (1958, p. 130-137). The same data also indicate that rocks having as little CaO as the Topopah Spring, especially in connection with the rather low water pressure indicated previously, should complete crystallization with only one feldspar, a sodic alkali feldspar. The common mantling of plagioclase by alkali feldspar (fig. 20) suggests that the Topopah Spring magma did, in fact, follow this course of crystallization. Fractional crystallization would have tended to reinforce this trend, and the phenocrysts whose optical properties are intermediate between plagioclase and alkali feldspar may represent incompletely reacted crystals resulting from this crystallization path. The crystal-poor rhyolites appear to have been erupted and quenched at an early stage of crystallization, accounting for both their low phenocryst content and their low ratio of alkali feldspar to plagioclase. The ratio of alkali feldspar to plagioclase is higher in the quartz latites, despite a more calcic bulk-rock composition, because of their more advanced degree of crystallization. Quartz is sparse in all rocks of the Topopah Spring Member and is either xenocrystic or had just begun to crystallize at the time of eruption.

A further objection to the hypothesis of fractionation by crystal accumulation is that the variations in phenocryst content could possibly account for, at most, about one-fourth of the range of bulk-rock compositional zonation. Most of the zonation results from

variations in composition of the groundmass. For the crystal-accumulation mechanism to have been dominant in the Topopah Spring Member, the variations in groundmass composition would require extensive resorption of phenocrysts. There is no evidence for such extreme resorption; although some phenocrysts show embayed outlines indicative of resorption, most are euhedral.

The phenocryst proportions and the relations between bulk-rock and groundmass compositions thus indicate that (1) crystallization occurred continuously throughout a liquid whose composition varied from bottom to top, (2) the compositional differences were not produced by accumulation of phenocrysts but were necessarily preexistent in order to produce the observed phenocryst relations, and (3) just prior to eruption the less silicic lower part of the magma was in a more advanced stage of crystallization than the rhyolitic upper part.

HYPOTHESES OF CRYSTAL-LIQUID FRACTIONATION AT HIDDEN DEPTH

The remainder of this discussion is devoted to consideration of the consequences of hypotheses of differentiation by separation of crystals and liquid, excluding that of simple accumulation of crystals in the quartz latitic part of the erupted magma. As we know of no simple way of distinguishing chemically the products of fractional crystallization from those of fractional melting, we consider both processes.

One preliminary point worth noting in consideration of any such hypothesis is the probability that the top of the magma chamber from which the tuffs were erupted had previously reached a rather shallow crustal level. This follows from current theories of ash-flow eruption and emplacement and from some regional evidence. Modern work on voluminous ash-flow cooling units (or ignimbrites) has shown that these deposits represent rapid outpouring from large magma reservoirs. This concept is supported both by the singular cooling of many ash flows in a unit, like the Topopah Spring, and by the prevalence of large caldera subsidence structures in known source areas of the large ash-flow sheets (Smith, 1960a). This in turn indicates the presence of rhyolitic magma in large units in the upper levels of the crust rather than in interconnecting fractures or deep crustal reservoirs. The several ash-flow sheets in southwestern Nevada for which sources have been identified were erupted from caldera structures (Christiansen and others, 1965; Christiansen and Noble, 1965).

The first hypothesis to be considered is that of fractional crystallization of a large body of quartz latitic or

rhyodacitic composition. Although it has already been shown that the quartz latitic part of the Topopah Spring magma was not merely a crystal accumulate, a plausible hypothesis is crystal fractionation by settling into a large volume of magma below that erupted to form the Topopah Spring Member. By this hypothesis, a volume of magma, possibly of batholithic dimensions, would have been emplaced to a shallow crustal level, the uppermost margin of the body would have chilled, and early crystallization of plagioclase and clinopyroxene and subsequently of alkali feldspar and biotite would have begun. The early formed crystals would have to have settled sufficiently rapidly to prevent effective reaction with the magmatic liquid in place, resulting in a compositional gradient toward the top of the chamber. With a progressive decrease in the thermal gradients and the extension of crystallization downward farther into the magma chamber, continuous removal of crystals from the upper part would have resulted in a steady progression in that part toward the composition of the ternary minimum of figure 26.

An important question concerning the crystal-settling hypothesis is whether settling velocities of phenocrysts could be adequate in view of the high viscosity characteristic of rhyolitic melts. This problem is difficult to evaluate quantitatively because many assumptions are required; however, order of magnitude can perhaps be approximated. If the partial pressure of water in the magma chamber was approximately 600 bars, as suggested by figure 26, then both the liquidus temperature and the water content can be estimated for the initial Topopah Spring magma from the experimental data of Tuttle and Bowen (1958) on the system Q-Or-Ab-H₂O. The lowest liquidus temperature for the quartz latites, about 860° C, and the greatest equilibrium water content, about 3 percent by weight, are obtained when water-vapor pressure equals lithostatic pressure. The experimental determinations of Shaw (1963) indicate that rhyolitic obsidians should have viscosities on the order of 10⁷ poises at this temperature and water content. If lithostatic pressure were greater than water pressure, the liquidus temperature would be higher and the equilibrium water content lower (Kennedy, 1955, fig. 1), and their effects on viscosity would tend to balance. Using a phenocryst radius of 1 mm and estimating the density of the melt at 2.2 gm per cu cm, a calculation with Stokes' law indicates a settling velocity of about 9,000 feet in 100,000 years for alkali feldspar, the dominant phenocryst. This seems adequate to allow crystal settling as a possible mechanism in a rhyolitic magma.

Another requirement of the crystallization fractionation hypothesis for the Topopah Spring rocks is that

the diffusion rate of silica in the magma has been low enough to maintain a nonequilibrium compositional gradient in the chamber during differentiation. This factor, too, is not susceptible to adequate evaluation, but qualitatively the properties of silicate liquids appear to indicate such low diffusion rates (Bowen, 1921).

One consequence of this hypothesis is that the degree of crystallization represented by the phenocrysts present in different parts of the ash-flow sheet does not represent the total extent of crystallization in the corresponding part of the magma chamber during the time between emplacement of the magma into the shallow chamber and eruption of the tuffs. These phenocrysts would represent only those crystals that were approximately in equilibrium with the liquid phase in that particular part of the magma chamber under the physical conditions obtaining at the time of eruption. Although the top of the magma chamber would have been the least crystal-rich part at the time of eruption, it would have produced more crystals than any other during the entire time between emplacement of the magma and pyroclastic eruption. At least 50 percent of the material at the top of the chamber would have had to crystallize and be removed to produce the observed differences in composition of groundmasses.

The second hypothesis considered here is that the compositional zonation of the Topopah Spring magma originated through fractional anatectic melting. At a water pressure of 600 bars, the first liquid to appear would have had a composition at the thermal minimum of figure 26 (lower diagram). Being less dense than its country rock, the liquid fraction should have tended to rise. Successive melting of progressively more mafic and refractory rock should have produced successive batches of liquid that followed the fractionation curve of figure 26 (lower diagram) away from the thermal minimum. These successive batches would also have tended to rise. The result might have been a column of liquid fractionated magma, in which silicic liquid occupied the upper part and graded downward into more mafic magma below.

Just how far upward this column would necessarily have moved would depend on the depth at which partial melting occurred. If anatexis can occur only as high as the base of the sialic crust (probably about 20 km in this region; see Roller and Healy, 1963, p. 5848), a great distance is required. If, on the other hand, the local geothermal gradient can, under some circumstances, be sufficiently steep to allow partial melting at lesser depths, such a fractional magma column might form with less upward movement.

Xenocrysts could not have been abundant in any Topopah Spring magma generated in such a manner,

judging by the close approximation of both bulk-rock and groundmass compositional trends to the experimental fractionation curves (fig. 26). Most of the crystals in the erupted tuffs are phenocrysts rather than xenocrysts, as indicated by compositional and textural features previously described. Anomalous plagioclase crystals that may be xenocrysts have also been mentioned, but they could also be survivors from early anatectic processes, or subsequent additions. Late introduction of these crystals, if they are xenocrysts, is suggested by the general lack of resorption features, even in the crystals most obviously out of equilibrium.

On the assumption that pyroclastic eruption means that water-vapor pressure reached or slightly exceeded lithostatic pressure at some point just before eruption and that the equilibrium water-vapor pressure of 600 bars was effective during phenocryst crystallization as well as during anatectic differentiation, a depth to the top of the preeruption magma chamber of about 2 km. is indicated. If anatectic melting is assumed to have begun at about the base of the sialic part of the crust, the fractionated magma column initially would have been undersaturated in water and would have risen almost 20 km. in the crust to collect in a shallow reservoir in sufficient volume to produce the Topopah Spring ash-flow sheet. The vertical rise involved would impose the following requirements: (1) That the magma rise without significant mixing of successively produced fractions, and (2) that crystallization be impeded during rise of the magma by the effect of decreasing total pressure relative to partial water pressure in lowering the liquidus temperature.

To the extent that either of the hypothetical mechanisms just reviewed could have actually occurred during the preeruption history of the Topopah Spring Member, they should have tended to reinforce each other. Any original compositional gradients produced during formation of the magma by fractional melting, either at depth or virtually in place, should have been of the same type as those produced by fractional crystallization in the preeruption magma chamber.

One other effect that may have been significant would have been a gradient of water content in the upper part of the magma chamber due to lower temperature and lithostatic pressure in that region (Kennedy, 1955, fig. 1). Any such gradient should have reinforced the tendency of the main chemical variation to depress the crystallization temperature of the upper rhyolitic part of the magma chamber during the advanced stages of differentiation and cooling in that region, allowing more extensive crystallization of the lower quartz latitic part.

REFERENCES CITED

- Aramaki, S., 1964, Geology of Akamizu-dake, Kagoshima Prefecture, and the welded pyroclastic deposits: *Geol. Soc. Japan Jour.*, v. 70, no. 830, p. 554-564.
- Bowen, N. L., 1921, Diffusion in silicate melts: *Jour. Geology*, v. 29, no. 4, p. 295-317.
- Bowen, N. L., and Tuttle, O. F., 1950, The system $\text{NaAlSi}_3\text{O}_8\text{-KAlSi}_3\text{O}_8\text{-H}_2\text{O}$: *Jour. Geology*, v. 58, no. 5, p. 489-511.
- Christiansen, R. L., Lipman, P. W., Orkild, P. P., and Byers, F. M., Jr., 1965, Structure of the Timber Mountain caldera, southern Nevada, and its relation to basin-range structure, *in Geological survey research 1965: U.S. Geol. Survey Prof. Paper 525-B*, p. B43-B48.
- Christiansen, R. L., and Noble, D. C., 1965, Black Mountain volcanism of southern Nevada [abs.], *in Abstracts for 1964: Geol. Soc. America Spec. Paper 82*, p. 246.
- Cook, E. F., 1958, Stratigraphic study of eastern Nevada Tertiary volcanic rocks [abs.]: *Geol. Soc. America Bull.*, v. 69, no. 12, p. 1548-1549.
- Cornwall, H. R., 1962, Calderas and associated volcanic rocks near Beatty, Nye County, Nevada, *in Engel, A. E. J., James, H. L., and Leonard, B. F., eds., Petrologic studies—a volume in honor of A. F. Buddington: Geol. Soc. America*, p. 357-372.
- Deer, W. A., Howie, R. A., and Zussman, J., 1963, Framework silicates, v. 4 of *Rock-forming minerals: London, Longmans, Green & Co.*, 435 p.
- Enlows, H. E., 1955, Welded tuffs of Chiricahua National Monument, Arizona: *Geol. Soc. America Bull.*, v. 66, no. 10, p. 1215-1246.
- Gianella, V. P., and Callaghan, Eugene, 1934, The earthquake of December 20, 1932, at Cedar Mountain, Nevada, and its bearing on the genesis of Basin Range structure: *Jour. Geology*, v. 42, no. 1, p. 1-22.
- Gilbert, C. M., 1938, Welded tuff in eastern California: *Geol. Soc. America Bull.*, v. 49, no. 12, pt. 1, p. 1829-1862.
- Goddard, E. N., chm., and others, 1948, Rock-color chart: Washington, Natl. Research Council (repub. by Geol. Soc. America, 1951), 6 p.
- Hess, H. H., 1949, Chemical composition and optical properties of common clinopyroxenes, pt. 1: *Am. Mineralogist*, v. 34, nos. 9-10, p. 621-666.
- Hinrichs, E. N., and Orkild, P. P., 1961, Eight members of the Oak Spring Formation, Nevada Test Site and vicinity, Nye and Lincoln Counties, Nevada, *in Short papers in the geologic and hydrologic sciences: U.S. Geol. Survey Prof. Paper 424-D*, p. D96-D103.
- Katsui, Y., 1963, Evolution and magmatic history of some Krakatoan calderas in Hokkaido, Japan: *Jour. Fac. Sci. Hokkaido Univ.*, ser. 4, *Geol. and Min.*, v. 11, p. 631-650.
- Kennedy, G. C., 1955, Some aspects of the role of water in rock melts, *in Poldervaart, Arie, ed., Crust of the earth—a symposium: Geol. Soc. America Spec. Paper 62*, p. 489-503.
- Kulp, J. L., 1961, Geologic time scale: *Science*, v. 133, no. 3459, p. 1111.
- Lipman, P. W., 1965, Chemical comparison of glassy and crystal-line volcanic rocks: *U.S. Geol. Survey Bull.* 1201-D, p. D1-D24.
- Lipman, P. W., and Christiansen, R. L., 1964, Zonal features of an ash-flow sheet in the Piapi Canyon Formation, southern Nevada, *in Geological survey research 1964: U.S. Geol. Survey Prof. Paper 501-B*, p. B74-B78.
- Locke, Augustus, Billingsley, P. R., and Mayo, E. B., 1940, Sierra Nevada tectonic patterns: *Geol. Soc. America Bull.*, v. 51, no. 4, p. 513-539.
- Longwell, C. R., 1960, Possible explanation of diverse structural patterns in southern Nevada: *Am. Jour. Sci.*, v. 258-A (Bradley volume), p. 192-203.
- Mackin, J. H., 1960, Structural significance of Tertiary volcanic rocks in southwestern Utah: *Am. Jour. Sci.*, v. 258, no. 2, p. 81-131.
- Marshall, P., 1935, Acid rocks of the Taupo-Rotorua volcanic district: *Royal Soc. New Zealand Trans. and Proc.*, v. 64, pt. 3, p. 323-366.
- Noble, D. C., Anderson, R. E., Ekren, E. B., and O'Connor, J. T., 1964, Thirsty Canyon Tuff of Nye and Esmeralda Counties, Nevada, *in Short papers in geology and hydrology: U.S. Geol. Survey Prof. Paper 475-D*, p. D24-D27.
- Nockolds, S. R., 1954, Average chemical compositions of some igneous rocks: *Geol. Soc. America Bull.*, v. 65, no. 10, p. 1007-1032.
- Nockolds, S. R., and Mitchell, R. L., 1948, The geochemistry of some Caledonian plutonic rocks; a study in the relationship between the major and trace elements of igneous rocks and their minerals: *Royal Soc. Edinburgh Trans.*, v. 61, pt. 2, p. 533-575.
- O'Connor, J. T., 1963, Petrographic characteristics of some welded tuffs of the Piapi Canyon Formation, Nevada Test Site, Nevada, *in Short papers in geology and hydrology: U.S. Geol. Survey Prof. Paper 475-B*, p. B52-B55.
- Orkild, P. P., 1965, Paintbrush and Timber Mountain Tuffs of Nye County, Nevada, *in Cohee, G. V., and West, W. S., Changes in stratigraphic nomenclature by the U.S. Geological Survey, 1964: U.S. Geol. Survey Bull.* 1224-A, p. A44-A51 [1966].
- Orville, P. M., 1963, Alkali ion exchange between vapor and feldspar phase: *Am. Jour. Sci.*, v. 261, no. 3, p. 201-237.
- Peterson, D. W., and Roberts, R. J., 1963, Relation between the crystal content and the chemical composition of welded tuffs: *Bull. Volcanol.*, v. 26, p. 113-123.
- Poole, F. G., Carr, W. J., and Elston, D. P., 1965, Salyer and Wahmonie Formations of southeastern Nye County, Nevada, *in Cohee, G. V., and West, W. S., Changes in stratigraphic nomenclature by the U. S. Geological Survey, 1964: U.S. Geol. Survey Bull.* 1224-A, p. A36-A44 [1966].
- Quinlivan, W. D., and Lipman, P. W., 1965, Compositional variations in some Cenozoic ash-flow tuffs, southern Nevada [abs.], *in Abstracts for 1964: Geol. Soc. America Spec. Paper 82*, p. 342.
- Rankama, Kalervo, and Sahama, T. G., 1950, *Geochemistry: Univ. Chicago Press*, 912 p.
- Ratté, J. C., and Steven, T. A., 1964, Magmatic differentiation in a volcanic sequence related to the Creede caldera, Colorado, *in Short papers in geology and hydrology: U.S. Geol. Survey Prof. Paper 475-D*, p. D49-D53.
- Roller, J. C., and Healy, J. H., 1963, Seismic-refraction measurements of crustal structure between Santa Monica Bay and Lake Mead: *Jour. Geophys. Research*, v. 68, no. 20, p. 5837-5849.
- Ross, C. S., and Smith, R. L., 1955, Water and other volatiles in volcanic glasses: *Am. Mineralogist*, v. 40, nos. 11-12, p. 1071-1089.
- 1961, Ash-flow tuffs—Their origin, geologic relations and identification: *U.S. Geol. Survey Prof. Paper 366*, 81 p.

- Shapiro, Leonard, and Brannock, W. W., 1962, Rapid analysis of silicate, carbonate, and phosphate rocks: U.S. Geol. Survey Bull. 1144-A, p. A1-A56.
- Shaw, H. R., 1963, Obsidian-H₂O viscosities at 1000 and 2000 bars in the temperature range 700° to 900° C: Jour. Geophys. Research, v. 68, no. 23, p. 6337-6343.
- Smith, R. L., 1960a, Ash flows: Geol. Soc. America Bull., v. 71, no. 6, p. 795-841.
- 1960b, Zones and zonal variations in welded ash flows: U.S. Geol. Survey Prof. Paper 354-F, p. 149-159.
- Thornton, C. P., and Tuttle, O. F., 1960, Differentiation index, pt. 1 of Chemistry of igneous rocks: Am. Jour. Sci., v. 258, no. 9, p. 664-684.
- Tröger, W. E., 1956, Optische Bestimmung der gesteinsbildenden Minerale, pt. 1, Bestimmungstabellen: Stuttgart, E. Schweizerbart'sche Verlag., 147 p.
- Turekian, K. K., and Wedepohl, K. H., 1961, Distribution of the elements in some major units of the earth's crust: Geol. Soc. America Bull., v. 72, no. 2, p. 175-191.
- Tuttle, O. F., 1952, Optical studies on alkali feldspars (Bowen volume): Am. Jour. Sci., pt. 2, p. 553-567.
- Tuttle, O. F., and Bowen, N. L., 1958, Origin of granite in the light of experimental studies in the system NaAlSi₃O₈-KAlSi₃O₈-SiO₂-H₂O: Geol. Soc. America Mem. 74, 153 p.
- Williams, Howel, 1942, The geology of Crater Lake National Park, Oregon, with a reconnaissance of the Cascade Range southward to Mount Shasta: Carnegie Inst. Washington Pub. 540, 162 p.
- Williams, P. L., 1960, A stained slice method for rapid determination of phenocryst composition of volcanic rocks: Am. Jour. Sci., v. 258, no. 2, p. 148-152.

